

A NUMERICAL MODEL FOR
THE MARMARA SEA

by

ERDEM A. ALBEK

B.S. in I.E., Boğaziçi University, 1984

Submitted to the Institute of Environmental Sciences
in partial fulfillment of the requirements
for the degree of
Master of Science

Bogazici University Library



39001100312837

14

Boğaziçi University

1987

Babaannem
Ayşe Saibe Kansu'nun
anısına

ACKNOWLEDGEMENTS

I would like to express my deep gratitude to Dr. Orhan Yenigün for his guidance and support at every stage of this work. I am also indebted to him for having introduced me into the fascinating field of numerical modeling.

I am thankful to Prof. Yüksel İnel for his support and for making departmental facilities available to me. I am also thankful to Dr. Osman Börekçi for his helpful comments.

I would like to express my thanks to Admiral Şevket Güçlüer and to Major Hüseyin Yüce of Seyir Hidrografi ve Oşinografi Dairesi, and to Dr. Barış Mater of İstanbul Üniversitesi Deniz Bilimleri Enstitüsü, for their efforts in providing information to me on the Marmara Sea. I am also thankful to Dr. D.J. Gunn, University College of Swansea, United Kingdom, for his helpful comments.

I am grateful to Nilüfer, Nilgün and Vildan for their patience in preparing drawings.

Finally, I am indebted to my parents and brother who always were by me.

ABSTRACT

In this study, a numerical model has been developed to predict currents and water levels prevailing in the Marmara Sea.

The model is a depth averaged two-layer transient model to adequately simulate stratified flow conditions in the sea. The nonlinear partial differential equations of the model have been solved by using an explicit finite difference scheme and employing a local integral method to reduce truncation and round-off errors and to improve accuracy.

Special emphasis has been laid on the prediction of currents and water levels under strong winds.

ÖZET

Bu çalışmada, Marmara denizi akıntılarının ve su seviyelerinin hesaplanabilmesi için nümerik bir model geliştirilmiştir.

Marmara denizinin iki katmanlı akıntı sistemini ortaya çıkarabilmek için, iki katmanlı, zamana bağımlı ve düşey ekseninde entegre edilmiş bir model kullanılmıştır. Modelin doğrusal olmayan kısmi diferansiyel denklemleri belirttik (explicit) bir sonlu farklar yöntemiyle çözülmüş, hataların kontrolü ve doğruluğun artmasının sağlanması için, bir yerel integral yöntemi uygulanmıştır.

Özellikle, kuvvetli rüzgarlar altında akıntı ve su seviyelerinin hesaplanmasına önem verilmiştir.

TABLE OF CONTENTS

	Page
Acknowledgements	iv
Abstract	v
Özet	vi
List of Figures	x
List of Tables	xi
List of Symbols	xii
I. INTRODUCTION	1
II. LITERATURE SURVEY	4
2.1 Depth-Averaged Models	4
2.2 Depth-Averaged Models of Stratified Flows	9
III. STRATIFIED FLOWS	15
3.1 Properties of Stratified Flows	15
3.2 Analytical Treatment of Stratified Flows	17
3.2.1 Stability of Stratified Flows	18
3.2.2 Internal Waves	18
3.2.3 Entrainment and Diffusion	19
3.2.4 Interfacial Friction	19
IV. THE MARMARA SEA	21
4.1 Geographical Setting	21
4.2 Physical Oceanography of the Marmara Sea	25
4.2.1 Vertical Distribution of Water	
Characteristics in the Marmara Sea	27
4.2.2 Horizontal Distribution of Water	
Characteristics in the Marmara Sea	34

4.2.3	Stability of Layering	36
V.	THE MODEL	38
5.1	Basic Assumptions	38
5.2	The Governing Equations	41
5.3	Shear Stresses	43
5.3.1	Wind Stress	43
5.3.2	Interfacial Stress	44
5.3.3	Bottom Stress	46
VI.	THE NUMERICAL METHOD	47
6.1	Finite Difference Methods	47
6.2	The Computational Grid	50
6.3	The Differencing Scheme for Spatial Derivatives	50
6.4	The Representation of Temporal derivatives: The Local Integral Method	52
6.5	The Finite Difference Equations	54
6.6	Boundaries and Boundary Conditions	59
6.6.1	Land Boundaries	59
6.6.2	Open Boundaries	61
6.7	The Computer Program	62
VII.	DISCUSSION OF THE RESULTS	63
7.1	The Boundary Conditions and Driving Mechanisms	63
7.1.1	The Upper Layer	63
7.1.2	The Lower Layer	64
7.2	The Circulation in the Absence of Wind	64
7.2.1	The Upper Layer	65
7.2.2	The Lower Layer	68

7.3	Upper Layer Circulation Under Wind Stress	68
7.3.1	Circulation and Water Levels in the Presence of a Strong South Wind	68
7.3.2	Circulation and Water Levels in the Presence of Northern Winds	70
VIII.	CONCLUSIONS AND RECOMMENDATIONS	80
IX.	REFERENCES	83
	APPENDIX I	88
	APPENDIX II	101
	APPENDIX III	115

LIST OF FIGURES

	<u>Page</u>
FIGURE 3.1 Density profile in a stratified fluid	15
FIGURE 4.1 Map of the Marmara Sea Region	22
FIGURE 4.2 Bathymetric map of the Marmara Sea	24
FIGURE 4.3 Layering in the Marmara Sea	27
FIGURE 4.4 Oceanographical stations in the Marmara Sea	29
FIGURE 4.5 Density profile at station 18	31
FIGURE 4.6 Salinity versus distance from the Bosphorus Strait	36
FIGURE 5.1 Variables used in the equations	40
FIGURE 6.1 The computational grid	51
FIGURE 6.2a Node closed in the negative x-direction	60
FIGURE 6.2b Node closed in the positive y-direction	60
FIGURE 7.1 Upper layer velocity field in the absence of wind	66
FIGURE 7.2 Upper layer velocity field in the absence of wind	67
FIGURE 7.3 Lower layer velocity field	69
FIGURE 7.4 Elevations above mean sea level	71
FIGURE 7.5 Upper layer currents	72
FIGURE 7.6 Elevations above mean sea level	73
FIGURE 7.7 Upper layer currents	75
FIGURE 7.8 Elevations above mean sea level	76
FIGURE 7.9 Upper layer currents	77
FIGURE 7.10 Elevations above mean sea level	78

LIST OF TABLES

		<u>Page</u>
TABLE 4.1	Some physical data on the Marmara Sea	21
TABLE 4.2	Temperature and salinity at station 18	28
TABLE 4.3	Density versus depth at station 18	32

LIST OF SYMBOLS

- A = smoothing constant for the local integral method
 B = bottom stress term in the momentum equation
 C = Chezy's bottom friction coefficient
 $C(z)$ = wind drag coefficient z meters above mean sea level
 F = densimetric Froude number
 f = Coriolis parameter
 g = gravitational acceleration
 H = maximum water depth
 H_m = water depth in single layer equations
 h = elevation of the sea bed above datum plane
 h_o = elevation of sea surface above datum plane
 h_1 = elevation of the interface above datum plane
 h_2 = elevation of the interface above datum plane
 i = x-coordinate of computational node
 j = y-coordinate of computational node
 K = interfacial friction coefficient
 m = subscript indicating upper or lower layer, also stands
for a mean density
 n = time step
 q = vector or scalar quantity
 s = a horizontal direction index
 Δs = a horizontal increment
 t = time
 T_b = bottom stress
 T_i = interfacial stress
 i

T = wind stress

U, V = depth averaged single layer velocity components

u_1, v_1 = upper layer velocity components

u_2, v_2 = lower layer velocity components

$V(z)$ = wind velocity z meters above sea level

x, y = Cartesian coordinates

$\Delta x, \Delta y$ = increments in the respective directions

GREEK LETTERS

ρ_a = density of air

ρ_1 = density of upper layer

ρ_2 = density of lower layer

ρ_m = mean density

$\Delta \rho$ = density difference

θ = latitude

Ω = angular rotation of the earth

I. INTRODUCTION

With the advent of high speed and high storage computers, numerical models of hydrodynamical systems have greatly replaced hydraulic models. Numerical models offer almost unlimited flexibility in the simulation of various conditions, whereas hydraulic models require extensive modifications for even a slight change in the modeled system. Moreover, numerical models are less expensive.

Fields of application of numerical models cover a wide range. In coastal engineering, simulation of flow patterns by a numerical model provides valuable data to be used in planning a coastal construction. Modeling of storm surges to predict maximum water-levels aids the efficient planning of flood defense works in areas vulnerable to frequent flooding by storms and hurricanes. Tidal computations in open channels and harbors are a useful tool for navigational purposes and construction projects.

Quite a number of marine environments today are heavily polluted by man. They require urgent intervention to regain back their aesthetical value and to become harmless and useful to any form of life. Numerical water quality modeling is a very efficient tool in aiding environmental planning of

such endangered marine systems. Water quality models are widely used to predict the behavior of pollutants released into a marine environment, their dispersion and fate.

The Marmara Sea in northwestern Turkey is one of the endangered marine systems. It lies in a region where a quarter of Turkey's population lives and almost half of the country's industry is located. The sea is continuously polluted by urban centers and industry. Owing to its geographical setting, the Marmara Sea has only limited access to open seas and this greatly reduces its regeneration capability by allowing the contaminants to disperse only in a confined area.

The Marmara Sea is important in the sense that it is a major international sea-way. Moreover, in the rapidly developing Marmara Region, it can serve much to transportation, especially in the eastern portion. The sea is also a productive fishing ground and recreational area.

In contrast to its importance, the Marmara Sea is little investigated. There is a lack of knowledge about its two-layer flow pattern. The general circulation in the sea is virtually unknown. There are no values for the transport of water in both upper and lower layers.

The foregoing study is thought to simulate the general circulation pattern in the Marmara Sea. The model developed is a quasi three-dimensional model. It is composed of two 2-D models to simulate variations in three dimensions. The model is designed to predict velocities and water levels for both layers under various conditions, like the response of the sea

to strong winds.

In its present form, the model will serve two purposes. First, the circulation pattern of the sea will be investigated and data for a water quality model will be obtained. Secondly, the applicability of the model to a large hydrodynamical system will be tested. Up to now, to the best knowledge of the author, no numerical model has been developed employing the full form of the equations describing fluid flow and covering such a large region.

II. LITERATURE SURVEY

2.1. Depth-Averaged Models

Mathematical modeling of fluid motion is accomplished by solving the Navier-Stokes equations which describe fluid motion in a hydrodynamical system. These equations are nonlinear partial differential equations and unless considerable simplifications are made by neglecting a number of terms and a very simple geometry of the system is assumed these equations do not have analytical solutions.

The advent of high speed, high storage digital computers has enabled the numerical solution of the Navier-Stokes equations, employing numerical techniques like finite difference and finite element methods. But even then, the handling of the 3-D equations is very complex and time consuming. This has necessitated some modifications in the equations, which has led to a class of numerical models, called depth-averaged models.

The modeling of a hydrodynamical system by depth averaged equations is based on two assumptions. The first one involves a comparison between the vertical acceleration in a system and the gravitational acceleration. In hydrodynamical systems, vertical accelerations are very small compared with

the gravitational acceleration. This results in the elimination of one equation from the system, the equation of motion in the vertical direction. But still, the system is 3-D.

The second assumption is that the system is well-mixed in the vertical direction. It is assumed that the flow properties do not change in the vertical direction. This allows an integration over the flow depth. The integration, usually called depth-averaging, results in a single velocity vector on the horizontal plane which is representative of all velocities along the flow depth. With this integration, the vertical coordinate is eliminated and the system is reduced to two dimensions. The resulting depth averaged equations are the following.

The equation of continuity

$$\frac{\partial h}{\partial t} + \frac{\partial(UH)}{\partial x} + \frac{\partial(VH)}{\partial y} \neq 0 \quad (2.1)$$

The equation of motion (longitudinal direction)

$$\frac{\partial U}{\partial t} + U \frac{\partial U}{\partial x} + V \frac{\partial U}{\partial y} - fV + g \frac{\partial h}{\partial x} + W + B \neq 0 \quad (2.2)$$

$$\frac{\quad}{A} \quad \frac{\quad}{C} \quad \frac{\quad}{P}$$

The equation of motion (lateral direction)

$$\frac{\partial V}{\partial t} + U \frac{\partial V}{\partial x} + V \frac{\partial V}{\partial y} + fU + g \frac{\partial h}{\partial y} + W + B \neq 0 \quad (2.3)$$

$$\frac{\quad}{A} \quad \frac{\quad}{C} \quad \frac{\quad}{P}$$

The continuity equation above arises from the consideration that inflow into a volume element in the system is equal to the outflow, given that the fluid is incompressible (sea water is slightly compressible but in a negligible amount). In the equations, x and y denote Cartesian coordinates, with x representing the longitudinal and y the lateral directions (this convention will be held throughout the text).

h in the equations represents water level elevation above a fixed reference plane, called a datum. H stands for the flow depth, U and V for depth-averaged components of the velocity vector and t for time.

The momentum equations, although they seem quite complex in fact arise from the simple, but very important equation of classical dynamics:

$$\text{Acceleration} = \text{force/mass}$$

The first three terms, labeled A, sum up to the acceleration term DU/Dt and DV/Dt , called the total derivative with $\partial U/\partial t$ and $\partial V/\partial t$ being the local derivatives and the other two being the convective accelerations. The terms labeled P, W and B are the components of forces acting on the system. P designates the components normal to the surface of the fluid volume (pressure force) and W and B stand for the tangential components (shear force). W is the wind stress acting on the sea surface and B the bottom stress acting along the sea bed. The term labeled C is the Coriolis term, arising from the Coriolis force which originates from the rotation of the earth. It is in fact an imaginary force,

used to transfer from axes fixed in space to axes fixed in the rotating earth. f is the Coriolis parameter.

Depth-averaged models have been extensively applied to predict motion and waterlevels in hydrodynamical systems. Liu (1) Leendertse, in their detailed survey on numerical modeling of estuaries and coastal seas, give a good description of depth-averaged models.

Hinwood and Wallis(2,3) compiled an extensive review of mathematical models by examining over hundred models for their predictive capability and limitations.

(4) Fisher, discusses the limitations of modeling of coastal flows by pointing out to the lack of knowledge on the controlling processes.

A good treatise on depth-averaged modeling may be found in Ponce and Yabusaki (5), where the authors claim that the greatest source of uncertainty in depth-averaged models is the inadequate representation of the shear stress terms. They also discuss the importance of the convective acceleration terms in adequately predicting circulation.

(6) Chintu Lai gives the most up-to-date review of hydrodynamical models. His work is confined to open channel flows but extensive information is present for depth-averaged modeling.

Depth-averaged models have been applied to a variety of hydrodynamical systems. The prediction of storm surges is an example. Reid and Bodine (7) modeled storm surges in Galveston bay with a simple 2-D model, neglecting the Coriolis force and convective accelerations. They used data, to calibrate

and verify their model, from two hurricanes.

(8)
Prandle modeled storm surges in the North Sea and River Thames where he used a 1-D model for the river and a separate 2-D one for the sea. The model provided data for maximum water-levels for the design of flood defense works. Another model of the North Sea is that of Pingree and Griffiths (9). Their model was used to predict currents driven by a uniform wind stress over the sea.

Tidal circulation in coastal areas has been a challenging field of study for numerical modeling. A classical paper on tidal computations is that of Dronkers (10), where a comprehensive study is presented for tidally induced currents in rivers and coastal areas. Flather and Heaps (11) modeled tides in Morecambe bay using a routine to incorporate the emergence and submergence of certain shallow areas of the bay. Gunn and Yenigün (12,13) developed a model for tidal currents in two estuaries, the Milford Haven and Tay estuaries. A numerical model for tidal circulation in harbors was developed by Falconer (14).

Depth-averaged models have also been used for water quality simulations. Williams and Hinwood (15) developed a 2-D pollutant transport model for the Port Philip bay in Australia which receives wastes from the city of Melbourne. In Liu and Leendertse (1), a model is presented for predicting coliform concentrations in Jamaica bay, New York, after a storm surge. Pollutant transport in a natural harbor was modeled by Falconer (16), utilizing depth-averaged equations.

2.2. Depth-Averaged Models of Stratified Flows

Stratified flows are characterized by fluid layers of different densities which are stacked in the vertical direction. The density differences between the layers are caused by differences in temperature, salinity or suspended matter concentration. The layers are separated from each other by intermediate regions where sharp density, temperature or salinity gradients occur. This intermediate layer effectively prevents mixing between the layers.

Several attempts have been made to model stratified flows. In general, two approaches have been employed. The first approach and the least used one is to utilize a 3-D model which employs a 3-D spatial network with a fixed number of grid boxes in both horizontal and vertical directions. The 3-D model requires extensive computer time and also has the disadvantage of having reduced vertical resolution in shallow regions where the number of grid boxes in the vertical direction is decreased.

The most widely used approach is to employ a layered model. The model assumes that layers in a stratified fluid are homogeneous in themselves and that each layer may be characterized by its own set of depth averaged-equations. The layers are separated from each other by interfaces of negligible thickness through which no transfer of mass or heat is allowed. Thus a layered model is an extension of the single layered depth-averaged model.

The resulting set of equations, with each set having its

own continuity equation and, depending on the nature of the system, one or two momentum equations, are coupled to each other. In the numerical solution procedure, all the equations have to be solved together. For a two-layered, 2-D system, the number of unknowns is six and there are six equations to be solved.

This type of model has been applied to many systems where stratified circulation exists, including thermally stratified lakes, estuaries where saline sea water is overlain by freshwater from rivers and, sea-straits where counterflows exist.

A numerical model of stratified flows is that of Grubert and Abbott⁽¹⁷⁾. The model assumed a 1-D two-layered system. Convective terms were included, as well as an expression for the bottom slope. The authors added terms to the equations which account for mass flux between the layers. But for this study they were assumed to be zero. The equations were solved by using an implicit finite difference scheme.

Lee and Liggett^(18,19) modeled a lake which showed thermal stratification. They used a hypothetical lake with arbitrary bottom and shoreline configuration. Their model was a steady-state one and convective terms were neglected. The 2-D equations included only the Coriolis acceleration, the pressure force and vertical friction terms. Due to the numerous approximations, quantitative accuracy appeared to be doubtful. Nevertheless some qualitative conclusions could be drawn. The interface slope was found to be greater than the free surface slope by a factor of $\Delta\eta/\delta$

($\Delta \rho$ = density difference between the layers, ρ = mean density). Magnitude for surface currents was less in the center of the lake than near shores. Downwind transport was observed to be greater near the shores.

A numerical model of flows in stratified estuaries is that of Hodgins et al⁽²⁰⁾. It is an unsteady-state two-layer depth-averaged model of the Fraser river estuary in Canada. The model is 1-D and includes convective accelerations. Friction terms were expressed as quadratic formulations. For the interfacial stress, the authors used an amplification factor by multiplying the quadratic expression with the densimetric Froude number. The resulting four equations were solved by using explicit central differences. Unlike in⁽¹⁷⁾, the model neglected transfer of mass between the layers. Moreover, lateral variations were not included, although the model was used for the main arm of the estuary which had an average width of 2000 meters.

Like estuaries, narrow bays may exhibit stratified flow patterns. Hyden⁽²¹⁾ developed a model (two-layered, depth averaged) of a narrow bay in Sweden and compared results with laboratory experiments and a hydraulic model of the bay. In the model, the author approximated the bay as a channel. The equations were one-dimensional, included convective terms and an expression to account for the bottom slope. Wind, interfacial and bottom stresses were formulated as quadratic equations. The solution procedure was the method of characteristics.

Two-layer, depth-averaged models have been applied to

sea-straits where counterflows exist. There are one-layered models of sea-straits like that of Laevastu⁽²²⁾ of the Gibraltar Strait. However a one-layer model does not accurately simulate flow conditions in a sea-strait where counterflows exist. A two-layer model is more appropriate.

Sümer and Bakioğlu⁽²³⁾ developed a two-layer model of the Bosphorus Strait. They neglected lateral variations and formulated the depth-averaged equations in one dimension. Wind stress and convective terms were neglected. The model was a steady-state one and assumed no mixing between the layers. It is however doubtful that mixing is small enough to be neglected in the Bosphorus Strait.

Another application of two-layered, depth-averaged models to sea-straits is the model of the Taiwan Strait by Yin and Chen⁽²⁴⁾. The model was designed to predict currents induced by tides in the strait. As the strait was wide (around 100 km), lateral variations were included, but convective terms neglected. The effect of wind was neglected and tide was considered to be the main driving force. A finite difference scheme was used for the solution of the equations.

In all these models, some simplifications are made. A common one is the neglectance of convective terms^(18,23,24). These terms are nonlinear and they have been shown to create instabilities in certain schemes. Benque et al⁽²⁵⁾, however, have shown that convective terms are important in modeling circulation and Ponce and Yabusaki⁽⁵⁾ point out that convective accelerations have to be included whenever

secondary currents need to be considered.

Another consideration is the dimension. The models of the estuaries concerned and the model of the Bosphorus Strait were 1-D. Lateral variations were neglected. For very long and very narrow flows, this reduction to 1-D may be justified. However, if the region modeled is wide so that secondary currents and circulations are likely to develop, 2-D models are more appropriate.

Shear stresses are the greatest pitfall of depth averaged formulations. When turbulence is accounted for in the equations of fluid motion (which is always done except for the case of laminar flow which is quite rare in hydrodynamical systems), terms like $\overline{u'v'}$, $\overline{u'u'}$ etc. arise where the primed variable denotes the fluctuating component of the velocity vector due to turbulence. These terms are called Reynolds stresses or shear stresses and represent tangential or frictional forces. When they are not parametrized, that is expressed in terms of quantities which can be observed or calculated from the equations, they lead to a closure of the equations; the set includes more variables than equations. Up to now no completely satisfactory representation of these stresses has been achieved, especially for the interfacial stress term in the two-layer models. Generally, quadratic formulations are used and these employ friction coefficients the adequacy of which is not known for modeled systems.

For two-layered flows, mixing across the interface creates problems. Mixing is usually neglected and it is done

not to render the problem more difficult. In some cases, especially for high shear flows, mixing is significant. However, to account for it is very difficult and it remains a challenging topic to include mixing into the equations.

III. STRATIFIED FLOWS

3.1. Properties of Stratified Flows

Stratification in hydrology is a term pertaining to the formation of distinct layers in a water body. In a stratified fluid, the densest water forms the lowest layer with lighter water occupying the overlying layers. Thus stratification is formed and maintained by density differences between the layers which are due to temperature and salinity gradients and variations in suspended matter concentrations in the vertical direction (Figure 3.1.).

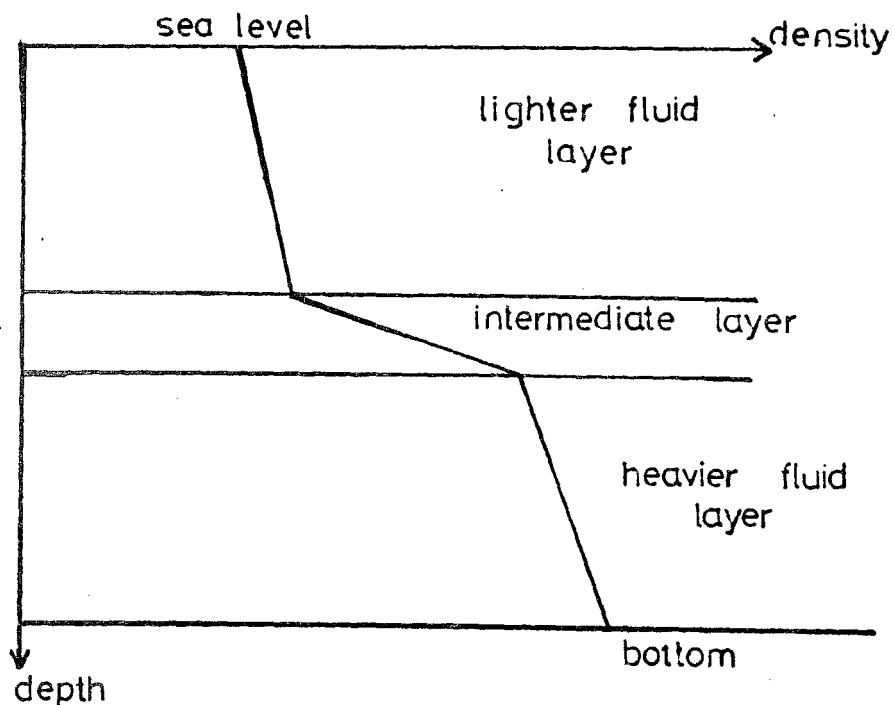


Fig 3.1. Density profile in a stratified fluid

The figure presents the simplest case of a stratified flow, the two-layer flow. Multilayer systems exist and systems where the vertical density gradient is continuous are not uncommon.

The intermediate layer plays a significant role in stratified flows. It is a region where the density has a sharp vertical gradient. If density differences are brought about by temperature differences, this region is called a thermocline. Salinity differences form a halocline. If the density differences are brought about by the combined effect of temperature and salinity differences, the intermediate layer is called a pycnocline.

The intermediate region acts as a barrier between the layers. It opposes vertical motion and greatly suppresses exchange of heat, salt or water between the layers.

Stratified flows occur everywhere in nature. Oceans are stratified by temperature. The top few hundred meters, well mixed by the wind are succeeded by a thermocline with a relatively sharp transition. The thermocline is mostly deeper than the upper layer, usually in excess of one kilometer. Below the thermocline is the bottom layer, formed by colder and denser water.

Lakes, particularly deep ones, are also mostly thermally stratified. However, the stratification is only seasonally stable, not permanent as in the oceans. Stratification in summer and in winter is broken down by fall and spring overturns when a homogeneous density distribution in the vertical is established.

In estuaries and fjords, salinity differences give rise to stratified flows. In an estuary, where fresh and saline waters meet, the fresh river water overlies saline sea water which is denser. The saline bottom layer may travel up the river for considerable distances, forming a salt wedge.

Sea-straits which connect sea basins of different characteristics, usually exhibit a two-layer flow pattern. Heavier waters of one basin flow beneath the lighter waters of the other basin, mostly as counterflows.

Sediment-laden river waters, upon entering a lake or reservoir, often give rise to underflows by plunging under the relatively clean and light lake waters. Such flows are only locally observable, the sediment settling quickly and the flow being diluted over a short distance.

3.2. Analytical Treatment of Stratified Flows

Mathematical description of stratified flows has been a subject for research for many years. Both theoretical studies and laboratory experiments have revealed many interesting features of such flows. Most research has been directed towards the understanding of two-layer systems, the simplest case. A thorough treatise may be found in Streeter⁽²⁶⁾. Three chapters devoted to the study of salt-wedge behavior in estuaries are present in Ippen⁽²⁷⁾.

In this section, some characteristics of stratified flows will be discussed and some mathematical relationships will be presented.

3.2.1. Stability of Stratified Flows

An important parameter in the study of layered flows is the densimetric Froude number. This dimensionless number is the ratio of inertial forces to the gravitational force and may be defined as (Abraham et al (28)):

$$F = \frac{(u_2 - u_1)^2}{\Delta \rho / \rho_m \cdot g \cdot (h_1 + h_2)} \quad (3.1)$$

where

u_1, u_2 = velocities of upper and lower layers

$\Delta \rho$ = density difference ($\rho_2 - \rho_1$)

ρ_2 = lower layer density

ρ_1 = upper layer density

ρ_m = mean density

g = gravitational acceleration

h_1 = depth of upper layer

h_2 = depth of lower layer

A densimetric Froude number less than unity indicates subcritical flow and stable stratification.

3.2.2. Internal Waves

Internal waves form at a density discontinuity or interface between layers and differ from surface waves by their much larger amplitude. Internal waves do not much affect surface waves, but small disturbances at the sea surface may form large internal waves at the density interfaces.

These waves contribute to mixing between layers. Abraham (28) et al have found out that if internal waves are stable, turbulent mixing is reduced. If internal waves are unstable and break, mixing across the interface occurs.

3.2.3. Entrainment and Diffusion

Entrainment is a process where a more turbulent layer erodes the less turbulent layer. Entrainment increases the thickness of the turbulent layer and creates mixing between the layers. The mixing by entrainment is a one-way process where there is a flux of mass from the less turbulent layer to the more turbulent layer (Carstens (29)).

Diffusion is a type of interfacial mixing. Molecular diffusion is usually neglected as its magnitude is far less than that of turbulent diffusion. Turbulent diffusion is a two-way process where equal volumes are exchanging places.

Interfacial mixing is the combination of these two processes. It is very difficult to determine the degree of mixing in stratified flows as many factors influence it. Laboratory experiments have revealed some features of interfacial mixing, but still many aspects remain unknown.

3.2.4. Interfacial Friction

Usually, in a stratified fluid, the layers tend to have different velocities. The difference in the velocity field gives rise to a shear stress between the layers. Several studies have been carried out to analyze this interfacial

friction. Most research was directed towards the determination of an interfacial friction coefficient. Several researchers correlated the friction coefficient with the Reynolds number and the densimetric Froude number (Macagno and Rouse⁽³⁰⁾, Dermassis and Partheniades⁽³¹⁾). The latter found out that the coefficient depends on these numbers and also on the relative density difference between the layers.

Abraham et al⁽²⁸⁾ conclude that the interfacial shear is influenced by turbulence both at the interface and bottom. They expressed the interfacial shear by a quadratic equation, which is the most widely used one. Their friction coefficients, however, are highly empirical.

IV. THE MARMARA SEA

4.1. Geographical Setting

The Marmara Sea is located in northwestern Turkey, in the Marmara region. Its coastline is shared by Thracia and Anatolia. It is an inland sea but has access and is in continuous water exchange with the Mediterranean Sea and the Black Sea via the narrow Dardanelles and Bosphorus Straits (Figure 4.1, Table 4.1).

Table 4.1. Some physical data on the Marmara Sea

Surface Area	11352 square kilometers
Maximum depth	1335 meters
Mean Depth	300 meters
Length	280 kilometers
Width	76 kilometers

The Marmara Sea shows an elongated shape, the length width ratio being 4 to 1. The sea, although very small in regard to surface area, shows the relief characteristics of a miniature ocean. Almost half of the sea is occupied by a shelf area which with a steep slope descends to deep

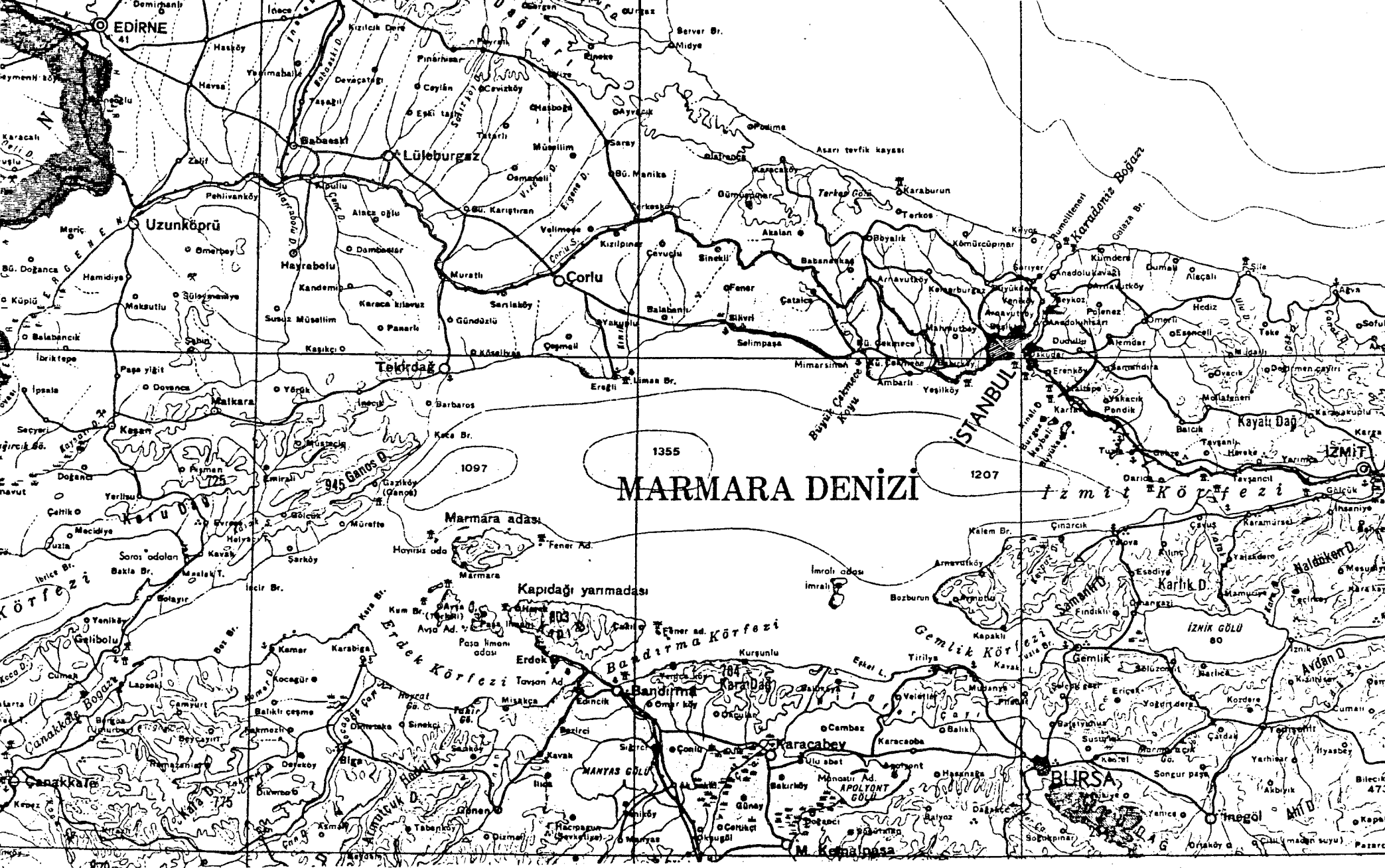


Fig. 4.1 Map of the Marmara Sea

depressions .

The coastline configuration shows marked differences between the Thracian and Anatolian coasts. The southern coastline is characterized by irregular topography. The shelf extends as far as 30 kilometers away from the coast, the edge having a depth of around 100 meters. There are several islands along the southern coastline, the principal ones being the Marmara, Avşa, Paşalimanı and İmralı islands. Two bays (Erdek and Bandırma) exist on each side of the Kapıdağ peninsula which formerly was an independent island but now is connected to the mainland by a tombolo.

The eastern coastline, again belonging to Anatolia, consists of two large bays. The Gemlik bay extends 40 kilometers into the land and is around 15 kilometers wide at the mouth. The Samandağ peninsula separates the Gemlik bay from the İzmit bay to the north which is narrower but longer, penetrating about 60 kilometers into the land.

The northern and northwestern coastline, belonging to Thracia, is strikingly regular, lacking both bays, peninsulas and off-shore islands. The shelf along the coast is, but, very narrow, rarely extending behind 10 kilometers. In some places, within a few kilometers, depths as great as 500 meters are encountered.

The shelf covers around half of the sea's area. The remaining portion is occupied by the slopes on the shelf edges and three deep depressions. The depressions lie in a more or less straight line. Separated by sills, they attain depths in excess of 1000 meters, the deepest being 1335

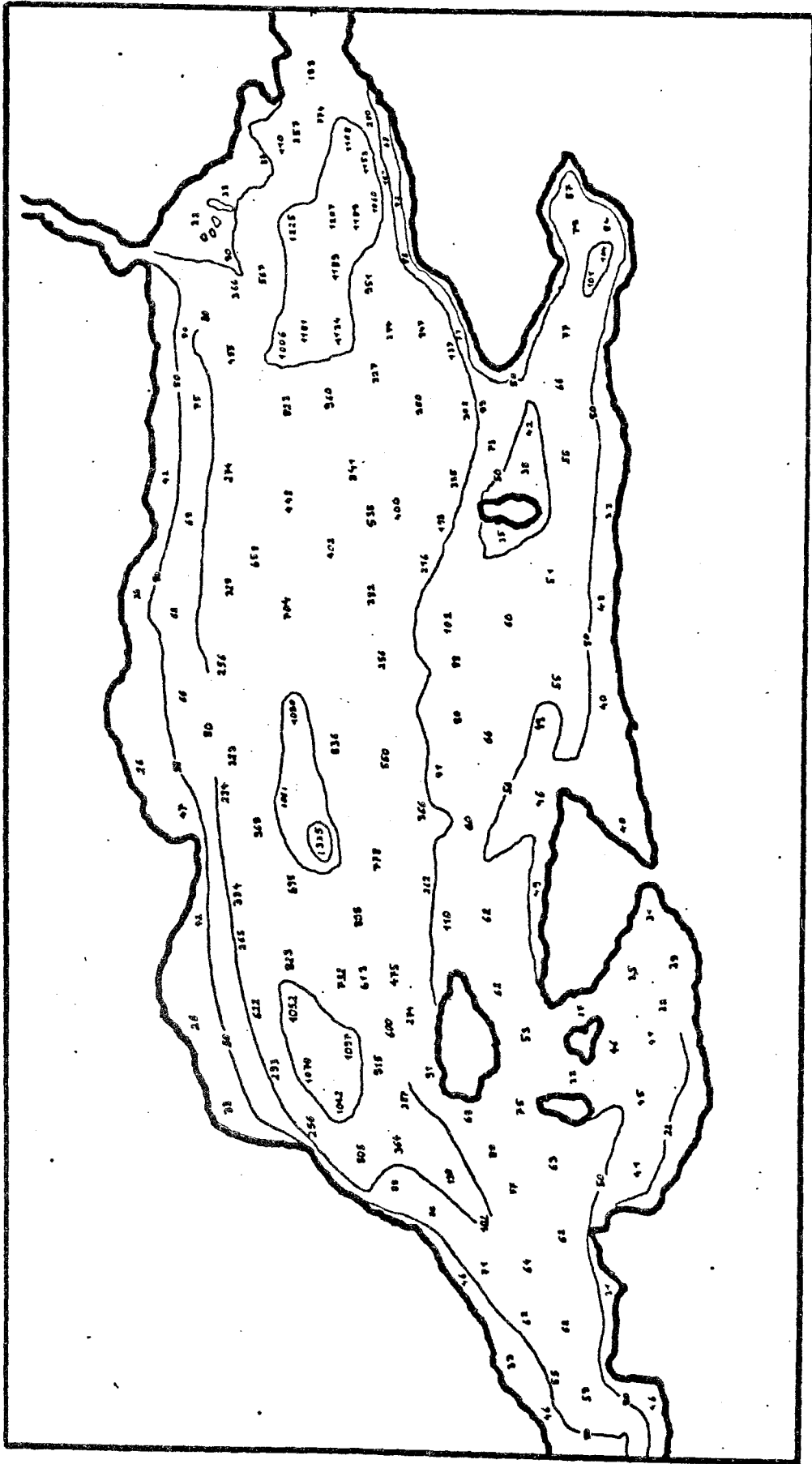


Fig.42. Bathymetric map of the Marmara Sea

meters.

The Marmara Sea basin is thought to be an extension of the North Anatolian fault line. The depression forming the basin stretches from the Sapanca lake to the east to the Saros bay in the Aegean Sea.

The sea is relatively young, having attained its present shape in the Quarternary period. It is thought to be a remnant of the great Sarmatian Sea of the Miocene epoch (İnandık⁽³²⁾). The Bosphorus and Dardanelles Straits are believed to be drowned river valleys. In its geological history, the Marmara Sea has been repeatedly flooded by the Mediterranean Sea, the most recent flooding occurring after the last glacial period.

The bottom of the sea is little investigated. Only in a few places have sediment analyses been made. A sediment cover of 1700 meters thickness is present which sits above carbonate rocks, tuff and clay. The layered sediment cover with alternating fresh and salt water fossil species reveals the evidence of the repeated floodings of the sea by the Mediterranean Sea and the interaction with the relatively fresh Black Sea during the interflooding periods. The recent sediments laid down after the last flooding consist of mud and are rich in foraminifera skeletons.

4.2. Physical Oceanography of the Marmara Sea

The Marmara Sea is a small inland sea having access to two larger sea basins, the Mediterranean Sea and the Black

Sea. It is the interaction with these two seas that gives the Marmara Sea unique characteristics, the most important one being the layered structure.

There exists a water exchange between the Mediterranean Sea and the Black Sea. The Black Sea, due to the excess of precipitation and river run-off over evaporation, has surplus water in the amount of around $300 \text{ km}^3/\text{year}$ ⁽²³⁾. The excess water is lost, as a result of sea level differences, through the straits and the Marmara Sea to the Mediterranean Sea as a surface current. But the loss is higher than the excess amount. The deficiency is compensated for by an undercurrent from the Mediterranean Sea by the same route.

⁽²³⁾ Sümer and Bakioğlu have found out, in their model of the Bosphorus Strait, that the loss from the Black Sea amounts to $620 \text{ km}^3/\text{year}$. In their model, they calculated the supply of Mediterranean water to the Black sea by the undercurrent to be around $230 \text{ km}^3/\text{year}$. Close values are obtained by solving salt and mass balance equations for the Black Sea.

There is some controversy on the behavior of the underflow. It is claimed that the undercurrent does not always reach the Black Sea, but mixes with the surface flow. It is argued that a sill in the northern entrance of the Bosphorus Strait forces the undercurrent to rise and mix with the surface waters. Moreover, strong northerly winds, driving the upper layer to high speeds, may even cause the lower layer to cease to flow and even return ⁽³³⁾.

There is a lack of knowledge about the behavior of this

complex water exchange pattern. The existence of Mediterranean waters below hundred meters in the Black Sea has been confirmed by surveys⁽³⁴⁾. But the seasonal variations in the discharges of both flows have not yet been adequately examined. The currents of the Dardanelles Strait, are, to a few surface current values, unknown. The currents of the Marmara Sea are also very little investigated. Apart from a detailed survey, conducted for the Gemlik bay⁽³⁵⁾, adequate circulation studies are missing.

4.2.1 Vertical Distribution of Water Characteristics in the Marmara Sea

As mentioned above, the Marmara Sea serves as a link between the Black Sea and the Mediterranean Sea. Like in the straits, there exists a two-layer circulation pattern in the sea. The upper few ten meters are occupied by fresh and cool Black Sea water, succeeded by an intermediate layer of a maximum thickness of 25 meters. The remaining bottom layer is occupied by Mediterranean water, being relatively warmer and saline. Figure 4.3. shows the layering in the sea.

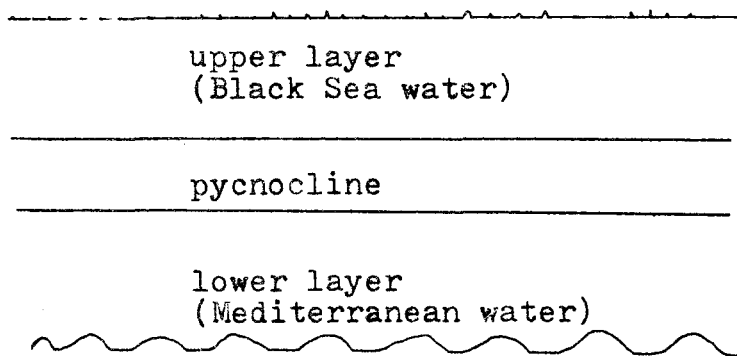


Fig. 4.3 Layering in the Marmara Sea

To get a more clear picture of the layering or stratification, the results of a field survey conducted by the Department of Navigation, Hydrography and Oceanography, a state authority, at 25 stations over the Marmara Sea in February, 1982, will be examined ⁽³⁶⁾. During the survey, at all stations, temperature and salinity measurements have been made at various depths. The stations were positioned as on Figure 4.4. on the next page.

Data gathered at all stations is given in Appendix I. In this chapter, results of measurements taken at station 18 will be examined.

Station 18 is situated between Hoşköy on the Thracian coast and the Marmara island. The depth at the station is 140 meters. Measurements of temperature and salinity have been made at the surface and at six depths (10, 20, 30, 50, 75 and 100 meters below sea surface). Table 4.2. displays the results.

Table 4.2. Temperature and salinity at station 18

Depth (m)	Temperature (C)	Salinity (ppt)
0	7.28	24.583
10	7.21	24.570
20	6.82	24.879
30	7.18	24.930
50	15.21	38.271
75	15.21	38.506
100	14.80	38.535

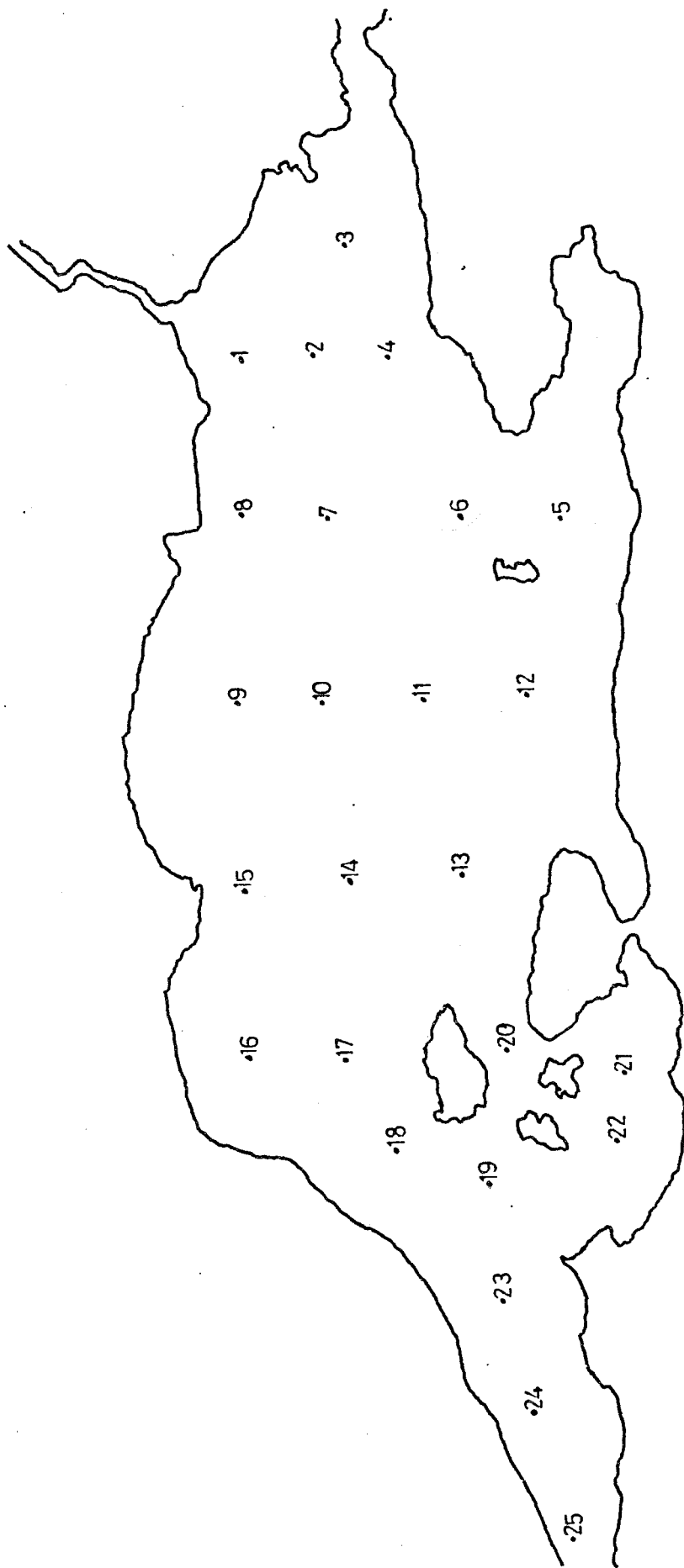


Fig. 44. Oceanographical stations in the Marmara Sea

Clearly visible from the table are the increases in both temperature and salinity between 30 and 50 meters. The temperatures for the first 30 meters are around 7 degrees C. At 50 meters one encounters a temperature of 15.21 C and afterwards no appreciable change down to 100 meters. Likewise the salinities. In the upper 30 meters, the salinity remains at 24 ppt. At 50 meters, a value of 38.271 ppt is recorded which then remains much the same down to 100 meters.

These values enable one to distinguish between two separate water masses. The upper 30 meters are occupied by a relatively fresh and cool water body with temperatures around 7 degrees C and salinities of about 24 ppt. After 50 meters and down to the bottom, a distinct water mass is observed with temperatures of 15 C and salinities of 38 ppt.

The upper layer is the layer occupied by Black Sea water. The bottom layer is occupied by Mediterranean water which is heavier, thus remaining below. These two water masses are separated by an intermediate layer where a steep gradient in both temperature and salinity is encountered. It is both a thermocline and a halocline.

If one looks at densities, the same picture emerges. Table 4.3. on the next page displays the distribution of density along the depth.

The upper 30 meters are occupied by light water of density 1019 kg/m^3 . Below 50 meters, the heavy Mediterranean waters have a density around 1028 kg/m^3 . Between 30 and 50 meters, in the intermediate layer, there is a region of a sharp density gradient, a pycnocline (Figure 4.5.)

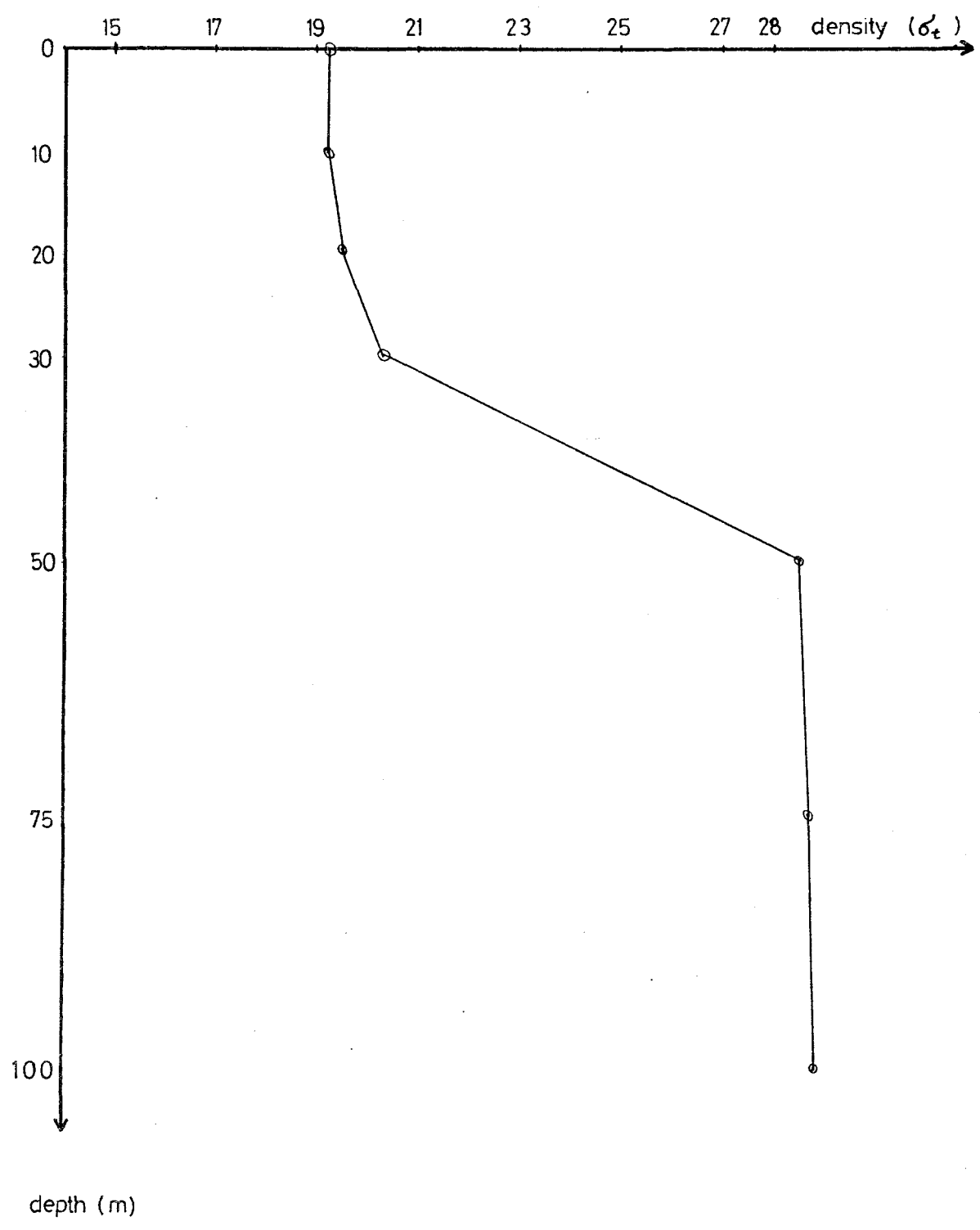


Fig 4 5 Density profile at station 18

Table 4.3. Density versus depth at station 18

Depth (m)	Density (kg/m ³)
0	1019.23
10	1019.23
20	1019.52
30	1020.38
50	1028.46
75	1028.64
100	1028.76

It is clear from the picture that the increase in density is a result of the increase in salinity. The increase in temperature does not affect the density as much as the salinity does. In fact, an increase in temperature lowers the density. Roughly, density decreases by 1 kg/m³ for a change of +5 degrees C, but increases by the same amount for a change of +1 ppt in salinity. Thus the density lowering effect of the temperature is greatly offset by the large increase in salinity.

This layering is encountered all over the Marmara Sea where depths exceed 50 meters. In areas shallower than 50 meters, the lower layer is either very thin or indistinguishable from the pycnocline.

In the upper layer, the temperatures and salinities increase with depth, although not comparably with the sharp gradients in the pycnocline. This suggests a transport of salt and heat from the lower layer, which but is limited. The

upward flux of heat and salt is largely hindered by the pycnocline.

The thickness of the intermediate layer changes from station to station, as well as the gradient. The minimum depth at which the pycnocline begins is 17 meters below surface at station 3, and 30 meters below surface at stations 8 and 18. Maximum thickness is attained at station 6 with 29 meters.

This variability in layer thicknesses makes it difficult to determine even the near exact location of the pycnocline. As the upper layer is considerably thin, external effects on it will easily be felt by the pycnocline, such as strong winds. Increased turbulence in the upper layer, caused by wind stirring, will erode the intermediate layer and entrain it.

The above conditions apply only for winter as the survey was conducted in February over a span of 3 days. It is not known how the profiles look like in other seasons or whether the stratification is stable throughout the year. However, some qualitative conclusions may be drawn.

It is the temperature that shows significant variations seasonally. The salinity distribution is not much affected by climatic conditions. This has been verified by the survey conducted in the Gemlik bay ⁽³⁵⁾. It has been found out, that although temperatures show a wide range of values yearly (6 C in winter, 23-25 C in summer), salinities do not change significantly. Furthermore, the survey has shown that the pycnocline is present throughout the year, changing only

in thickness, being two or three meters thicker in winter. Thus the stratification is stable throughout the year.

Although it has not yet been verified by surveys, the same situation may be assumed for the Marmara Sea. As the salinities do not change significantly throughout the year, the stratification may be regarded as stable the whole year.

4.2.2. Horizontal Distribution of Water Characteristics in the Marmara Sea

The horizontal distribution of surface temperatures throughout the Marmara Sea is nearly homogeneous, both in winter and in summer. There is only a change of 1-2 C between the straits. For the lower layer, only winter values are available and these show almost no change. Thus it can be concluded that the Mediterranean water passes the Marmara Sea without any significant loss of heat.

The horizontal salinity distribution shows some differences. Salinity increases as one moves from the Bosphorus Strait to the southwest. This shows that there is a flux of salt from the lower layer to the upper layer. (37) Pickard states that the water leaving the Black Sea with a salinity of 16 ppt reaches the Mediterranean Sea with a salinity of 30 ppt. The underflow, leaving the Mediterranean Sea with a salinity of 38 ppt, has it reduced to 35 to 30 ppt by the time it reaches the Black Sea. Pickard concludes that much of the mixing takes place along the straits due to high current shear and turbulence as a result of the narrowness of

these passages.

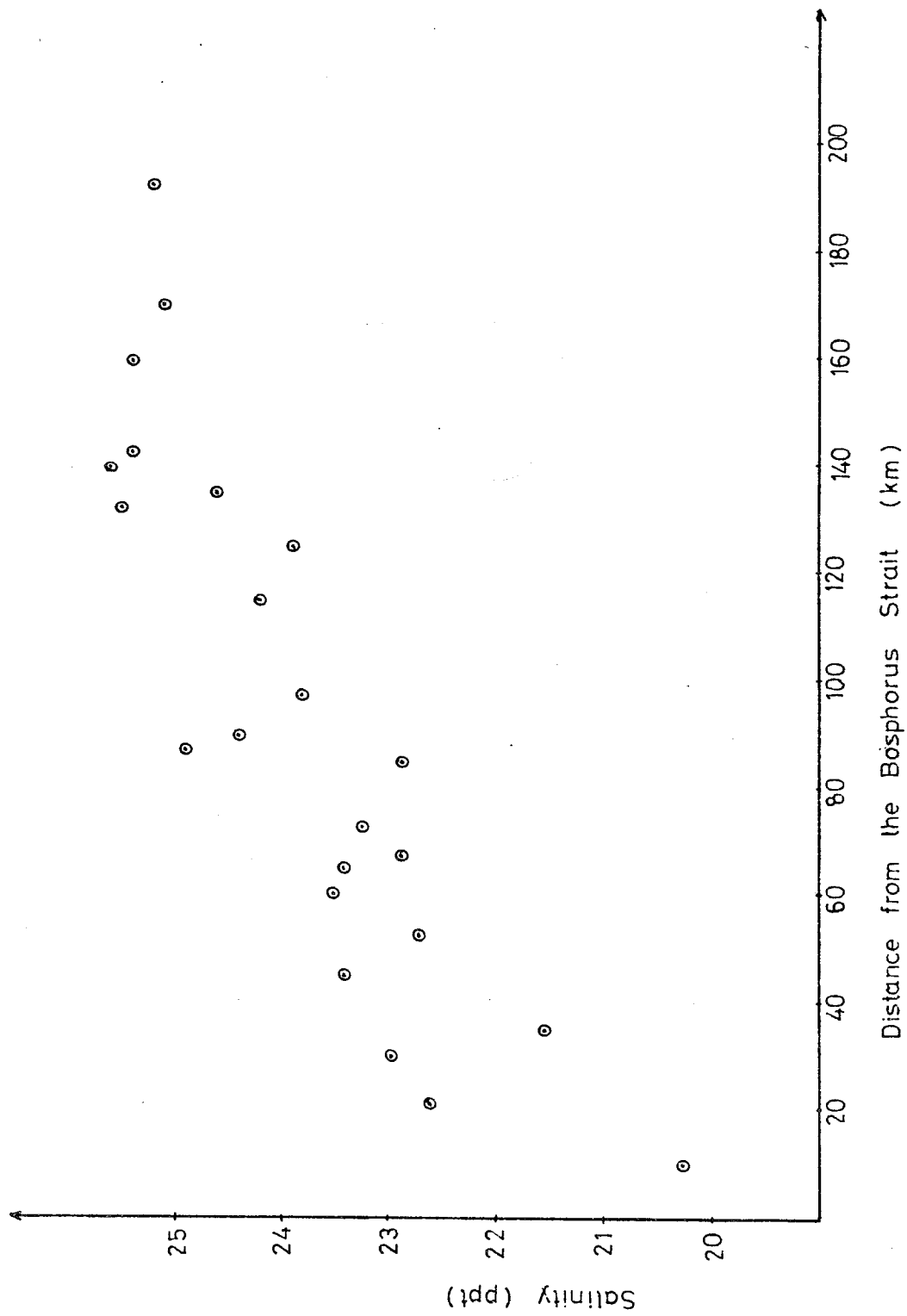
A plot of the change in surface salinities with increasing distance from the Bosphorus Strait will indicate the extent of mixing occurring in the Marmara Sea (Figure 4.6. on the next page).

The figure clearly shows the increase in salinity with increasing distance from the Bosphorus Strait. Considering two stations which are furthest apart from each other (stations 1 and 25), the increase in salinity is 5 ppt in 182 kilometers or 0.027 ppt/km. If it is assumed that the increase in salinity of Black Sea water is 4 ppt along the 35 kilometers while flowing through the Bosphorus Strait, a rate of 0.11 ppt/km is obtained. The rate of increase of salinity along the Dardanelles Strait comes out to be 0.08 ppt/km . These are rough values but it may be concluded that the straits contribute to much of the mixing of the layers (around 87%) and there is considerably less mixing in the Marmara Sea.

In contrast to the horizontal salinity gradient in the upper layer, the salinity of the lower layer does not change along the route in the Marmara Sea. The salinities are all around 38 ppt.

4.2.3. Stability of the Layering

As mentioned in the previous chapter, the stability of the layering in a hydrodynamical system may be analyzed by the dimensionless densimetric Froude number (eq. 3.1).



Assigning the following values to the variables in the expression

$$u_1 = 0.1 \text{ m/sec}$$

$$u_2 = 0.05 \text{ m/sec}$$

$$\rho_1 = 1019.28 \text{ kg/m}^3$$

$$\rho_2 = 1028.65 \text{ kg/m}^3$$

$$h_1 = 25 \text{ meters}$$

$$h_2 = 300 \text{ meters}$$

the densimetric Froude number comes out to be 8×10^{-5} . This number is far less than one, so the flow is subcritical. Here h_2 is taken to be the mean thickness of the lower layer. There are coastal regions where the lower layer attains thicknesses less than 20 meters. Even in such cases the Froude number is less than unity.

V. THE MODEL

5.1. Basic Assumptions

Considering the stratified flow pattern prevailing in the Marmara Sea, a two-layer, two-dimensional, depth-averaged transient model has been constructed. In formulating the governing equations, the following assumptions have been made.

i) Vertical accelerations are small enough compared to the gravitational acceleration and are neglected.

ii) For each layer, flow properties do not change over the flow depth.

These are the underlying assumptions for depth-averaged models. As discussed in chapter 2, the first assumption enables one to drop the equation of motion in the vertical direction. The second assumption allows the integration of the equations over the flow depth, obtaining depth-averaged variables and equations. Thus the support of the system is reduced to two dimensions by eliminating the vertical coordinate and velocity component.

iii) The intermediate layer is assumed to have no thickness. The layers are separated by an interface.

Each two layer system has an intermediate region between

the layers as outlined in chapter 3. In some systems, this layer has a thickness comparable with those of the others. In numerical modeling of stratified flows, however, this intermediate layer is defined to be an interface of zero thickness ⁽¹⁾. Otherwise, it would be necessary to employ a three-layer model with appropriate equations to describe motion in the intermediate region. These equations would necessarily be 3-D because of the sharp density gradient in the layer. Very little is known about the dynamic behavior of these regions and up to now only one numerical model has been developed to simulate flow conditions in the intermediate layers. ⁽³⁸⁾ Davies developed a 3-D model of a stratified sea by employing the variation of the eddy viscosity in the vertical direction. His model, however, requires accurate knowledge about the eddy viscosity profile which is very limited. Davies, in his calculations, used arbitrary eddy viscosity profiles the applicability of which is quite doubtful.

iv) It is assumed that there is no transport of heat, salt or water between the layers across the interface. Only momentum exchange is allowed.

This last assumption leads to the neglectance of interfacial mixing. The fluxes of salt and heat across the interface are never known exactly as it is very difficult to measure them, even in laboratory experiments. In numerical models, the use of the mixing concept necessitates the introduction of new variables and equations, besides ⁽¹⁾ diffusion coefficients. For the Marmara Sea, the

interfacial mixing is assumed to be negligible. There are indications that there is some mixing, but its magnitude is unknown. Rough estimates, as discussed in chapter 4, however, indicate that mixing is kept at low levels by the intermediate layer acting as a barrier and the neglectance is justified.

5.2. Governing Equations

Figure 5.1 displays the variables used in the equations of the model.

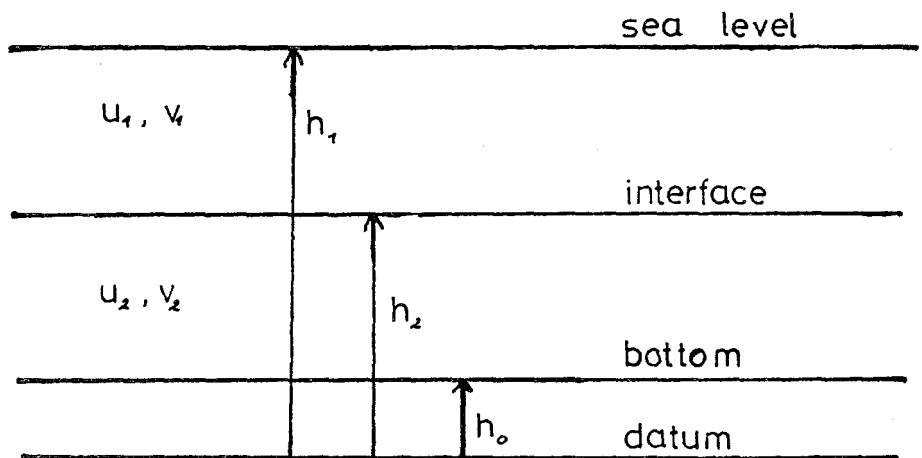


Fig 5.1. Variables used in the equations

The subscripts for the velocities u and v denote layers (1 for the upper layer, 2 for the lower layer). h_1 is the sea level elevation, h_2 the interfacial elevation and h_0 the bottom elevation. The datum has been chosen to be 1400 meters below mean sea level. All elevations are computed relative to

this fixed reference plane. The coordinate system employed is Cartesian coordinates with x being the longitudinal and y the latitudinal direction. t in the equations denotes time.

The equations are as follows.

Upper layer

The equation of continuity

$$\begin{aligned} \frac{\partial h_1}{\partial t} - \frac{\partial h_2}{\partial t} + \frac{\partial u_1}{\partial x}(h_1 - h_2) + u_1\left(\frac{\partial h_1}{\partial x} - \frac{\partial h_2}{\partial x}\right) \\ + \frac{\partial v_1}{\partial y}(h_1 - h_2) + v_1\left(\frac{\partial h_1}{\partial y} - \frac{\partial h_2}{\partial y}\right) = 0 \end{aligned} \quad (5.1)$$

The equation of motion (longitudinal direction)

$$\begin{aligned} \frac{\partial u_1}{\partial t} + u_1\frac{\partial u_1}{\partial x} + v_1\frac{\partial u_1}{\partial y} - fv_1 + g\frac{\partial h_1}{\partial x} \\ - \frac{T_{wx}}{\rho_1(h_1 - h_2)} + \frac{T_{ix1}}{\rho_1(h_1 - h_2)} = 0 \end{aligned} \quad (5.2)$$

The equation of motion (lateral direction)

$$\begin{aligned} \frac{\partial v_1}{\partial t} + u_1\frac{\partial v_1}{\partial x} + v_1\frac{\partial v_1}{\partial y} + fu_1 + g\frac{\partial h_1}{\partial y} \\ - \frac{T_{wy}}{\rho_1(h_1 - h_2)} + \frac{T_{iy1}}{\rho_1(h_1 - h_2)} = 0 \end{aligned} \quad (5.3)$$

Lower layer

The equation of continuity

$$\begin{aligned} \frac{\partial h_2}{\partial t} + \frac{\partial u_2}{\partial x}(h_2 - h_0) + u_2\left(\frac{\partial h_2}{\partial x} - \frac{\partial h_0}{\partial x}\right) \\ + \frac{\partial v_2}{\partial y}(h_2 - h_0) + v_2\left(\frac{\partial h_2}{\partial y} - \frac{\partial h_0}{\partial y}\right) = 0 \end{aligned} \quad (5.4)$$

The equation of motion (longitudinal direction)

$$\begin{aligned} \frac{\partial u_2}{\partial t} + u_2 \frac{\partial u_2}{\partial x} + v_2 \frac{\partial u_2}{\partial y} - fv + g \frac{\rho_1}{\rho_2} \cdot \frac{\partial h_1}{\partial x} + g \frac{(\rho_1 - \rho_2)}{\rho_2} \cdot \frac{\partial h_2}{\partial x} \\ + \frac{T_{bx}}{\rho_2(h_2 - h_0)} + \frac{T_{ix2}}{\rho_2(h_2 - h_0)} \neq 0 \end{aligned} \quad (5.5)$$

The equation of motion (lateral direction)

$$\begin{aligned} \frac{\partial v_2}{\partial t} + u_2 \frac{\partial v_2}{\partial x} + v_2 \frac{\partial v_2}{\partial y} + fu_2 + g \frac{\rho_1}{\rho_2} \cdot \frac{\partial h_1}{\partial y} + g \frac{(\rho_1 - \rho_2)}{\rho_2} \cdot \frac{\partial h_2}{\partial y} \\ + \frac{T_{by}}{\rho_2(h_2 - h_0)} + \frac{T_{iy2}}{\rho_2(h_2 - h_0)} = 0 \end{aligned} \quad (5.6)$$

The equations are based on the Eulerian equations of motion and continuity (Pond and Pickard⁽³⁹⁾). Liu and Leendertse⁽¹⁾ presented the same equations, with no convective terms however, and a combined friction factor. Lai⁽⁶⁾ presents 1-D equations with convective terms.

ρ_1 and ρ_2 are the densities of the upper and lower layers respectively. They have been obtained from the tables in Appendix I. as $\rho_1 = 1019.28 \text{ kg/m}^3$ and $\rho_2 = 1028.65 \text{ kg/m}^3$. The gravitational acceleration g has the value of 9.81 m/s^2 .

f in the equations represents the Coriolis coefficient. Its value depends on latitude, being zero at the equator and attaining its maximum value at the poles. For small distances, the latitudinal variation is small to be negligible and the coefficient is assumed to be constant. For the Marmara Sea, this coefficient has been computed from the equation below (McLellan⁽⁴⁰⁾).

$$f = 2.\Omega.\sin\theta \quad (5.7)$$

where

Ω = angular velocity of the earth

θ = latitude

Ω is 0.729×10^{-4} sec and for the Marmara Sea, the latitude has been taken to be $40^{\circ} 41'$. Using these values, the Coriolis coefficient comes out to be 10^{-4} sec.

5.3. Shear Stresses

T_w, T_i, T_b represent shear or tangential forces. In this model, they have been formulated as quadratic expressions.

5.3.1. Wind Stress

Wind is a primary driving force of currents. Wind, blowing over the sea surface transfers momentum and energy to the water. It acts both tangentially and normal to the sea surface but the tangential (shear) action is much larger than the normal one.

The wind stress acting on the sea surface is formulated as follows (Safaie⁽⁴¹⁾).

$$T = \rho_a \cdot C(z) \cdot V(z)^2 \quad (5.8)$$

where

ρ_a = mass density of air

$C(z)$ = wind stress coefficient

$V(z)$ = wind speed at height z above water surface

It is convenient to fix the height to ten meters and in evaluating the wind stress, the velocity of the wind is determined at ten meters above sea-level. The wind stress coefficient is found empirically (Wu⁽⁴²⁾, Safaie⁽⁴¹⁾). In this model, the value of the coefficient has been taken from Safaie⁽⁴¹⁾ as

$$C(10) = 5.2 \times 10^{-4} \cdot V(10)^{0.44} \quad (5.9)$$

Inserting this value into equation 5.8. and using the value 1.29 kg/m^3 for the density of air, the wind stress becomes

$$T = 6.7 \times 10^{-4} \cdot V^{2.44} \quad (5.10)$$

This vector is decomposed into its components as follows.

$$T_{wx} = 6.7 \times 10^{-4} \cdot V^{2.44} \cdot \sin \theta \quad (5.11)$$

$$T_{wy} = 6.7 \times 10^{-4} \cdot V^{2.44} \cdot \cos \theta$$

where θ is the angle between the wind vector and the y-axis.

5.3.2. Interfacial Stress

In stratified flows, layers usually have different velocities. This difference gives rise to interfacial shear. Several studies have been made in this field, a classical treatment being that of Macagno and Rouse⁽³⁰⁾. Abraham et

(28)
 al found that the interfacial shear varies with the stage of development of the intermediate layer and that it is affected by turbulence generated at the interface and at the bottom. They proposed a quadratic expression for the shear as

$$T_i = K_i \cdot \rho_m \cdot (u_2 - u_1)^2 + \frac{h_1}{h_1 + h_2} K_b \cdot \rho_m \cdot u_2^2 \quad (5.12)$$

where

u_1, u_2 = velocities of upper and lower layers respectively

ρ_m = mean density

h_1 = thickness of upper layer

h_2 = thickness of lower layer

K_i, K_b = shear stress coefficients

The first term in equation 5.12 is the contribution of the interfacial turbulence and the second term the contribution of turbulence generated at the bottom. For the coefficients, the values of 4×10^{-4} and $(11 \text{ to } 12) \times 10^{-4}$ were proposed, for K_i and K_b respectively.

(20)
 Hodgins et al in their model of the Fraser estuary, used also a quadratic formulation. They used an amplification factor, equal to the densimetric Froude number to render the stress more sensitive to the velocity shear.

In this model for the Marmara Sea, the following expression has been employed.

$$T_{im} = K_i \cdot \rho_m \cdot (u_2 - u_1) \cdot |u_2 - u_1| \quad (5.13)$$

where $m=1,2$ for upper and lower layers respectively and K_i is the interfacial friction coefficient.

The value of the interfacial friction coefficient is

difficult to determine. All measurements rely on laboratory experiments and their applicability to real hydrodynamical systems is doubtful. Dermisis and Partheniades⁽³¹⁾, in laboratory experiments, have found out that the interfacial friction coefficient is best correlated with the number RF where R and F are the Reynolds and Froude numbers respectively, and with the relative density difference between the layers.

In the model of the Marmara Sea, the value suggested by Abraham et al⁽²⁸⁾ as 4×10^{-4} has been adopted. The contribution of bottom turbulence has been neglected as the lower layer is relatively thick over most of the Marmara Sea. It has been found out that varying this coefficient between 1×10^{-3} and 1×10^{-4} had no effect on the results. Neglecting the stress did also not create significant differences. Scaling the equations showed that the interfacial stress term contributed little to the equations. It is however included in the following manner.

$$\begin{aligned} T_{ixm} &= \rho_m \cdot 4 \times 10^{-4} \cdot (u_2 - u_1) \cdot (u_m^2 - v_m^2)^{0.5} \\ T_{iym} &= \rho_m \cdot 4 \times 10^{-4} \cdot (v_2 - v_1) \cdot (u_m^2 - v_m^2)^{0.5} \end{aligned} \quad (5.14)$$

where $m=1,2$ for upper and lower layers respectively.

5.3.3. Bottom Stress

The bottom stress or the shear force acting on the fluid as a result of its drag over the bottom has been formulated according to Yenigün⁽⁴³⁾ as

$$T_{bx} = \rho_2 \cdot g \cdot u_2 \cdot (u_2^2 - v_2^2)^{0.5} / C^2 \quad (5.15)$$

$$T_{by} = \rho_2 \cdot g \cdot v_2 \cdot (u_2^2 - v_2^2)^{0.5} / C^2$$

where C is the Chezy coefficient.

The Chezy coefficient may be obtained from the Manning coefficient (Chow⁽⁴⁴⁾). The Manning coefficient is, however, mainly used for open channel flows. For the model the Chezy coefficient has been adopted from Dronkers⁽¹⁰⁾ as

$$C = 50 \text{ m}^{1/2} / \text{sec}$$

VI. THE NUMERICAL METHOD

6.1. Finite Difference Methods

Finite difference methods (explicit and implicit) have been widely used for the numerical solution of the equations describing fluid flow. Liu and Leendertse⁽¹⁾ have given a detailed description of implicit and explicit methods applied to estuaries and coastal seas. Dronkers⁽¹⁰⁾ has discussed several finite difference schemes for tidal computations in rivers and coastal areas. Flather and Heaps⁽¹¹⁾ in their model of the Morecambe bay have developed a finite difference method in which they accounted for the emergence and submergence of shallow areas in the bay (drying nodes). In their approach to modeling circulation in depth-averaged flow, Ponce and Yabusaki⁽⁵⁾ have employed a mixed scheme, where the continuity and x-momentum equations were solved implicitly and the y-momentum equation was solved explicitly. An up-to-date review of the application of finite difference methods, particularly to open-channel flows, may be found in Lai⁽⁶⁾ where several implicit and explicit schemes are thoroughly discussed.

In models of stratified flows, finite difference methods have been applied in most cases. Grubert and

(17)
 Abbott utilized an implicit finite difference scheme and a double sweep algorithm to solve their 1-D equations. Hodgins et al (20) for their model of the Fraser River estuary, (24) employed explicit central differences. Yin and Chen also employed explicit finite differences to compute tidal currents in the Taiwan Strait.

The criteria for choosing between explicit or implicit schemes depend on the characteristics of the model and on the capabilities of the computer used. To achieve accuracy and stability is of primary concern in choosing a scheme.

Implicit finite difference schemes are unconditionally stable. They, however, consume large computer storage and time and may be uneconomical in some cases. Explicit schemes do not require that much computer storage and time. They are also easier to construct and to code. However, explicit schemes are vulnerable to instabilities and are restricted in the time increment used.

For the numerical model of the Marmara Sea, an explicit finite difference scheme was adopted. The particular scheme (12,13) was developed by Gunn and Yenigün and was successfully used in modeling tidal motion in two separate estuaries. A nonstaggered computational grid was adopted where all variables were evaluated at the centers of the grid boxes. Slip boundary conditions were employed at land boundaries.

6.2. The Computational Grid

In finite difference methods, the aim is to compute flow properties, e.g. velocities and elevations, at prescribed points over the modeled area by constructing a computational grid. The grid for the Marmara Sea is given in Figure 6.1 on the next page.

The grid consists of squares, each with a side length of 5000 meters. Every square or node is designated by two integers which define its location. The index i corresponds to the x-coordinate in the equations, whereas the index j stands for the y coordinate. The origin is located in the lower left corner of the grid.

Two types of nodes make up the grid.

i) Dry nodes are land nodes where no computations are carried out for the velocities and elevations.

ii) Wet nodes are those where velocities and elevations are computed from the equations. Three such types of nodes are recognized.

a) Open sea nodes are those which do not have a dry node adjacent to them in the cardinal directions.

b) Land boundary nodes have a dry node adjacent to them in one or more cardinal direction.

c) Boundary condition nodes are those at which boundary conditions for velocities and elevations are specified.

6.3. The Differencing Scheme for Spatial Derivatives

To approximate the spatial derivatives by finite

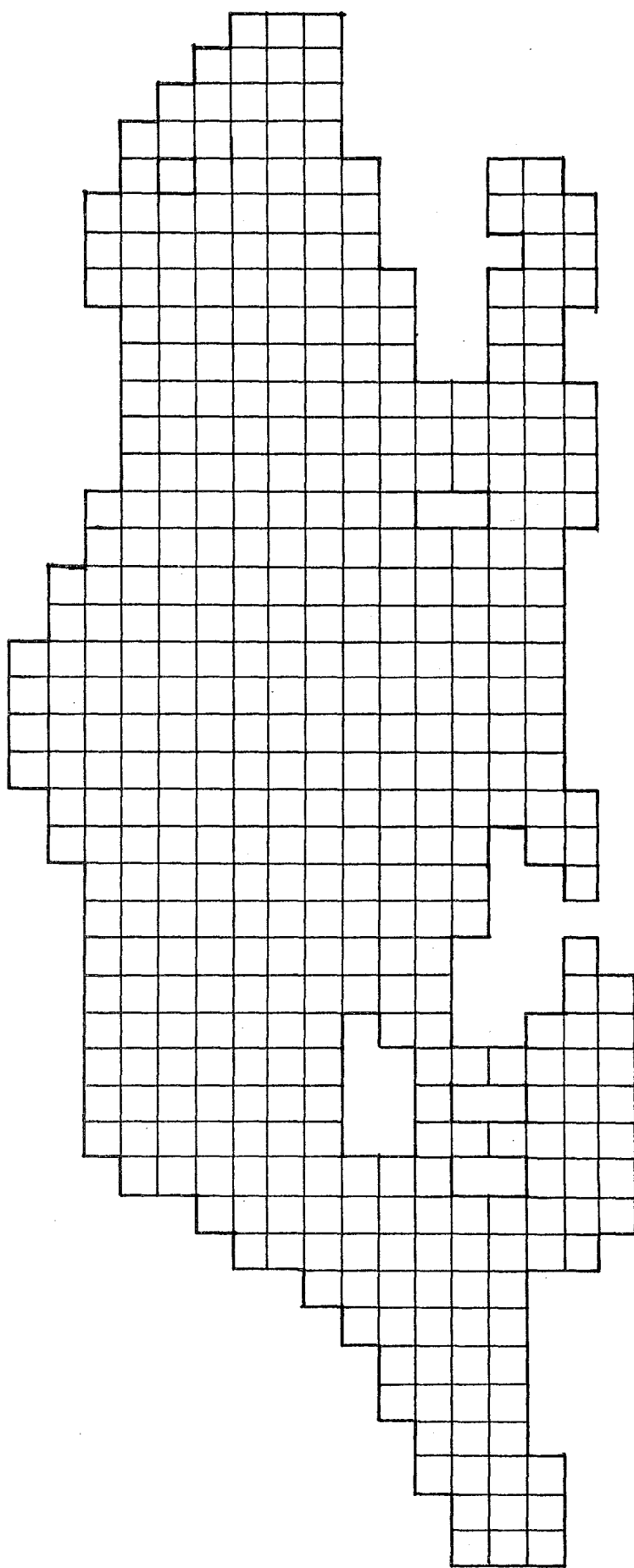


Fig. 61. The Computational Grid

differences, central differencing which yields second order accuracy was adopted. The finite difference forms of the derivative of the property q (which is velocity or elevation at node (i,j)) with respect to the spatial directions x and y are

$$\frac{dq}{dx} = (q_{i-1,j} - q_{i+1,j}) / 2\Delta x \quad (6.1)$$

$$\frac{dq}{dy} = (q_{i,j-1} - q_{i,j+1}) / 2\Delta y$$

where x and y are spatial increments.

Thus the derivative of a property at a node i,j is expressed by the difference of the values of the property at the two adjacent nodes divided by twice the spatial increment. For the nodes at land boundaries, a different approach is used, the slip boundary conditions which will be described in section 6.6 .

6.4. The Representation of the Temporal Derivatives :

The Local Integral Method

In the representation of the temporal derivatives by finite differences, a local integral method was used. The method was developed by Gunn and Yenigün is given in Gunn and Yenigün⁽¹²⁾ and Yenigün⁽⁴³⁾ .

The temporal derivatives are approximated at first by a forward difference.

$$\frac{dq}{dt} = \frac{q^{n+1} - q^n}{\Delta t} \quad (6.2)$$

where n is the time level and Δt the time increment.

Then, the lower time value of q (q^n) is expressed as a local integral and the derivative takes the following form

$$\frac{dq}{dt} = \left(q^{n+1} - \frac{1}{2\Delta s} \int_{I-1}^{I+1} q^n ds \right) / \Delta t \quad (6.3)$$

where s is a spatial direction (x or y), Δs a spatial increment (x or y) and I stands for i or j .

The purpose of this local integral is to reduce round-off and truncation errors in the numerical integration (Yenigun⁽⁴³⁾). Further discretization of the local integral yields the following finite difference form for the temporal derivative

$$\frac{dq}{dt} = \left(q_I^{n+1} - \frac{1}{A+2} (q_{I+1}^n + Aq_I^n + q_{I-1}^n) \right) / \Delta t \quad (6.4)$$

Here A is a parameter which defines the particular formula for integration.

The local integral method has been employed in the models for the Milford Haven and Tay estuaries (12,13,43). It has been found out that the parameter A had a strong relationship to the time increment (t) employed. For every fixed time increment t , there is a maximum value of A (A_{\max}) beyond which the solutions of the equations tend to be unstable. Furthermore the choice of A affects the accuracy of the solutions. It has been found out that the greatest accuracy was achieved by the value of A at its stability limit (A_{\max}).

This local integral method with its properties of

controlling round-off and truncation errors and improving accuracy was used for the discretization of the temporal derivatives in the model of the Marmara Sea.

6.5. The Finite Difference Equations

In the explicit finite difference method, the values of a property at a time step is computed from known values of the previous time step. In this model, a time splitting procedure is employed (Yenigün⁽⁴³⁾, Roache⁽⁴⁵⁾). The iterations are carried out in two half time steps. In the first half-time step, intermediate values are computed from known values of the properties at the previous time step n . Integration is carried out only in the x -direction. The explicit formulations are as follows:

First half-time step $n+1/2$

$$\begin{aligned}
 h_{1,i,j}^{n+1/2} &= \left(\frac{\Delta t}{A+2} \right) (h_{1,i+1,j}^n + Ah_{1,i,j}^n + h_{1,i-1,j}^n) - \\
 &\left(\frac{\Delta t}{2\Delta x} \right) (h_{1,i,j}^n - h_{2,i,j}^n) (u_{1,i+1,j}^n - u_{1,i-1,j}^n) - \\
 &\left(\frac{\Delta t}{2\Delta x} \right) u_{1,i,j}^n (h_{1,i+1,j}^n - h_{1,i-1,j}^n - h_{2,i+1,j}^n - h_{2,i-1,j}^n)
 \end{aligned}
 \tag{6.4}$$

$$\begin{aligned}
u_{1,i,j}^{n+1/2} &: \left(\frac{\Delta t}{A+2} \right) (u_{1,i+1,j}^n + Au_{1,i,j}^n + u_{1,i-1,j}^n) - \\
&\left(\frac{\Delta t}{2\Delta x} \right) u_{1,i,j}^n (u_{1,i+1,j}^n - u_{1,i-1,j}^n) - \\
&\left(\frac{\Delta t}{2\Delta x} \right) u_{1,i,j}^n g (h_{1,i+1,j}^n - h_{1,i-1,j}^n) \quad (6.5)
\end{aligned}$$

$$\begin{aligned}
v_{1,i,j}^{n+1/2} &: \left(\frac{\Delta t}{A+2} \right) (v_{1,i+1,j}^n + Av_{1,i,j}^n + v_{1,i-1,j}^n) - \\
&\left(\frac{\Delta t}{2\Delta x} \right) u_{1,i,j}^n (v_{1,i+1,j}^n - v_{1,i-1,j}^n) \quad (6.6)
\end{aligned}$$

$$\begin{aligned}
h_{2,i,j}^{n+1/2} &: \left(\frac{\Delta t}{A+2} \right) (h_{2,i+1,j}^n + Ah_{2,i,j}^n + h_{2,i-1,j}^n) - \\
&\left(\frac{\Delta t}{2\Delta x} \right) (h_{2,i,j}^n - h_{0,i,j}^n) (u_{2,i+1,j}^n - u_{2,i-1,j}^n) - \\
&\left(\frac{\Delta t}{2\Delta x} \right) u_{2,i,j}^n (h_{2,i+1,j}^n - h_{2,i-1,j}^n - h_{0,i+1,j}^n + h_{0,i-1,j}^n) \quad (6.7)
\end{aligned}$$

$$\begin{aligned}
u_{2,i,j}^{n+1/2} &: \left(\frac{\Delta t}{A+2} \right) (u_{2,i+1,j}^n + Au_{2,i,j}^n + u_{2,i-1,j}^n) - \\
&\left(\frac{\Delta t}{2\Delta x} \right) u_{2,i,j}^n (u_{2,i+1,j}^n - u_{2,i-1,j}^n) - \\
&\left(\frac{\Delta t}{2\Delta x} \right) g (\beta_1/\beta_2) (h_{1,i+1,j}^n - h_{1,i-1,j}^n) - \\
&\left(\frac{\Delta t}{2\Delta x} \right) g ((\beta_2 - \beta_1)/\beta_2) (h_{2,i+1,j}^n - h_{2,i-1,j}^n) \quad (6.8)
\end{aligned}$$

$$\begin{aligned}
v_{2,i,j}^{n+1/2} &= (\Delta t/A+2)(v_{2,i+1,j}^n + Av_{2,i,j}^n + v_{2,i-1,j}^n) - \\
&(\Delta t/2\Delta x)v_{2,i,j}^n (v_{2,i+1,j}^n - v_{2,i-1,j}^n) - \\
&(\Delta t/2\Delta x)g(\rho_1/\rho_2)(hh_{1,i+1,j}^n - h_{1,i-1,j}^n) - \\
&(\Delta t/2\Delta x)g((\rho_2 - 1)/\rho_2)(h_{2,i+1,j}^n - h_{2,i-1,j}^n)
\end{aligned}
\tag{6.9}$$

These intermediate values do not have any physical significance. They are used in the second half-time step, appearing in the right-hand sides of the expressions from which values for the time step $n+1$ are computed.

Second half-time step $n+1$

$$\begin{aligned}
h_{1,i,j}^{n+1} &= (\Delta t/A+2)(h_{1,i,j+1}^{n+1/2} + Ah_{1,i,j}^{n+1/2} + h_{1,i,j-1}^{n+1/2}) \\
&(\Delta t/2\Delta x)(h_{1,i,j}^{n+1/2} - h_{2,i,j}^{n+1/2})(v_{1,i,j+1}^{n+1/2} - v_{1,i,j-1}^{n+1/2}) - \\
&(\Delta t/2\Delta x)v_{1,i,j}^{n+1/2}(h_{1,i,j+1}^{n+1/2} - h_{1,i,j-1}^{n+1/2} - h_{2,i,j-1}^{n+1/2} * h_{2,i,j-1}^{n+1/2})
\end{aligned}
\tag{6.10}$$

$$\begin{aligned}
u_{1,i,j}^{n+1} &= (\Delta t/A+2)(u_{1,i,j+1}^{n+1/2} + Au_{1,i,j}^{n+1/2} + u_{1,i,j-1}^{n+1/2}) - \\
&(\Delta t/2\Delta x)v_{1,i,j}^{n+1/2}(u_{1,i,j+1}^{n+1/2} - u_{1,i,j-1}^{n+1/2}) + fv_{1,i,j}^{n+1/2} \Delta t + \\
&T_w^{n+1/2} (\Delta t)/\rho_1 (h_{1,i,j}^{n+1/2} - h_{2,i,j}^{n+1/2})
\end{aligned}$$

(cont...)

$$T_{i,1}^{n+1/2} (\Delta t) / \beta_1 (h_{1,i,j}^{n+1/2} - h_{2,i,j}^{n+1/2}) \quad (6.11)$$

$$v_{1,i,j}^{n+1} = (\Delta t / A + 2) (v_{1,i,j+1}^{n+1/2} + Av_{1,i,j}^{n+1/2} + v_{1,i,j-1}^{n+1/2}) -$$

$$(\Delta t / 2\Delta y) v_{1,i,j}^{n+1/2} (v_{1,i,j+1}^{n+1/2} - v_{1,i,j-1}^{n+1/2}) - fu_{1,i,j}^{n+1/2} \Delta t -$$

$$T_w^{n+1/2} (\Delta t) / \beta_1 (h_{1,i,j}^{n+1/2} - h_{2,i,j}^{n+1/2}) -$$

$$T_{i,1}^{n+1/2} (\Delta t) / \beta_1 (h_{1,i,j}^{n+1/2} - h_{2,i,j}^{n+1/2}) \quad (6.12)$$

$$h_{2,i,j}^{n+1} = (\Delta t / A + 2) (h_{2,i,j+1}^{n+1/2} + Ah_{2,i,j}^{n+1/2} + h_{2,i,j-1}^{n+1/2}) -$$

$$(\Delta t / 2\Delta y) (h_{2,i,j}^{n+1/2} - h_{0,i,j}^{n+1/2}) (v_{2,i,j+1}^{n+1/2} - v_{2,i,j-1}^{n+1/2}) -$$

$$(\Delta t / 2\Delta y) v_{2,i,j}^{n+1/2} (h_{2,i,j+1}^{n+1/2} - h_{2,i,j-1}^{n+1/2} - h_{0,i,j+1}^{n+1/2} + h_{0,i,j-1}^{n+1/2}) \quad (6.13)$$

$$u_{2,i,j}^{n+1} = (\Delta t / A + 2) (u_{2,i,j+1}^{n+1/2} + Au_{2,i,j}^{n+1/2} + u_{2,i,j-1}^{n+1/2}) -$$

$$(\Delta t / 2\Delta y) v_{2,i,j}^{n+1/2} (u_{2,i,j+1}^{n+1/2} - u_{2,i,j-1}^{n+1/2}) + fv_{2,i,j}^{n+1/2} \Delta t -$$

$$T_b^{n+1/2} (\Delta t) / \beta_2 (h_{2,i,j}^{n+1/2} - h_{2,i,j}^{n+1/2}) -$$

$$T_{i,2}^{n+1/2} (\Delta t) / \beta_2 (h_{2,i,j}^{n+1/2} - h_{2,i,j}^{n+1/2}) \quad (6.14)$$

$$v_{2,i,j}^{n+1} = (\Delta t / A + 2) (v_{2,i,j+1}^{n+1/2} + Av_{2,i,j}^{n+1/2} + v_{2,i,j-1}^{n+1/2}) -$$

$$(\Delta t / 2\Delta y) g(\beta_1 / \beta_2) (h_{1,i,j-1}^{n+1/2} - h_{1,i,j-1}^{n+1/2}) + fu_{2,i,j}^{n+1/2} \Delta t -$$

(cont..)

$$\begin{aligned}
& (\Delta t / 2\Delta y) g ((\rho_2 - \rho_1) / \rho_2) (h_{2,i,j+1}^{n+1/2} - h_{2,i,j-1}^{n+1/2}) - \\
& T_b^{n+1/2} (\Delta t) / \rho_2 (h_{2,i,j}^{n+1/2} - h_{0,i,j}^{n+1/2}) - \\
& T_{i,2}^{n+1/2} (\Delta t) / \rho_2 (h_{2,i,j}^{n+1/2} - h_{0,i,j}^{n+1/2}) \quad (6.15)
\end{aligned}$$

At this second half-time step, the integration is carried out for the y-direction.

Thus the iteration process from time step n to time step n+1 is carried out in two half-time steps. Terms which are not expressed as functions of variables in neighbouring nodes (Coriolis, friction terms) are taken care of in the second half-time step.

The time increment t is bounded by an upper value which is obtained from the Friedrichs-Courant-Lewy stability condition ⁽⁴³⁾ which has the following form

$$(2gH_m)^{1/2} \frac{\Delta t}{\Delta S} \leq 1 \quad (6.16)$$

where H_m is the maximum depth in the modeled region.

Due to its two-layer structure, there are two t values for the Marmara Sea, one for each layer.

Taking the maximum depth of the upper layer to be 40 meters, the maximum allowable time increment comes out to be 500/3 seconds. The lower layer, with a maximum depth of 1300 meters, allows a time increment of less than 100/3 seconds to be used. This second time increment limit was adopted for the model and time increments were chosen to be less than this value.

6.6. Boundaries and Boundary Conditions

6.6.1. Land Boundaries

At land boundaries, a wet node is adjacent to one or more dry nodes. The treatment of land boundary nodes is done according to slip boundary conditions. Figures 6.2a and 6.2b on the next page show two examples of land boundary nodes.

The dry node in Fig. 6.2a($i-1, j$) is a node where velocities and elevations are not computed. The central differences for node (i, j) however contain variables of node ($i-1, j$). To take care of this and to attain a zero flux condition across the boundary, the following modifications are made.

$$\begin{aligned} h_{m,i-1,j} &= h_{m,i,j} \\ u_{m,i-1,j} &= -u_{m,i,j} \\ v_{m,i-1,j} &= v_{m,i,j} \end{aligned} \quad (6.17)$$

where $m=1,2$ for upper and lower layers, respectively

The variables at the fictitious node ($i-1, j$) are thus replaced by those of the node for which the computations are done. For the quantity which should have a zero flux across the boundary (the longitudinal velocity component u for the case in Fig. 6.2.), a negation is performed.

For the case in Fig. 6.2b, the following modifications are done

$$h_{m,i,j+1} = h_{m,i,j}$$

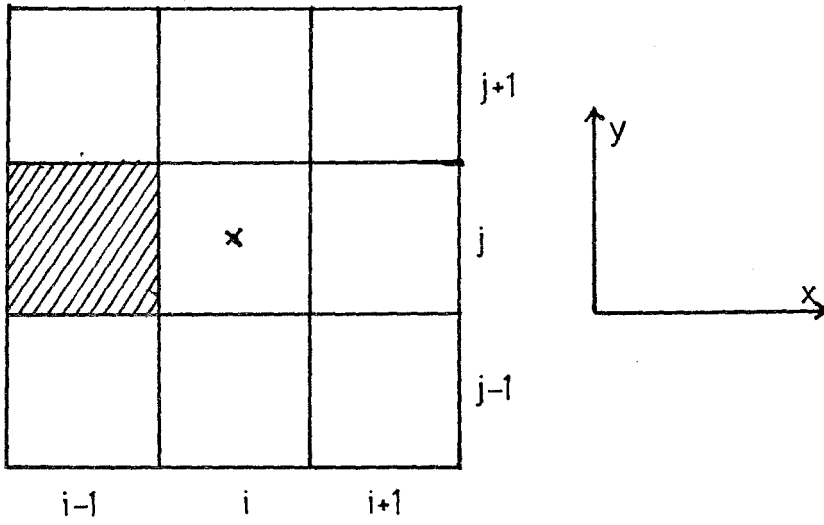


Fig.6.2a Node closed in the negative x -direction

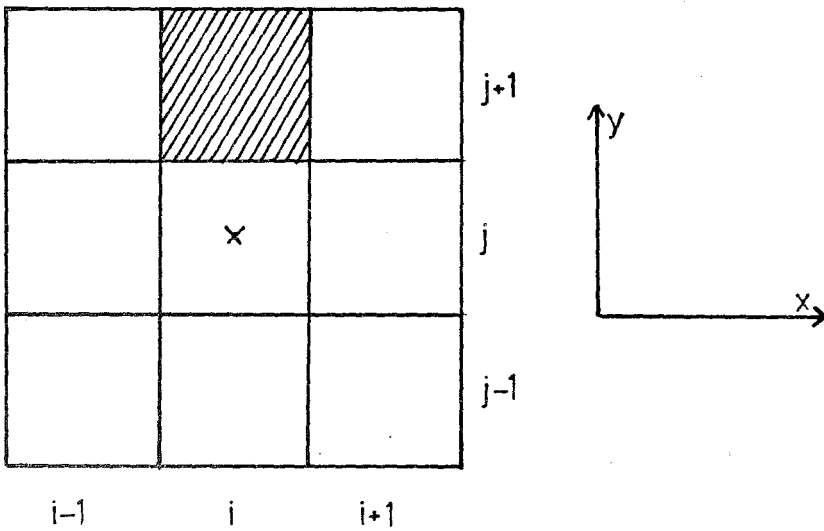


Fig.6.2b Node closed in the positive y -direction

$$u_{m,i,j+1} = u_{m,i,j} \quad (6.18)$$

$$v_{m,i,j+1} = -v_{m,i,j}$$

where $m=1,2$ for upper and lower layers respectively.

In this case, the lateral component of the velocity is negated as it should have zero flux across the land boundary.

6.6.2. Open Boundary Conditions

Unlike at land boundaries where kinematic boundary conditions are specified, the treatment of open boundaries is quite difficult. Open boundary conditions greatly influence the stability and accuracy of the solutions.

In the model of the Marmara Sea, the open boundaries are at the entrances of the straits. Inflow and outflow occur at these boundaries.

It is convenient to specify velocities at the inflows and elevations at the outflows ⁽¹⁾. There are two inflow and two outflow boundaries in the Marmara Sea and there are six variables for which boundary conditions have to be specified.

For the upper layer, the inflow is at the Bosphorus Strait entrance. At the three boundary nodes there, the upper layer velocities u_1 and v_1 are specified. The outflow is at the Dardanelles Strait entrance where the sea-level elevation is given.

For the lower layer, the reverse case applies. The inflow is at the entrance of the Dardanelles Strait where the lower layer velocities u_2 and v_2 are specified. The

interfacial elevation h is given at the outflow, at the entrance of the Bosphorus Strait.

In most numerical models, tidal variations are specified as boundary conditions, as tide is a primary driving force in most hydrodynamical systems. In the Marmara Sea, tidal variations of the sea-level are small and their effect on the circulation is negligible ⁽³³⁾.

6.7. The Computer Program

A computer program in Fortran V was written (Appendix II) to solve the finite difference equations given in section 6.5 . The computations were carried out in two steps.

In the first step, a separate program was utilized to generate initial conditions. In the equations, the convective terms were neglected. Moreover, the stress terms were also not taken into consideration and a hypothetical bottom configuration was used. The first step computed velocities to be fed into the main program where the convective and stress terms were included and the real bottom topography was used. In the second step, the simulation time was 12 hours. Runs were made (on the CDC Cyber 170 on the campus of the Bosphorus University) for conditions with no wind and wind. Boundary conditions (velocities and elevations) were specified as time varying functions, increasing from zero at the beginning of the iterations to a maximum value after 12 hours simulation time.

VII. DISCUSSION OF THE RESULTS

7.1. The Boundary Conditions and Driving Mechanisms

7.1.1. The Upper Layer

The upper layer in the Marmara Sea is driven by the wind and sea-level differences between the straits. There obviously exists a flow due to horizontal density gradients, but its magnitude should be small and it was also neglected in the model.

Due to the lack of data at the open boundaries, the simulations were carried out with a wide range of boundary conditions. Several sea-level differences were specified as boundary conditions for the upper layer and the response of the sea to the surface gradients was tested with and without wind forcing. The velocities at the boundary nodes were specified based on data from a report prepared by the Seyir (46) Hidrografi ve Oşinografi Dairesi. The data, however, was not time-dependent and the location of the current measurements also did not coincide exactly with the boundary nodes. Therefore, in the simulations, the velocities also were varied.

7.1.2. The Lower Layer

The lower layer is driven by the interfacial gradient. The bottom slope was neglected as its inclusion led to increase due to the roughness of the sea bed.

The interfacial slope, however, constituted a weak force to establish a flow in the lower layer. Even with interfacial elevation differences up to 40 meters between the straits, which is quite unrealistic, the sea-level difference offset the effect of the interfacial slope. The upper layer dragged the lower layer along.

This inefficiency of the interfacial slope to drive the lower layer suggested another mechanism for the lower layer currents. The main driving force of these bottom waters, however, has up to now not been explained adequately, let alone expressed mathematically.

In order to obtain reasonable results for the lower layer, the term which stood for the effect of the upper layer on the lower layer in the equations of the model was dropped. This omission rendered the lower layer insensitive to sea level differences, but enabled to specify reasonable interfacial slopes. A flow was obtained. Its quantitative accuracy, however, is doubtful due to the omission of the term as mentioned above. Therefore, the lower layer results should be approached with care.

7.2. The Circulation in the Absence of Wind

7.2.1. The Upper Layer

The upper layer circulation in the absence of wind is governed by the sea-level difference. Several values were assigned to it. Here, two simulations will be examined.

In Appendix III, the numerical results of these simulations are given. In Figures 7.1 and 7.2 on the next two pages, the vector plots are shown.

As observable from the figures, the flow is predominantly to the west. The waters, after leaving the Bosphorus Strait, turn to the right and spread out. Near the Marmara island, the currents encounter a narrower channel, gain in speed and leave the sea through the Dardanelles Strait. There exists a faint and not well defined circulation in the eastern portion of the sea and a branching into the Gemlik bay.

In the two simulations, due to the large grid size, secondary circulations near land boundaries are not well reproduced. Moreover, the currents to the east of the Bosphorus Strait and along the southern coastline seem to be too slow. As no data exists to calibrate and verify the model, much cannot be said about their adequacy.

In the simulations, sea-level differences were 16 and 10 centimeters, respectively. The results of the first run differed from the second run by the velocity magnitudes. Currents were faster. As also different boundary velocities were specified at the Bosphorus Strait entrance, velocities slightly varied from each other in the eastern portion.

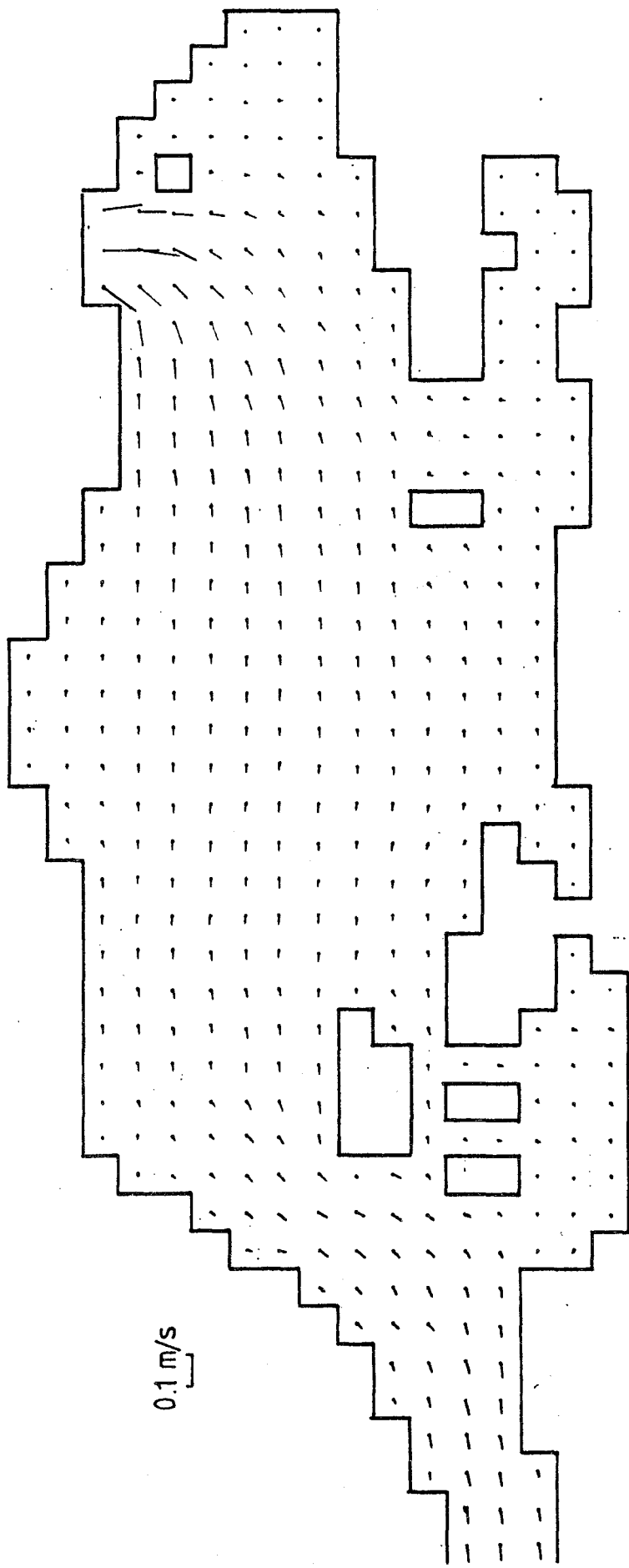


Fig. 71. Upper layer velocity field in the absence of wind
(Sea level difference 16 cm)

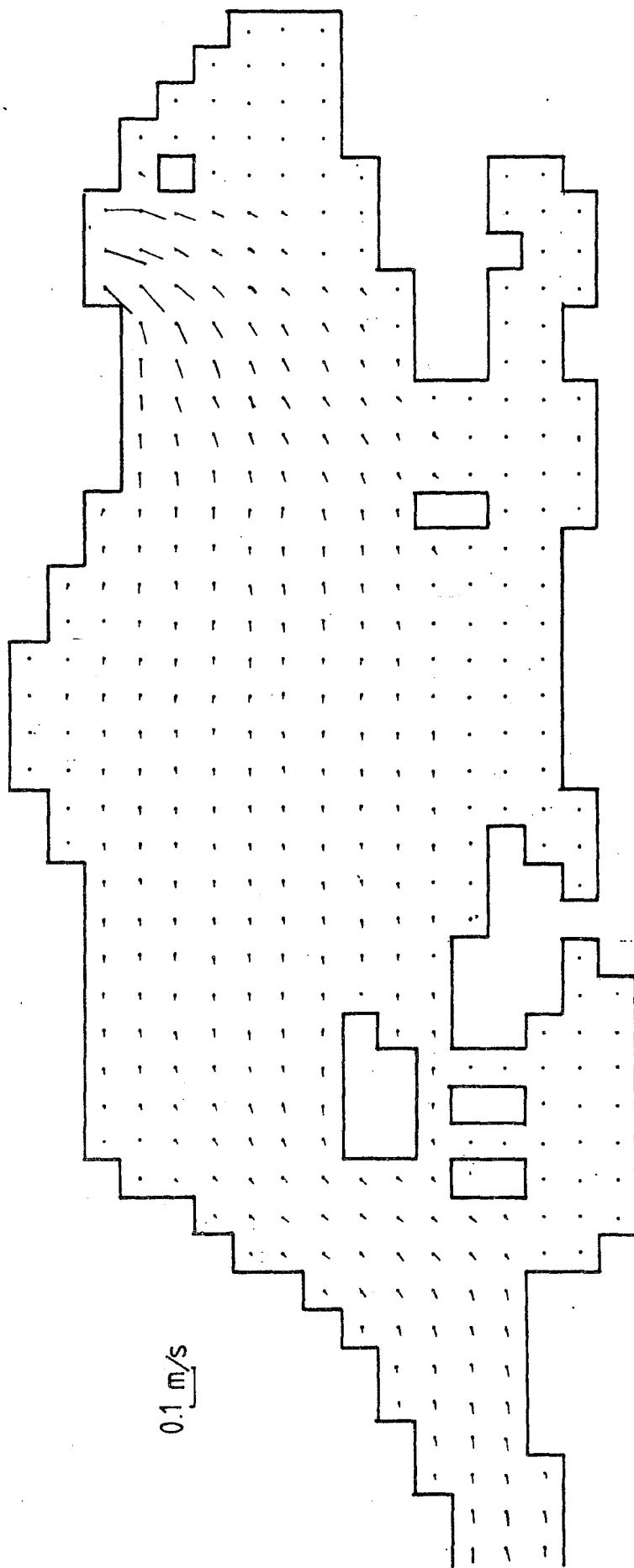


Fig. 7.2. Upper layer velocity field in the absence of wind
(Sea level difference 10 cm)

7.2.2. The Lower Layer

As mentioned above, the lower layer currents were made insensitive to sea-level fluctuations. Therefore, the results of the lower layer were only dependent on the interfacial slope and velocities specified as boundary conditions. Several values were specified to the interfacial slope ranging from 8 to 15 meters. As for the upper layer, no data set existed for calibration and verification.

In Figure 7.3 the flow in the lower layer is displayed. In general, the bottom waters flow in the opposite direction of the surface waters. The magnitudes are around three times slower than those of upper layer currents. The circulation in the eastern portion of the sea is well-defined.

All simulations of lower layer currents gave similar results, therefore they will not be considered anymore. The numerical results of each simulation, however, are given in Appendix III.

7.3. Upper Layer Circulation under Wind Stress

As the simulation time employed (12 hours) was not long enough to examine the response of the sea to long term average conditions, the behavior of the sea under strong winds over a small time period was tested.

7.3.1. Circulation and Water-Levels in the Presence of a Strong South Wind

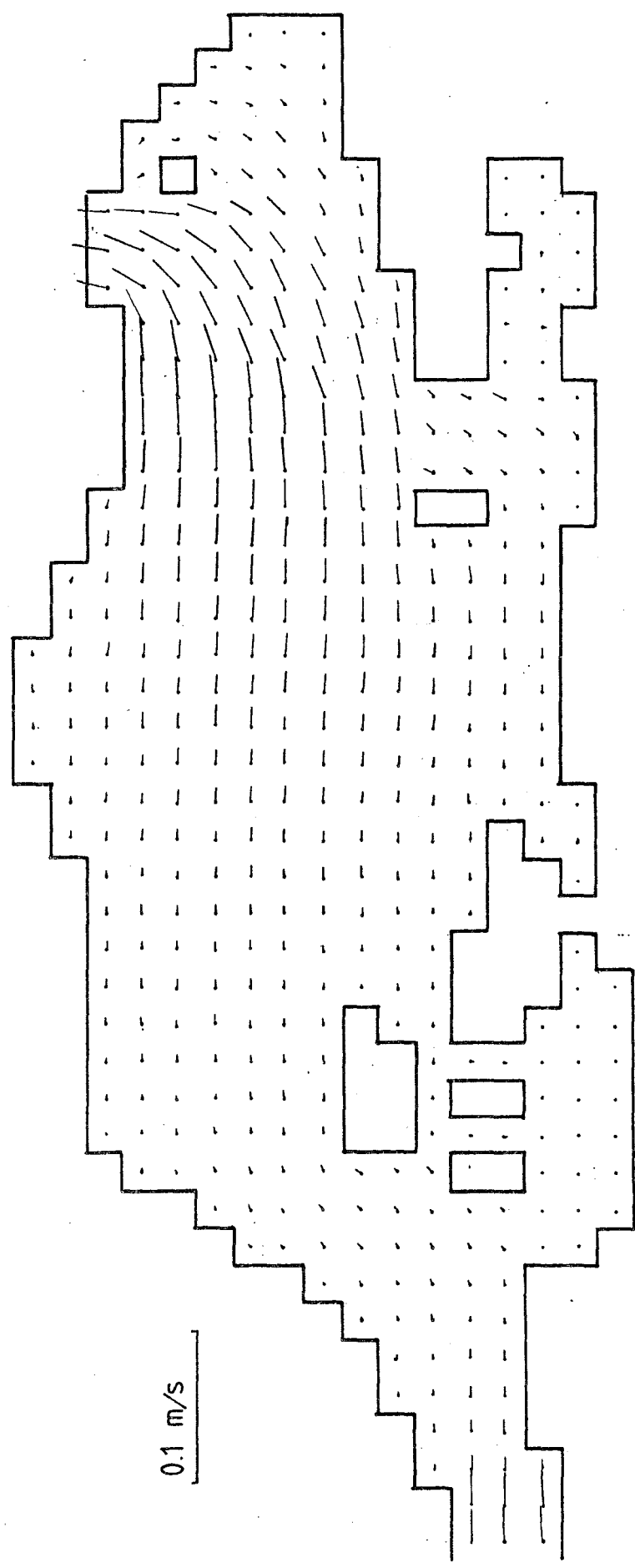


Fig. 73. Lower layer velocity field

The Marmara Region is frequently subject to strong winds from the south (lodos). It has been observed that on windy days, waters pile up along the northern coasts up to one meter ⁽³³⁾. Two simulation runs were made for a southern wind, blowing with a speed of 20 meters/sec (gale according to the Beaufort scale). In the first run, the sea-level difference between the straits was 8 centimeters.

This small difference and the strong wind resulted in velocities partially reversed from those in normal cases. In the western portion of the sea, the flow appeared to be to the northeast. The sea-level difference between the northern and southern coasts amounted to around 30 centimeters (Figure 7.4).

In the second run, the same wind stress was applied. However, the sea-level difference was increased to 24 centimeters. No reversal of the currents occurred, but their magnitudes were severely reduced (Figure 7.5). A general trend towards west-northwest appeared. As the inflow through the Bosphorus Strait was increased and the outflow through the Dardanelles Strait was reduced due to the wind, waters piled up in the sea, especially along the northern coastlines and in the eastern portion (Figure 7.6).

7.3.2. Circulation and Water Levels in the Presence of Northern Winds

For winds blowing from the northern directions, several runs were made for light and strong winds from northeast and

Elevation (cm)

0-10

11-20

21-30

31-40

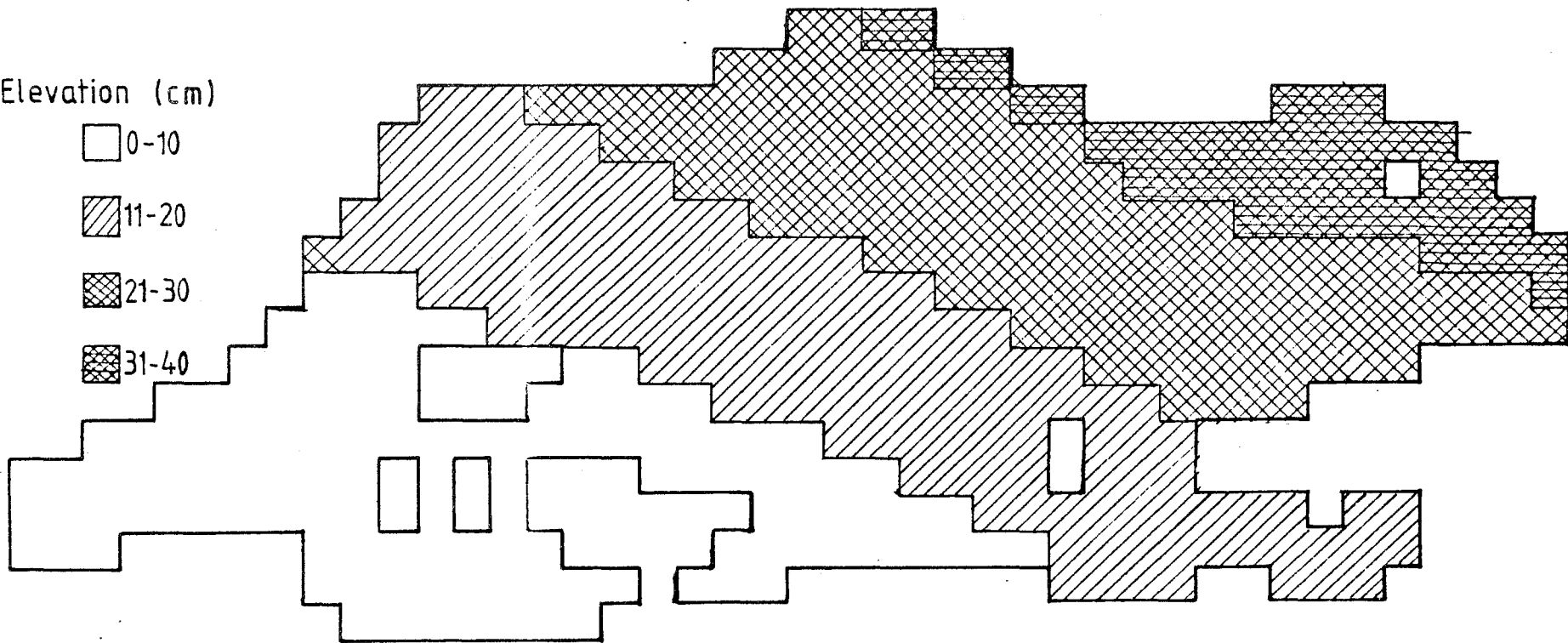


Fig. 7.4 Elevations above mean sea level

20 M/S

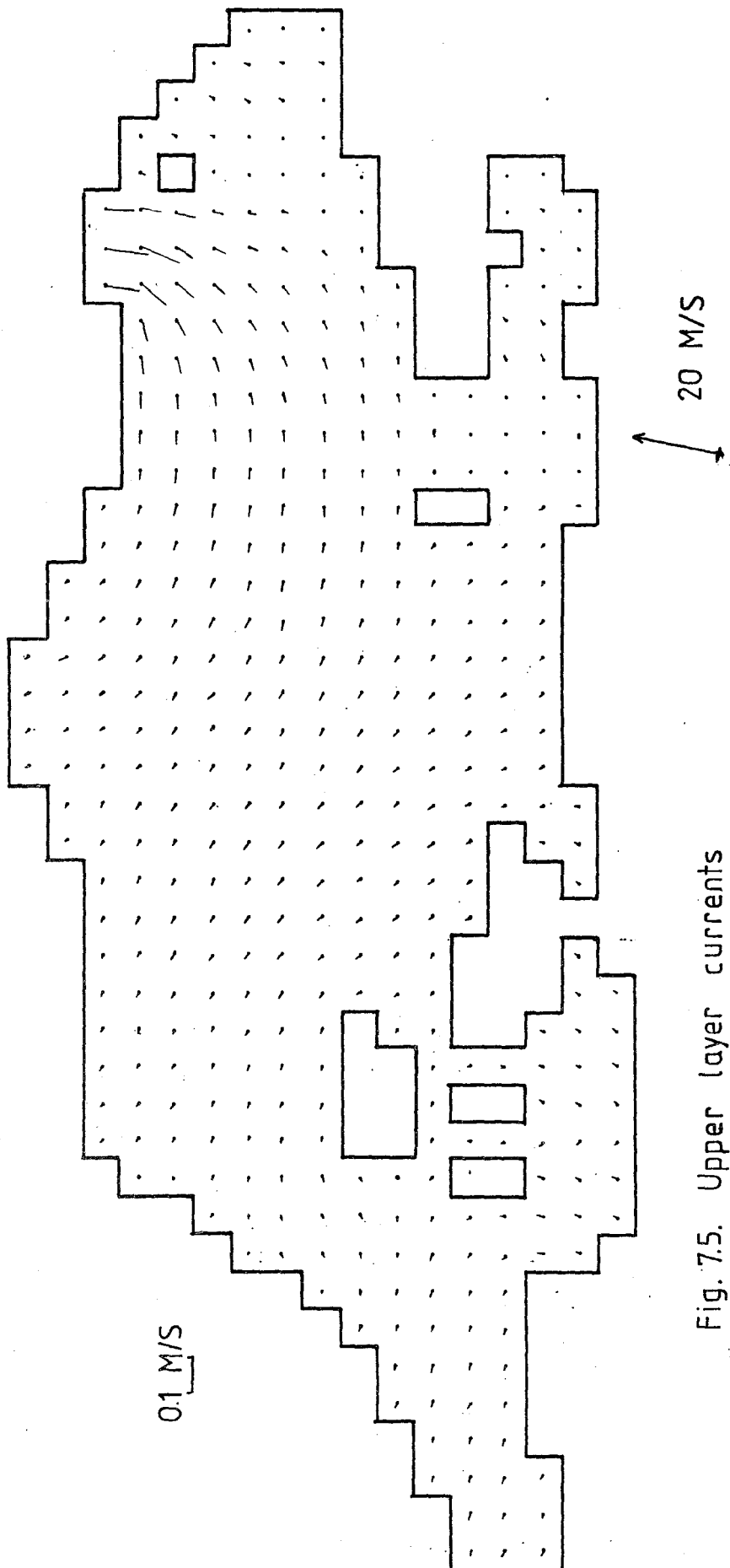


Fig. 7.5. Upper layer currents

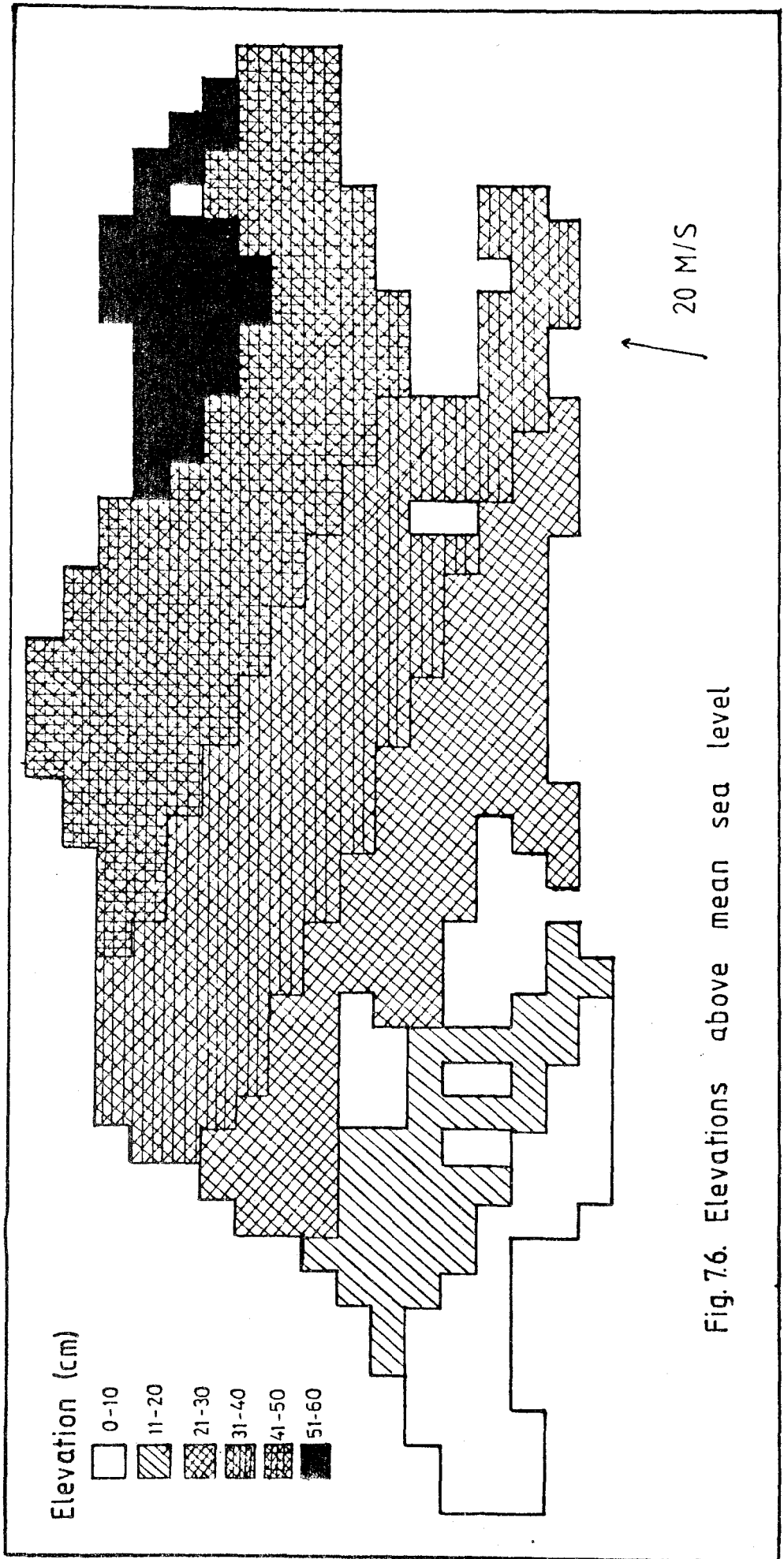


Fig. 7.6. Elevations above mean sea level

northwest. Here, results of two simulations will be displayed.

In the first run, wind was blowing from the northeast with a speed of 17 meters/sec (gale-near gale). The sea-level difference was 16 centimeters. The results showed an increase in magnitude of the western-bound currents. (Figure 7.7). Comparing the results with the first simulation with no wind and the same sea-level difference (Section 7.2.1), it can be observed that currents nearly doubled their speeds. The strong northeasterly wind resulted in the piling of waters in the western portion of the sea (Figure 7.8).

In the second simulation, a calmer wind was specified blowing from northwest with a speed of 13 m/sec (strong breeze). The sea-level difference was 15 centimeters. The wind decreased the magnitude of the westward flow, although not reversing it. A counterclockwise circulation, faint and not well-defined at its eastern boundary, appeared around the islands to the west of the Kapıdağ peninsula (Figure 7.9). Waters piled up along the southern coasts (Figure 7.10).

As observed from the figures of the velocity fields and water levels, the Marmara Sea currents show significant variations according to variations in forces applied to it and variations in boundary conditions. A partial reversal of currents may be caused by strong winds and low inflows. Coastal circulations are more readily altered or completely reversed than open sea currents.

As currents and sea-levels at the open boundary nodes are dependent on each other (they are functions of the

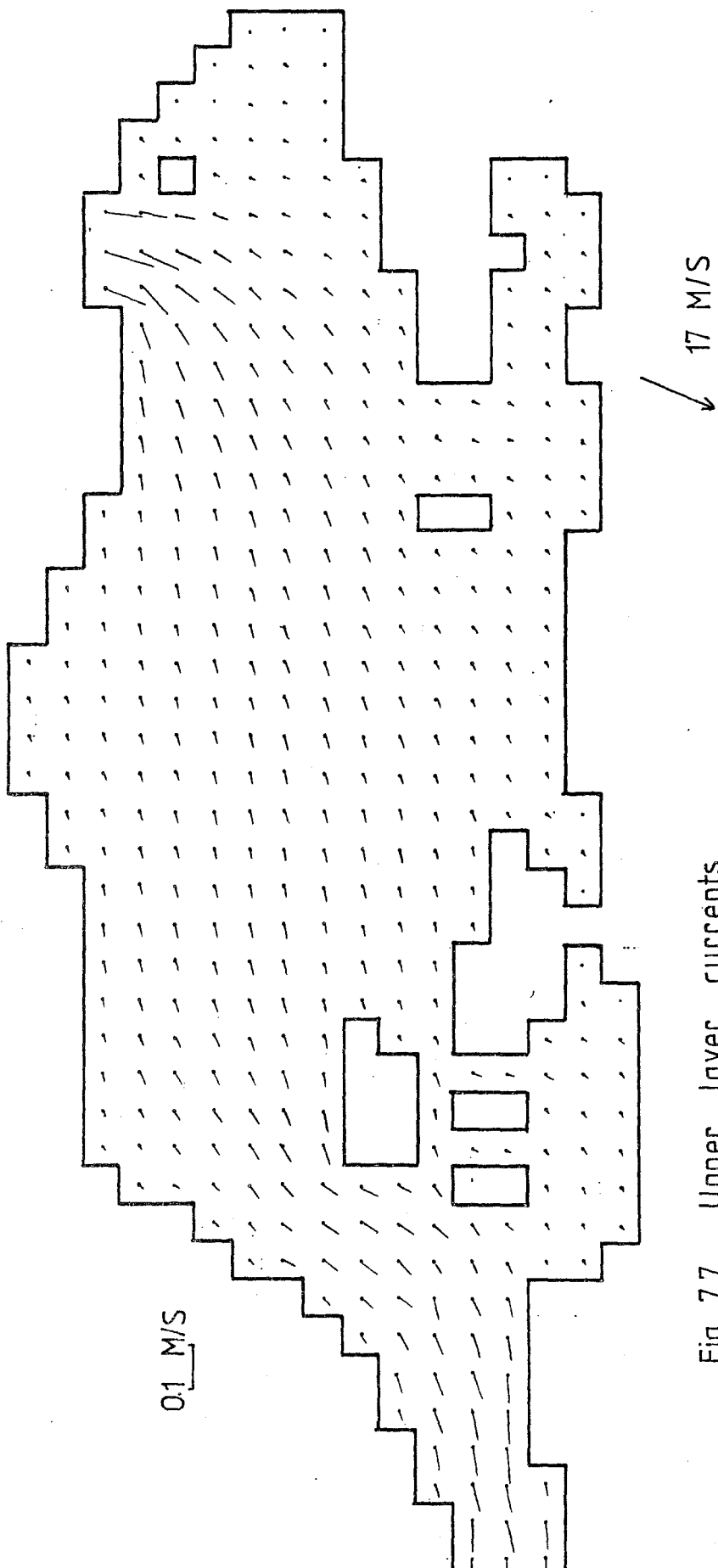


Fig 77 Upper layer currents

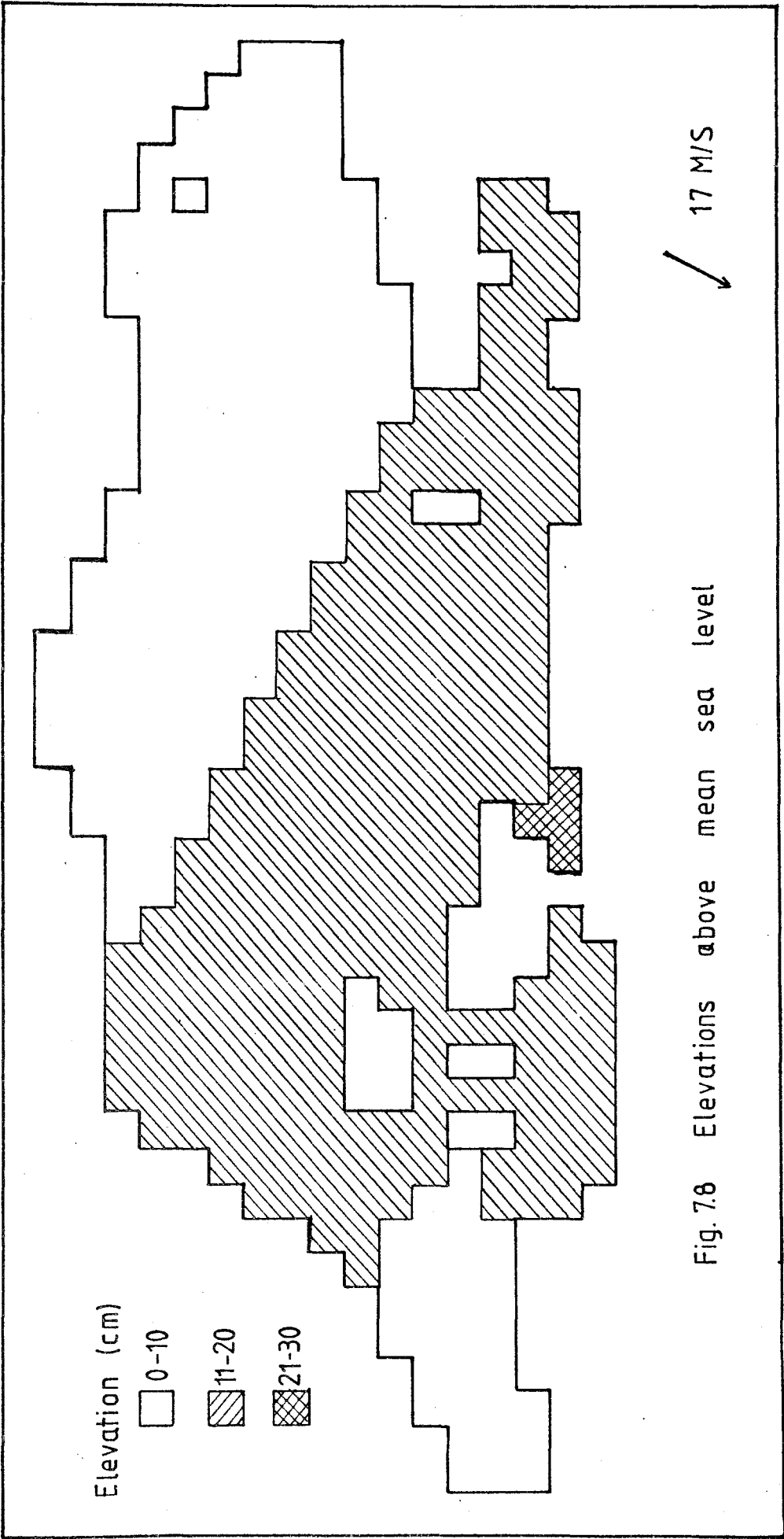


Fig. 7.8 Elevations above mean sea level

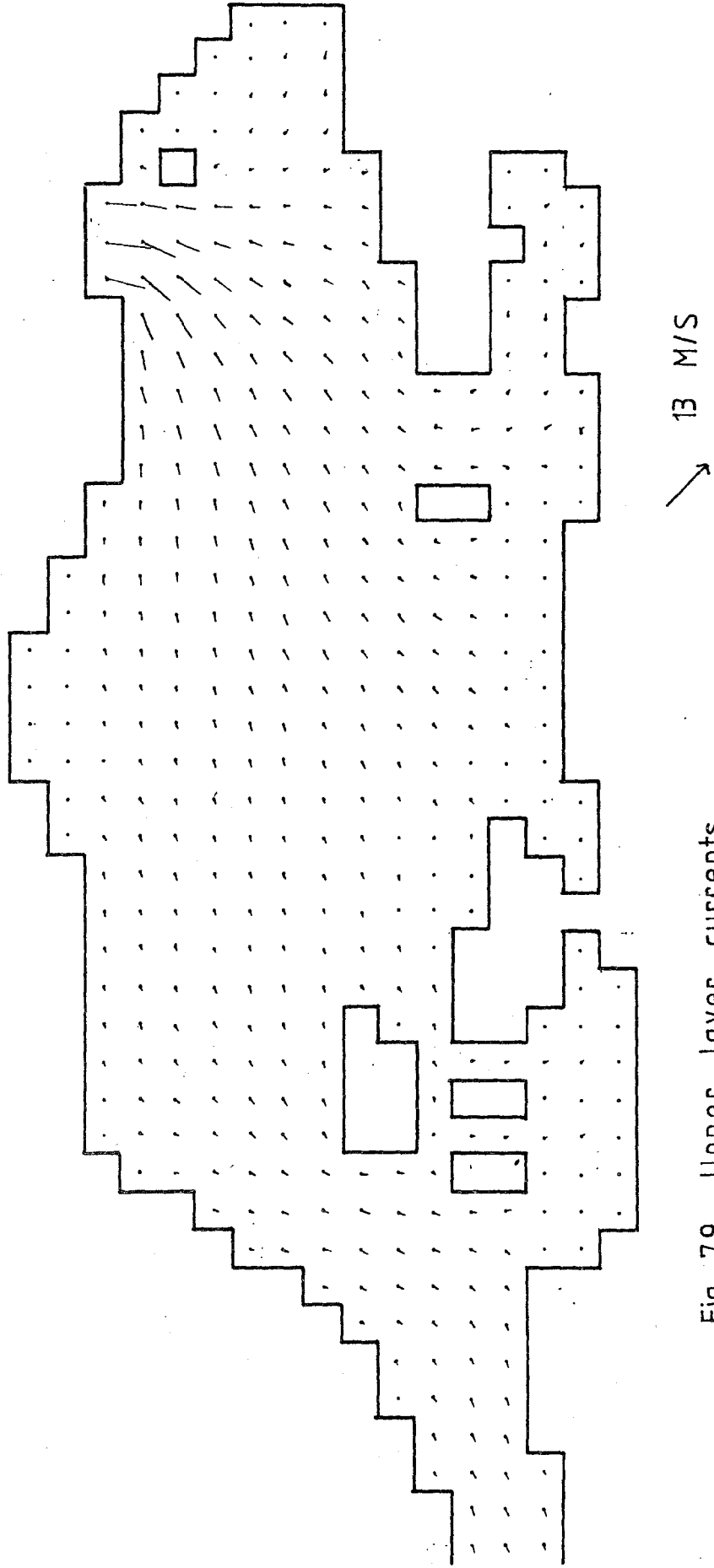
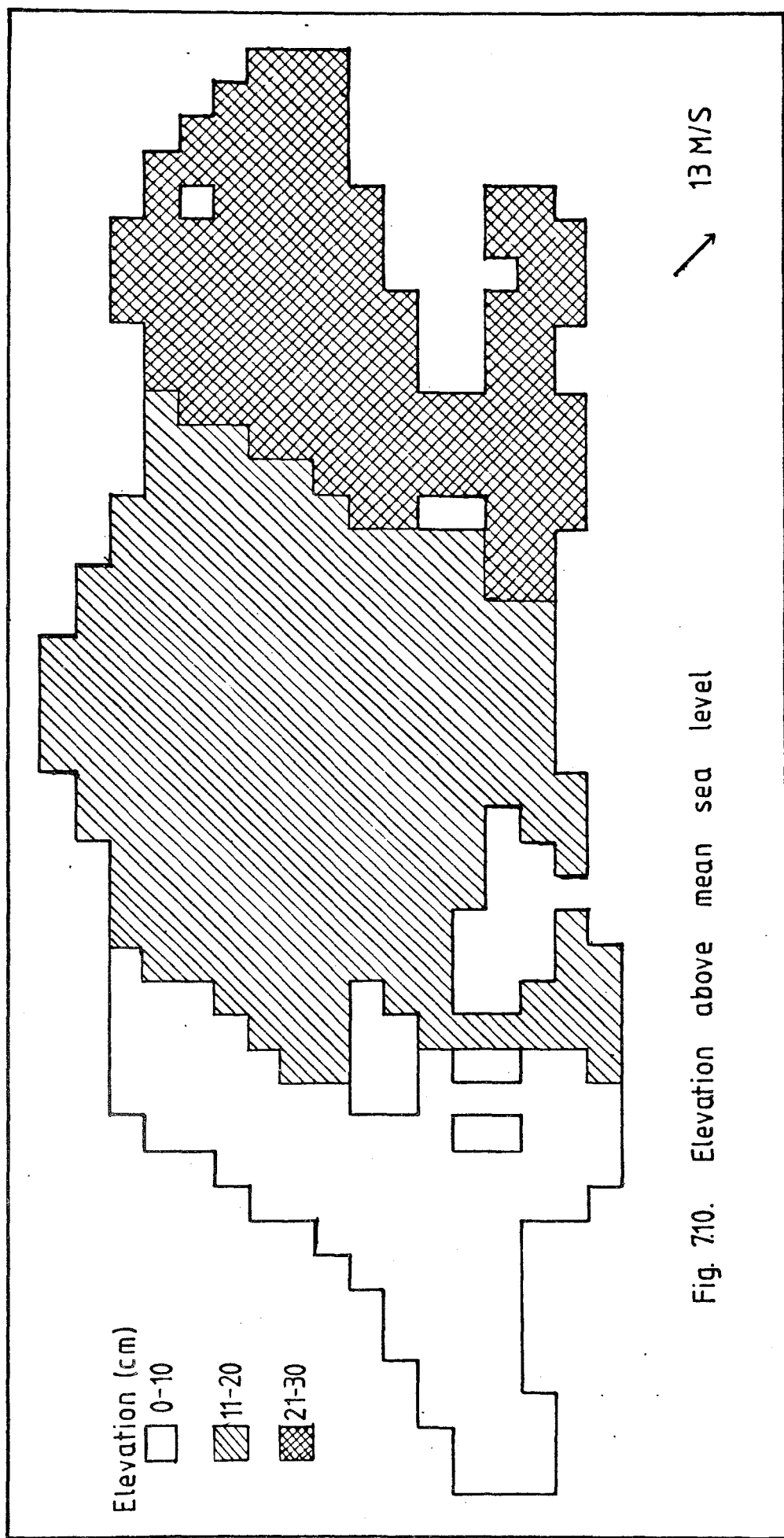


Fig 79 Upper layer currents



inflows and outflows), a certain correlation should exist between them. Lack of data did not allow this correlation to be determined. So, in the simulations, it is quite possible that actual conditions in regard to extreme boundary velocities and water levels were not met and, this may have resulted in loss of information on the flow.

VIII. CONCLUSIONS AND RECOMMENDATIONS

The results of the simulation runs have shown that the depth-averaged two-layer model could be applied to the Marmara Sea to predict water levels and currents. However, some aspects should be considered.

Lack of data sets prevented a calibration and verification of the model. So for further use, this problem should be overcome by obtaining data sets to calibrate and verify the model.

It has been found out that the greatest uncertainty was about the boundary conditions. As they affect the results significantly, in future applications, it is recommended that the boundary conditions be based on time-dependent data obtained under the conditions simulated in the runs. Although its amplitude is small, tide should also be included in the model as a driving force.

The driving mechanism of the lower layer should be more accurately defined, and expressed mathematically. Besides the interfacial slope and the gravitational pull down the bottom slope, there should be another force to set up and maintain a flow in the lower layer. This force is obviously a pressure force arising from the density differences between the Black

Sea and the Mediterranean Sea. However, along the Marmara Sea, significant horizontal density differences are not observed in the lower layer (chapter 4). An expression to account for pressure forces arising from a horizontal density gradient thus fails to establish a flow. Therefore, a large scale interaction between the two seas should be considered.

A horizontal density gradient also exists for the upper layer as a result of interfacial transfer of salt and heat from the lower layer. This has been neglected in the model. However, terms can be added to the equations to account for interfacial mixing.

The computation of transport in hydrodynamical systems is of importance. However, this task required work beyond the scope of this study. At first, to compute the transport of water through the sea, a much larger time period should be employed in the simulations. One season (three months) is adequate for such a purpose. It is clear that the average transport cannot be computed from a simulation time of 12 hours when one considers that a water molecule needs around hundred days to move from one strait to the another. For the lower layer, this time should be increased by approximately threefold. Moreover, for the computation of the transport, the average wind stress and the discharges (as inflows) through the straits during the period should be known.

Secondary circulations in coastal areas could not be adequately modeled because of the large grid size. A finer grid was considered to be uneconomical as the computer time required (around 2000 CPU seconds at present for the main

program) would increase too much. It is recommended that separate models of coastal areas with fine grids be developed which utilize the main model as data donor at the open boundaries. This will help to reproduce secondary currents more accurately.

BIBLIOGRAPHY

- 1- Liu, S., Leendertse, J.J., "Multidimensional Numerical Modeling of Estuaries and Coastal Seas," Advances in Hydroscience, Vol.11, pp. 95-164, 1978.
- 2- Hinwood, J.B., Wallis, I.G., " Classification of Models of Tidal Waters," ASCE, Journal of the Hydraulics Division, Vol. 101, No. HY10, pp. 1315-1331, 1975.
- 3- Hinwood, J.B., Wallis, I.G., " Review of Models of Tidal Waters," ASCE, Journal of the Hydraulics Division, Vol. 101, No. HY11, pp. 1405-1425, 1975.
- 4- Fisher, H.B., " Some Remarks on Computer Modeling of Coastal Flows," ASCE, Journal of the Waterways, Harbors, and Coastal Engineering Division, Vol. 102, No. WW4, pp. 395-406, 1976.
- 5- Ponce, V.M., Yabusaki, S.B., " Modeling Circulation in Depth Averaged Flow," ASCE, Journal of the Hydraulics Division, Vol. 107, No. HY11, pp. 1501-1517, 1981.
- 6- Lai, C., " Numerical Modeling of Unsteady Open Channel Flows," Advances in Hydroscience, Vol. 14, p. 161, 1986.
- 7- Reid, R.O., Bodine, B.R., " Numerical Model for Storm Surges in Galveston Bay," ASCE, Journal of the Waterways and Harbors Division, Vol.94, No.WW1, p. 33, 1968
- 8- Prandle, D., " Storm Surges in the Southern North Sea and River Thames," Proc. R. Soc. Lond., A334, pp. 509-539, 1975
- 9- Pingree, R.D., Griffiths, D.K., " Currents driven by a uniform wind stress on the shelf seas around the British Isles," Oceanologica Acta, Vol. 3, No. 2, pp. 227-236, 1980
- 10- Dronkers, J.J., " Tidal Computations for Rivers, Coastal Areas and Seas," ASCE, Journal of the Hydraulics Division, Vol. 95, No. HY1, pp. 29-77, 1969.
- 11- Flather, R.A., Heaps, N.S., " Tidal Computations for Morecambe Bay," Geophys. J. R. astr. Soc., 42, p. 489, 1975.

- 12- Gunn, D.J., Yenigün, O., " Modeling of Tidal Motion in Shoaling Waters: The Estuary of Milford Haven," Estuarine, Coastal and Shelf Science, 21, pp. 337-356, 1985.
- 13- Gunn, D.J., Yenigün, O., " A Model for Tidal Motion and Level in the Tay Estuary," Proceedings of the Royal Society of Edinburgh, Series B, to be published.
- 14- Falconer, R.A., " Numerical Modeling of Tidal Circulation in Harbors," ASCE, Journal of the Waterway, Port, Coastal and Ocean Division, Vol. 106, No. WW1, pp. 31-48, 1980.
- 15- Williams, B.J., Hinwood, J.B., " Two-Dimensional Mathematical Water Quality Model," ASCE, Journal of the Environmental Engineering Division, Vol. 102, No. EE1, 1976
- 16- Falconer, R.A., " Water Quality Simulation Study of a Natural Harbor," ASCE, Journal of the Waterway, Port, Coastal and Ocean Engineering Division, Vol. 112, No. 1, pp. 15-34, 1986.
- 17- Grubert, J.P., Abbott, M.A., " Numerical Computation of Stratified Nearly Horizontal Flows," ASCE, Journal of the Hydraulics Division, Vol. 98, No. HY10, pp. 1847-1865, 1972.
- 18- Lee, K.K., Liggett, J.A., " Computation for Circulation in Stratified Lakes," ASCE, Journal of the Hydraulics Division, Vol. 96, No. HY10, pp. 2089-2115, 1970.
- 19- Lee, K.K., Liggett, J.A., " Properties of Circulation in Stratified Lakes," ASCE, Journal of the Hydraulics Division, Vol. 97, No. HY1, pp. 15-29, 1971.
- 20- Hodgins, D.O., Osborn, T.R., and Quick, M.C., "Numerical Model of Stratified Estuary Flows," ASCE, Journal of the Waterways, Port, Coastal and Ocean Division, Vol. 103, No. WW1, pp. 25-42, 1977.
- 21- Hyden, H., " Water Exchange in Two-Layer Stratified Waters," ASCE, Journal of the Hydraulics Division, Vol. 100 No. HY3, pp. 345-361, 1974.
- 22- Laevastu, T., " Reproduction of Currents and Water Exchange in the Strait of Gibraltar with Hydrodynamical Numerical Model of Walter Hansen," Studies in Physical Oceanography, Vol. 2, Gordon and Breach Science Publishers, 1972.
- 23- Sümer, B.M., Bakioglu, M. Sea-Strait Flow With Special Reference to Bosphorus. İstanbul Teknik Üniversitesi İnşaat Fakültesi, 1981.

- 24- Yin, F., Chen, S., "Tidal Computation on Taiwan Strait," ASCE, Journal of the Waterways, Port, Coastal and Ocean Division, Vol. 108, No. WW4, pp. 539-553, 1982.
- 25- Benque, J.P., Cunge, J.A., Feuillet, J., Haugual, A., and Holly, Jr., F.M., " New Method for Tidal Current Computation," ASCE, Journal of the Waterways, Port, Coastal and Ocean Division, Vol. 108, No. WW3, pp. 396-417, 1982.
- 26- Streeter, V.L.(ed.), Handbook of Fluid Dynamics, McGraw Hill Company, Inc., 1961.
- 27- Ippen, A.T.(ed.), Estuary and Coastline Hydrodynamics McGraw Hill Company, Inc., 1966.
- 28- Abraham, G., Karelse, M., and Van Os, A.G., " On the Magnitude of Interfacial Shear of Subcritical Flows in Relation with Interfacial Stability," Journal of Hydraulic Research, Vol. 17, No. 4, pp. 273-287, 1979.
- 29- Carstens, T., " Turbulent Diffusion and Entrainment in Two-Layer Flow," ASCE, Journal of the Waterways and Harbors Division, Vol. 96, No. WW1, pp. 97-104, 1970.
- 30- Macagno, E.O., Rouse, H., " Interfacial Mixing in Stratified Flow," ASCE, Transactions, Vol. 127, Part I., pp. 102-128, 1962.
- 31- Dermissis, V., Partheniades, E., " Interfacial Resistance in Stratified Flows," ASCE, Journal of the Waterways, Port, Coastal and Ocean Engineering, Vol. 110, No. 2, pp. 231-250, 1984.
- 32- İnandık, H., " Türkiye Çevresindeki Denizlerin Başlıca Özellikleri," İstanbul Üniversitesi Coğrafya Enstitüsü Dergisi, Cilt 7, Sayı 14, 1964.
- 33- Darkot, B., Tuncel, M. Marmara Bölgesi Coğrafyası, İstanbul Üniversitesi Coğrafya Enstitüsü Yayınları, No. 118, İstanbul, 1981.
- 34- Büyüközden, A., Yüce, H., Bayraktar, T., " Akdeniz Suyunun İstanbul Boğazı Boyunca ve Karadenizde İncelenmesi" Doğa Bilim Dergisi, Seri B, Cilt 9, Sayı 3, 1985.
- 35- Curi, K., Gemlik Deniz Deşarjı. Boğaziçi Üniversitesi Çevre Bilimleri Enstitüsü, 1982.
- 36- Marmara Denizi Oşinografik Mesaha Sonuçları, Kış 1982 ; Seyir, Hidrografi ve Oşinografî Dairesi, Oşinografî Şube Dördürlüğü, İstanbul, 1982.
- 37- Pickard, G.L., Descriptive Physical Oceanography. 2nd edition, Pergamon International Library, 1975.

- 38- Davies, A.M., " On computing the three dimensional flow in a stratified sea using the Galerkin method," Applied Mathematical Modeling, Vol. 6, pp. 347-362, 1982.
- 39- Pond, S., Pickard, G.L., Introductory Dynamic Oceanography, Pergamon International Library, 1978.
- 40- McLellan, H.J., Elements of Physical Oceanography. Pergamon Press, 1975.
- 41- Wu, J., " Wind Stress and Surface Roughness at Air-Sea Interface," Journal of Geophysical Research, Vol. 74, No.2, pp. 444-455, 1969.
- 42- Safaie, B., " Wind Stress at Air-Water Interface," ASCE, Journal of the Waterways, Port, Coastal and Ocean Engineering, Vol. 110, No.2, pp. 287-293, 1984.
- 43- Yenigun, O., " Modeling of Tidal Motion in Estuaries, " Ph.D. Dissertation, University of Wales, 1983.
- 44- Chow, V.T., Open Channel Hydraulics. McGraw Hill, 1959.
- 45- Roache, P.J., Computational Fluid Dynamics. Hermosa Publishers, Albuquerque, 1976.
- 46- İstanbul Boğazı Kanalizasyon Projesine İlişkin Oşinografik, Jeolojik, Sismik ve Hidrografik Çalışma Raporu, Seyir, Hidrografi ve Oşinografi Dairesi, 1980.

APPENDICES

APPENDIX I

TABLES

STATION NUMBER 1
 LONGITUDE 28 55 00
 LATITUDE 40 54 36
 CORRESPONDING GRID LOCATION (35,15)
 DATE OF SAMPLING 26/02/1982
 MAXIMUM DEPTH (M) 79
 WIND
 DIRECTION 210
 SPEED (M/S) 3.605
 PRESSURE (MBAR) 1000
 TEMPERATURE (C)
 DRY BULB 9.9
 WET BULB 9.7

DEPTH (M)	TEMPERATURE (C)	SALINITY (PPT)	DENSITY (KG/M3)
0	6.15	20.264	1015.97
10	6.64	22.572	1017.73
20	8.86	27.111	1021.00
30	13.84	35.882	1026.50
50	15.40	38.377	1026.50

STATION NUMBER 2
 LONGITUDE 28 55 54
 LATITUDE 40 48 00
 CORRESPONDING GRID LOCATION (35,12)
 DATE OF SAMPLING 26/02/1982
 MAXIMUM DEPTH (M) 970
 WIND

DIRECTION 210
 SPEED (M/S) 1.030
 PRESSURE (MBAR) 1000
 TEMPERATURE (C)
 DRY BULB 9.8
 WET BULB 7.4

DEPTH (M)	TEMPERATURE (C)	SALINITY (PPT)	DENSITY (KG/M3)
0	6.95	22.640	1017.75
7	6.70	23.479	1018.44
13	6.66	24.183	1018.99
20	7.55	24.856	1019.42
32	15.45	38.166	1026.33
50	15.21	38.446	1026.60
60	15.16	38.501	1026.65
100	14.95	38.548	1026.74
134	14.81	38.555	1026.77
204	14.58	38.554	1026.82
350	14.44	38.565	1026.86
420	14.40	38.562	1026.87
580	14.43	38.561	1026.86

STATION NUMBER 3
 LONGITUDE 29 10 00
 LATITUDE 40 45 12
 CORRESPONDING GRID LOCATION (39,11)
 DATE OF SAMPLING 26/02/1982
 MAXIMUM DEPTH (M) 1100
 WIND
 DIRECTION 240
 SPEED (M/S) 1.030
 PRESSURE (MBAR) 1001
 TEMPERATURE (C)
 DRY BULB 10.0
 WET BULB 7.5

DEPTH (M)	TEMPERATURE (C)	SALINITY (PPT)	DENSITY (KG/M3)
0	6.81	22.973	1010.03
5	6.44	23.076	1010.15
17	7.71	25.106	1019.59
20	10.25	30.083	1025.10
45	15.45	38.256	1020.40
60	15.16	38.489	1020.64
80	14.94	38.533	1020.73
129	14.72	38.531	1020.77
172	14.62	38.530	1020.80
210	14.42	38.538	1020.86
430	14.41	38.543	1020.85
520	14.40	38.565	1020.87
715	14.44	38.546	1020.85

STATION NUMBER 4
 LONGITUDE 28 55 36
 LATITUDE 40 42 12
 CORRESPONDING GRID LOCATION (35,10)
 DATE OF SAMPLING 20/02/1982
 MAXIMUM DEPTH (M) 710
 WIND
 DIRECTION 260
 SPEED (M/S) .515
 PRESSURE (MBAR) 1002
 TEMPERATURE (C)
 DRY BULB 9.5
 WET BULB 7.5

DEPTH (M)	TEMPERATURE (C)	SALINITY (PPT)	DENSITY (KG/M3)
0	6.53	-	1017.21
10	6.88	-	1016.25
20	6.55	-	1019.02
30	15.38	-	1020.19
49	15.39	-	1020.58
74	15.05	-	1020.71
99	14.89	-	1020.76
140	14.75	-	1020.79
190	14.62	-	1020.83
297	14.44	-	1020.88
300	14.43	-	1020.86
495	14.40	-	1020.87

STATION NUMBER 5
 LONGITUDE 23 36 30
 LATITUDE 40 26 50
 CORRESPONDING GRID LOCATION (30,05)
 DATE OF SAMPLING 27/02/1982
 MAXIMUM DEPTH (M) 49
 WIND
 DIRECTION 75
 SPEED (M/S) .515
 PRESSURE (MBAR) 1006
 TEMPERATURE (C)
 DRY BULB 7.4
 WET BULB 6.0

DEPTH (M)	TEMPERATURE (C)	SALINITY (PPT)	DENSITY (KG/M3)
0	7.23	22.750	1017.81
10	7.36	24.307	1019.01
20	9.89	29.630	1022.81
30	13.22	34.923	1025.31

STATION NUMBER 6
 LONGITUDE 23 36 07
 LATITUDE 40 37 07
 CORRESPONDING GRID LOCATION (30, 8)
 DATE OF SAMPLING 26/02/1982
 MAXIMUM DEPTH (M) 393
 WIND
 DIRECTION 180
 SPEED (M/S) 1.030
 PRESSURE (MBAR) 1004
 TEMPERATURE (C)
 DRY BULB 8.5
 WET BULB 7.0

DEPTH (M)	TEMPERATURE (C)	SALINITY (PPT)	DENSITY (KG/M3)
0	6.51	22.737	1017.87
9	6.67	23.611	1018.54
19	6.90	24.782	1019.43
29	10.93	32.487	1024.85
46	15.50	38.433	1025.52
73	15.09	38.530	1026.69
97	14.95	38.541	1026.73
140	14.76	38.551	1026.78
190	14.56	38.557	1026.83
294	14.46	38.554	1026.85

STATION NUMBER 7
 LONGITUDE 28 36 36
 LATITUDE 40 44 06
 CORRESPONDING GRID LOCATION (30,11)
 DATE OF SAMPLING 26/02/1982
 MAXIMUM DEPTH (M) 720
 WIND
 DIRECTION 225
 SPEED (M/S) 1.030
 PRESSURE (MBAR) 1003
 TEMPERATURE (C)
 DRY BULB 7.4
 WET BULB 6.0

DEPTH (M)	TEMPERATURE (C)	SALINITY (PPT)	DENSITY (KG/M3)
0	6.74	23.393	1017.50
9	6.63	23.023	1018.09
18	6.74	24.816	1019.48
28	15.35	37.883	1020.13
48	15.53	38.409	1020.50
71	15.32	38.499	1020.61
95	15.07	38.537	1020.70
142	14.79	38.568	1020.79
190	14.71	38.568	1020.80
280	14.48	38.557	1020.85
478	14.44	38.547	1020.85
575	14.41	38.562	1020.87

STATION NUMBER 8
 LONGITUDE 23 36 36
 LATITUDE 41 53 48
 CORRESPONDING GRID LOCATION (30,14)
 DATE OF SAMPLING 23/02/1982
 MAXIMUM DEPTH (M) 174
 WIND
 DIRECTION 40
 SPEED (M/S) 6.130
 PRESSURE (MBAR) 1006
 TEMPERATURE (C)
 DRY BULB 9.7
 WET BULB 9.5

DEPTH (M)	TEMPERATURE (C)	SALINITY (PPT)	DENSITY (KG/M3)
0	6.27	21.555	1010.97
10	6.20	21.543	1010.97
20	6.70	23.850	1010.73
30	7.30	25.249	1019.75
50	14.34	37.987	1020.44
75	15.38	38.465	1020.57
100	15.26	38.517	1020.64
150	15.00	38.552	1020.73

STATION NUMBER 9
 LONGITUDE 28 17 36
 LATITUDE 40 54 06
 CORRESPONDING GRID LOCATION (25,14)
 DATE OF SAMPLING 28/02/1982
 MAXIMUM DEPTH (M) 308
 WIND
 DIRECTION 40
 SPEED (M/S) 8.240
 PRESSURE (MBAR) 1006
 TEMPERATURE (C)
 DRY BULB 9.7
 WET BULB 9.5

DEPTH (M)	TEMPERATURE (C)	SALINITY (PPT)	DENSITY (KG/M3)
0	6.78	23.530	1010.48
9	6.78	23.593	1010.52
10	6.90	24.160	1010.95
27	6.86	25.905	1020.32
44	15.47	38.393	1020.50
67	15.21	38.559	1020.68
93	15.02	38.597	1020.76
133	14.81	38.623	1020.82
170	14.60	38.597	1020.85

STATION NUMBER 10
 LONGITUDE 28 17 00
 LATITUDE 40 44 30
 CORRESPONDING GRID LOCATION (24,11)
 DATE OF SAMPLING 27/02/1982
 MAXIMUM DEPTH (M) 510

WIND
 DIRECTION 90
 SPEED (M/S) 2.575
 PRESSURE (MBAR) 1006
 TEMPERATURE (C)
 DRY BULB 7.0
 WET BULB 6.0

DEPTH (M)	TEMPERATURE (C)	SALINITY (PPT)	DENSITY (KG/M3)
0	6.65	23.304	1010.35
7	6.79	25.006	1019.62
10	6.87	25.630	1020.11
24	6.78	25.729	1020.19
40	15.50	38.186	1020.33
62	15.30	38.017	1020.71
81	15.02	38.603	1020.76
123	14.85	38.012	1020.81
165	14.69	38.659	1020.88
250	14.49	38.689	1020.95

STATION NUMBER 11
 LONGITUDE 28 16 54
 LATITUDE 40 37 18
 CORRESPONDING GRID LOCATION (24, 8)
 DATE OF SAMPLING 27/02/1982
 MAXIMUM DEPTH (M) 76
 WIND
 DIRECTION 90
 SPEED (M/S) 2.575
 PRESSURE (MBAR) 1006
 TEMPERATURE (C)
 DRY BULB 7.5
 WET BULB 6.1

DEPTH (M)	TEMPERATURE (C)	SALINITY (PPT)	DENSITY (KG/M ³)
0	6.57	23.259	1016.28
10	7.00	24.412	1019.13
20	6.86	25.117	1019.70
30	9.44	30.531	1025.60
50	15.55	33.441	1026.52

STATION NUMBER 12
 LONGITUDE 28 17 36
 LATITUDE 40 27 10
 CORRESPONDING GRID LOCATION (25, 5)
 DATE OF SAMPLING 27/02/1982
 MAXIMUM DEPTH (M) 50
 WIND

DIRECTION 25
 SPEED (M/S) 0.515
 PRESSURE (MBAR) 1005
 TEMPERATURE (C)
 DRY BULB 9.8
 WET BULB 9.6

DEPTH (M)	TEMPERATURE (C)	SALINITY (PPT)	DENSITY (KG/M ³)
0	6.75	22.849	1017.94
10	6.96	25.033	1019.62
20	6.86	25.511	1020.01
30	11.33	33.913	1025.80

STATION NUMBER 13
 LONGITUDE 23 57 05
 LATITUDE 40 37 06
 CORRESPONDING GRID LOCATION (19,08)
 DATE OF SAMPLING 27/02/1982
 MAXIMUM DEPTH (M) 53
 WIND
 DIRECTION 90
 SPEED (M/S) 1.030
 PRESSURE (MBAR) 1007
 TEMPERATURE (C)
 DRY BULB 11.0
 WET BULB 8.6

DEPTH (M)	TEMPERATURE (C)	SALINITY (PPT)	DENSITY (KG/M3)
0	7.50	23.253	1010.65
10	7.15	24.811	1019.43
20	7.49	25.759	1020.13
30	14.74	37.494	1027.97

STATION NUMBER 14
 LONGITUDE 27 38 30
 LATITUDE 40 22 48
 CORRESPONDING GRID LOCATION (19,11)
 DATE OF SAMPLING 27/02/1982
 MAXIMUM DEPTH (M) 1000
 WIND

 DIRECTION 45
 SPEED (M/S) 10.3
 PRESSURE (MBAR) 1007
 TEMPERATURE (C)
 DRY BULB 9.5
 WET BULB 7.5

DEPTH (M)	TEMPERATURE (C)	SALINITY (PPT)	DENSITY (KG/M3)
0	6.75	24.419	1019.10
9	6.69	24.532	1019.20
19	6.07	25.418	1019.90
28	8.12	27.915	1021.73
47	15.30	33.447	1020.58
71	15.11	38.535	1020.69
95	14.75	38.553	1020.74
142	14.73	38.551	1020.78
190	14.61	38.560	1020.82
235	14.45	38.552	1020.83
478	14.42	38.548	1020.85
570	14.42	38.560	1020.80
774	14.45	38.541	1020.84

STATION NUMBER 15
 LONGITUDE 27 53 00
 LATITUDE 40 52 50
 CORRESPONDING GRID LOCATION (19,14)
 DATE OF SAMPLING 23/02/1932
 MAXIMUM DEPTH (M) 1150
 WIND
 DIRECTION 70
 SPEED (M/S) .000
 PRESSURE (MBAR) 1005
 TEMPERATURE (C)
 DRY BULB 7.5
 WET BULB 5.0

DEPTH (M)	TEMPERATURE (C)	SALINITY (PPT)	DENSITY (KG/M3)
0	7.19	24.950	1019.49
0	7.12	24.912	1019.51
14	7.09	24.901	1019.57
21	7.10	25.251	1019.97
34	15.31	36.014	1020.24
50	15.32	33.493	1020.61
60	15.10	38.525	1020.66
100	14.92	33.502	1020.75
141	14.75	33.530	1020.79
217	14.53	36.540	1020.85

STATION NUMBER 16
 LONGITUDE 27 38 30
 LATITUDE 40 44 42
 CORRESPONDING GRID LOCATION (14,11)
 DATE OF SAMPLING 23/02/1932
 MAXIMUM DEPTH (M) 600
 WIND
 DIRECTION 45
 SPEED (M/S) 4.300
 PRESSURE (MBAR) 1000
 TEMPERATURE (C)
 DRY BULB 5.0
 WET BULB 5.0

DEPTH (M)	TEMPERATURE (C)	SALINITY (PPT)	DENSITY (KG/M3)
0	6.72	24.222	1019.02
0	6.63	24.210	1019.01
17	6.57	24.277	1019.00
20	7.17	25.349	1019.65
40	15.42	38.202	1020.41
67	15.30	38.517	1020.63
80	15.09	36.503	1030.93
130	15.88	38.016	1020.80
177	15.65	33.624	1020.80
267	15.59	36.625	1020.80

STATION NUMBER 17
 LONGITUDE 27 33 30
 LATITUDE 40 52 06
 CORRESPONDING GRID LOCATION (14,14)
 DATE OF SAMPLING 23/02/1982
 MAXIMUM DEPTH (M) 1040
 WIND
 DIRECTION 45
 SPEED (M/S) 6.690
 PRESSURE (MBAR) 1006
 TEMPERATURE (C)
 DRY BULB 7.5
 WET BULB 5.0

DEPTH (M)	TEMPERATURE (C)	SALINITY (PPT)	DENSITY (KG/M3)
0	6.61	24.237	1019.02
2	6.58	23.810	1018.71
10	6.58	24.427	1019.19
27	7.26	25.436	1019.88
45	15.23	38.252	1020.44
67	15.20	38.515	1020.65
89	15.04	38.549	1020.72
135	14.36	38.573	1020.70
181	14.63	38.583	1020.82
274	14.50	38.577	1020.80
465	14.43	38.585	1020.88

STATION NUMBER 18
 LONGITUDE 27 25 54
 LATITUDE 40 40 13
 CORRESPONDING GRID LOCATION (10,09)
 DATE OF SAMPLING 23/02/1982
 MAXIMUM DEPTH (M) 140
 WIND
 DIRECTION 45
 SPEED (M/S) 6.180
 PRESSURE (MBAR) 1006
 TEMPERATURE (C)
 DRY BULB 8.0
 WET BULB 5.0

DEPTH (M)	TEMPERATURE (C)	SALINITY (PPT)	DENSITY (KG/M3)
0	7.20	24.563	1019.25
10	7.21	24.570	1019.25
20	6.82	24.879	1019.52
30	7.18	24.930	1020.30
50	15.21	38.271	1020.40
75	15.21	38.506	1020.64
100	14.80	38.535	1020.70

STATION NUMBER 19
 LONGITUDE 27 24 00
 LATITUDE 40 33 55
 CORRESPONDING GRID LOCATION (10, 7)
 DATE OF SAMPLING 23/02/1982
 MAXIMUM DEPTH (M) 07
 WIND
 DIRECTION 45
 SPEED (M/S) 7.725
 PRESSURE (HBAR) 1006
 TEMPERATURE (C)
 DRY BULB 8.0
 WET BULB 5.5

DEPTH (M)	TEMPERATURE (C)	SALINITY (PPT)	DENSITY (KG/M3)
0	6.38	25.394	1019.92
10	6.85	25.381	1019.91
20	6.70	25.634	1020.12
30	14.02	37.234	1027.90
50	15.12	38.343	1020.54

STATION NUMBER 20
 LONGITUDE 27 30 24
 LATITUDE 40 32 48
 CORRESPONDING GRID LOCATION (14, 7)
 DATE OF SAMPLING 27/02/1982
 MAXIMUM DEPTH (M) 02
 WIND

DIRECTION 80
 SPEED (M/S) 2.575
 PRESSURE (HBAR) 1007
 TEMPERATURE (C)
 DRY BULB 9.9
 WET BULB 7.1

DEPTH (M)	TEMPERATURE (C)	SALINITY (PPT)	DENSITY (KG/M3)
0	7.50	25.921	1010.69
10	7.30	24.707	1010.69
20	7.20	25.499	1019.95
30	11.43	33.932	1020.79
50	14.39	38.515	1020.72

STATION NUMBER 21
 LONGITUDE 27 30 42
 LATITUDE 40 22 50
 CORRESPONDING GRID LOCATION (14,03)
 DATE OF SAMPLING 27/02/1982
 MAXIMUM DEPTH (M) 36
 WIND
 DIRECTION 315
 SPEED (M/S) .515
 PRESSURE (MDAP) 1006
 TEMPERATURE (C)
 DRY BULB 9.5
 WET BULB 7.5

DEPTH (M)	TEMPERATURE (C)	SALINITY (PPT)	DENSITY (KG/M3)
0	7.55	25.543	1019.95
10	6.81	25.366	1020.29
20	6.77	25.888	1020.32
30	11.26	33.713	1025.75

STATION NUMBER 22
 LONGITUDE 27 30 42
 LATITUDE 40 22 43
 CORRESPONDING GRID LOCATION (11, 3)
 DATE OF SAMPLING 27/02/1982
 MAXIMUM DEPTH (M) 42
 WIND
 DIRECTION 30
 SPEED (M/S) .515
 PRESSURE (MDAP) 1006
 TEMPERATURE (C)
 DRY BULB 12.0
 WET BULB 9.2

DEPTH (M)	TEMPERATURE (C)	SALINITY (PPT)	DENSITY (KG/M3)
0	7.53	25.646	1020.04
10	6.75	25.949	1020.37
20	6.76	26.124	1020.50
30	13.72	36.591	1027.47

STATION NUMBER 23
 LONGITUDE 27 11 36
 LATITUDE 40 33 00
 CORRESPONDING GRID LOCATION (6, 7)
 DATE OF SAMPLING 27/02/1982
 MAXIMUM DEPTH (M) 07
 WIND
 DIRECTION 45
 SPEED (M/S) 8.240
 PRESSURE (MDAP) 1006
 TEMPERATURE (C)
 DRY BULB 8.0
 WET BULB 5.5

DEPTH (M)	TEMPERATURE (C)	SALINITY (PPT)	DENSITY (KG/M3)
0	6.03	25.380	1019.90
10	6.05	25.421	1019.43
20	6.85	25.692	1020.15
30	13.78	35.495	1026.78
50	15.05	38.530	1028.70

STATION NUMBER 24
 LONGITUDE 27 00 12
 LATITUDE 40 30 48
 CORRESPONDING GRID LOCATION (3, 6)
 DATE OF SAMPLING 27/02/1982
 MAXIMUM DEPTH (M) 52
 WIND
 DIRECTION 75
 SPEED (M/S) 6.130
 PRESSURE (MBAR) 1006
 TEMPERATURE (C)
 DRY BULB 8.5
 WET BULB 6.0

DEPTH (M)	TEMPERATURE (C)	SALINITY (PPT)	DENSITY (KG/M3)
0	6.87	25.152	1019.71
10	6.85	25.167	1019.74
20	6.80	25.301	1019.85
30	13.67	37.382	1020.11

STATION NUMBER 25
 LONGITUDE 26 49 24
 LATITUDE 40 28 18
 CORRESPONDING GRID LOCATION OUT OF GRID
 DATE OF SAMPLING 27/02/1982
 MAXIMUM DEPTH (M) 23
 WIND
 DIRECTION 145
 SPEED (M/S) 2.575
 PRESSURE (MBAR) 1006
 TEMPERATURE (C)
 DRY BULB 9.9
 WET BULB 9.7

DEPTH (M)	TEMPERATURE (C)	SALINITY (PPT)	DENSITY (KG/M3)
0	7.09	25.221	1019.70
10	7.00	25.217	1019.76
20	6.70	25.559	1020.07

APPENDIX II
COMPUTER PROGRAM LISTING

```

PROGRAM HAR(BDND1,CABS1,RES1,VHRD1,RD1,TAPE10=BDND1,TAPE9=CA
*TAPE12=RES1,TAPE11=VHRD1,TAPE13=RD1)
DIMENSION IDM(43,19),IRR(5),ISCA(43,19),JSCA(43,19),h3(43,19)
COMMON /S1/IP,IM,IXP,IXM
COMMON /S2/JP,JM,JYP,JYM
COMMON /S3/H1(43,19),U1(43,19),V1(43,19),H2(43,19),U2(43,19)
*J2(43,19)
COMMON /S4/H12(43,19),U12(43,19),V12(43,19),H22(43,19)
*U22(43,19),V22(43,19)
COMMON /S5/NU(43,19),DB(43,19)
COMMON /S6/SX(43,19),SY(43,19)
COMMON /S7/AS,R1,R2,R3,R4,R5,R6,R7,RI,RB,RWX,RWY,GR
H1B(TA,GR,TT,CSE)=CSE-(TA*GR/TT)
H2D(TA,DIFL,TT,DUL)=DUL-(TA*DIFL/TT)
INITIALIZATION
G=7.81
JD=1019.28
JD=1028.65
CA=0.0001
DI=5000.
IPFD=IDI=IDT=IGR=ITT=ICTI=IDIS=0
IRI=INR=ITA=IPM=0
IRR(1)=IRR(2)=IRR(3)=IRR(4)=IRR(5)=0
IEV=IPD=0
IT=0.0
DO 11 I=1,43
DO 11 J=1,19
H1(I,J)=H12(I,J)=0.0
U1(I,J)=V1(I,J)=0.0
H2(I,J)=U2(I,J)=V2(I,J)=0.0
J12(I,J)=V12(I,J)=0.0
H22(I,J)=U22(I,J)=V22(I,J)=0.0
DB(I,J)=SX(I,J)=SY(I,J)=0
ISCA(I,J)=JSCA(I,J)=0
IDM(I,J)=NU(I,J)=0
11 CONTINUE
A1=CS=J.0
AR14=AR15=AR16=0.0
A14=A15=A16=0.0
UD14=UD15=UD16=0.0
UB35=UB36=UB37=0.0
A35=A36=A37=0.0
AB35=AB36=AB37=0.0
AD14=AD15=AD16=0.0
BL35=BL36=BL37=0.0
AR1=A2=D1=D2=0.0
QLD=QU0=QLB=QUB=1.0
NIH=NIP=NJM=NJP=0
IP=IM=IXP=IXM=0
JP=JM=JYP=JYM=0
NIP=NIH=NJP=NJM=1
K=L=IER=1=0
ISC=JSC=0
R1=R2=R3=R4=R5=R6=R7=R8=0.0
AS=W=AW=0.0
RWX=RWY=ISX=WSY=1.0
RI=RB=DT=0.0

```

```

INPUT FROM DATA FILES
FILE CABS
READ(9,90) IEN, CS
90 FORMAT(1X, I3, //, 1X, F7.5)
READ(9,88) SLX, SLY, SN
88 FORMAT(1X, F7.5, //, 1X, F7.5, //, 1X, F4.1)
READ(9,93) GR
93 FORMAT(1X, F5.3)
READ(9,94) DI FL, DUL
94 FORMAT(1X, F5.1, //, 1X, F6.1)
READ(9,171) C, FI
171 FORMAT(1X, F5.1, //, 1X, F7.5)
READ(9,92) W, AW
92 FORMAT(1X, F6.3, //, 1X, F5.1)
READ(9,95) UD14, UD15, UD16, A14, A15, A16
READ(9,95) UB35, UB36, UB37, A35, A36, A37
95 FORMAT(3(1X, F6.3, //), 1X, F5.1, //, 1X, F5.1, //, 1X, F5.1)
READ(9,96) AS, DT, TT
96 FORMAT(/, 1X, F4.1, //, 1X, F5.1, //, 1X, F8.1, //)
READ(9,97) INR, (IRR(I), I=1,5)
97 FORMAT(1X, I1, //, 5(1X, I5, //))
FILE BOND
DO 532 I=1,43
READ(10,99) (NU(I,J), J=1,19)
532 CONTINUE
99 FORMAT(5X, 19I2)
DO 10 I=1,43
READ(10,98) (IDM(I,J), J=1,19)
10 CONTINUE
98 FORMAT(1X, 19I4)
DO 283 I=1,43
DO 283 J=1,19
UB(I,J)=FLOAT(IDM(I,J))
283 CONTINUE
INPUT FROM VHRD
READ(11,300) IEN1
300 FORMAT(50X, I3)
DO 15 I=1,43
READ(11,190) (U1(I,J), J=1,19)
READ(11,190) (V1(I,J), J=1,19)
READ(11,190) (U2(I,J), J=1,19)
READ(11,190) (V2(I,J), J=1,19)
15 CONTINUE
190 FORMAT(1X, 19F6.3)
DO 191 I=1,43
DO 191 J=1,19
U12(I,J)=U1(I,J)
V12(I,J)=V1(I,J)
U22(I,J)=U2(I,J)
V22(I,J)=V2(I,J)
191 CONTINUE

```

```

LAND BOUNDARY CONFIGURATIONS
DO 330 I=1,42
DO 330 J=2,18
IF(NU(I,J).EQ.0)GO TO 331
IF(NU(I,J).EQ.-1)GO TO 332
GO TO 330
332 ISCA(I,J)=4
JSCA(I,J)=4
GO TO 330
331 NIP=NU(I+1,J)
NIM=NU(I-1,J)
ISCA(I,J)=NTD(NIP,NIM)
NJP=NU(I,J+1)
NJM=NU(I,J-1)
JSCA(I,J)=NTD(NJP,NJM)
330 CONTINUE
DO 310 I=1,43
DO 310 J=1,19
H12(I,J)=H1(I,J)=CSE=1400.+GR
H22(I,J)=H2(I,J)=DUL
310 CONTINUE
INITIAL COMPUTATIONS
BOUNDARY CONDITIONS
DARDANELLEN BOUNDARY
J2(1,4)=U22(1,4)=UD14*COSD(450.-A14)
J2(1,5)=J22(1,5)=UD15*COSD(450.-A15)
U2(1,6)=J22(1,6)=UD16*COSD(450.-A16)
V2(1,4)=V22(1,4)=UD14*SIND(450.-A14)
V2(1,5)=V22(1,5)=UD15*SIND(450.-A15)
V2(1,6)=V22(1,6)=UD16*SIND(450.-A16)
BOSPHORUS BOUNDARY
J1(35,16)=U12(35,16)=UB35*COSD(450.-A35)
J1(36,16)=U12(36,16)=UB36*COSD(450.-A36)
U1(37,16)=U12(37,16)=UB37*COSD(450.-A37)
V1(35,16)=V12(35,16)=UB35*SIND(450.-A35)
V1(36,16)=V12(36,16)=UB36*SIND(450.-A36)
V1(37,16)=V12(37,16)=UB37*SIND(450.-A37)
WIND FIELD
WSX=.00067*(W**(2.44))*COSD(450.-AW)
WSY=.00067*(W**(2.44))*SIND(450.-AW)
SHORT NOTATIONS
R1=1./(AS+2.)
R2=DT/(2.*DI)
R3=R2*G
R4=R3*(UD/BD)*CS
R5=R3*((BD-UD)/BD)
R6=DT*CA
R7=(BD-UD)/BD
RWX=WSX*DT/UD
RWY=WSY*DT/UD
RI=DT*FI
RB=DT*G/(C**2.)

```

```

OUTPUT FILE
IDI=INT(DI)
ITT=INT(TT)
IDT=INT(DT)
ICTI=ITT/IDT
IDIS=0
WRITE(12,200)IEN,ITT,DIS,IDT,ICTI,IDI
200 FORMAT(//,40X,20HRESULTS OF EXECUTION,1X,I3,//,30X,
*15HSIMULATION TIME,1X,I6,1X,7HSECONDS,/,30X,
*32HMAXIMUM ALLOWABLE TIME INCREMENT,1X,I3,1X,7HSECONDS,/,30X,
*23HTIME INCREMENT EMPLOYED,1X,I3,1X,7HSECONDS,/,30X,
*34HCORRESPONDING NUMBER OF ITERATIONS,1X,I4,/,30X,13HGRID DISTAN
*,1X,I4,1X,6HMETERS,/)
254 WRITE(12,202)UD,BD
202 FORMAT(/,30X,19HUPPER LAYER DENSITY,1X,F7.2,1X,7HKG/M**3,
/,30X,19HLOWER LAYER DENSITY,1X,F7.2,1X,7HKG/M**3)
WRITE(12,203)CA
203 FORMAT(30X,22HCORIOLIS ACCELERATION=,1X,F6.4,1X,5H1/SEC,/)
WRITE(12,204)W,AW
204 FORMAT(30X,11HWIND SPEED=,1X,F6.3,1X,5HM/SEC,/,30X,
*11HWIND ANGLE=,1X,F5.1,1X,7HDEGREES,/)
WRITE(12,205)C,FI
205 FORMAT(30X,36HCHEZY'S BOTTOM FRICTION COEFFICIENT=,1X,F5.1,
*1X,10HN**0.5/SEC,/,30X,33HINTERFACIAL FRICTION COEFFICIENT=,
*1X,F7.5,/)
WRITE(12,206)GR
206 FORMAT(30X,17HSEA LEVEL EXCESS ,F6.2,1X,6HMETERS)
WRITE(12,207)
207 FORMAT(//,30X,41HBOUNDARY CONDITIONS AT BOSPHORUS ENTRANCE,/,30X
*41(1H-),/,30X,34HVELOCITIES AT THREE BOUNDARY NODES,/,30X,
*11HUPPER LAYER,/,20X,4HNODE,5X,21HCURRENT SPEED (M/SEC),5X,
*30HDIRECTION (NORTH IS 0 DEGREES),/20X,4(1H-),5X,21(1H-),5X
*,30(1H-),/)
WRITE(12,208)UB35,A35,UB36,A36,UB37,A37
208 FORMAT(19X,7H(35,16),8X,F6.3,10X,F5.1,/,19X,7H(36,16),8X,F6.3,1
*,F5.1,/,19X,7H(37,16),8X,F6.3,10X,F5.1,/)
WRITE(12,209)
209 FORMAT(30X,43HBOUNDARY CONDITIONS AT DARDANELLEN ENTRANCE,/,30X
*43(1H-),/,30X,34HVELOCITIES AT THREE BOUNDARY NODES,/,30X,
*11HUPPER LAYER,/,20X,4HNODE,5X,21HCURRENT SPEED (M/SEC),5X,
*30HDIRECTION (NORTH IS 0 DEGREES),/20X,4(1H-),5X,21(1H-),5X
*,30(1H-),/)
WRITE(12,210)UD14,A14,UD15,A15,UD16,A16
210 FORMAT(19X,7H(1,4),8X,F6.3,10X,F5.1,/,19X,7H(1,5),8X,F6.3,1
*,F5.1,/,19X,7H(1,6),8X,F6.3,10X,F5.1,/)
WRITE(12,211)INR
211 FORMAT(/,30X,26HRESULTS HAVE BEEN PRINTED ,11,1X,5HTIMES,/)

```

```

COMPUTATIONS
DO 1 L=1,INR
IRI=IRR(L)/INT(DT)
DO 2 K=1,IRI
ITA=ITA+IDT
TA=FLOAT(ITA)
H1(1,4)=H1(1,5)=H1(1,6)=H1B(TA,GR,TT,CSE)
H12(1,4)=H12(1,5)=H12(1,6)=H1B(TA,GR,TT,CSE)
H2(35,16)=H2(36,16)=H2(37,16)=H2D(TA,DIFL,TT,DUL)
H22(35,16)=H22(36,16)=H22(37,16)=H2D(TA,DIFL,TT,DUL)
FIRST TIME STEP
DO 7 I=1,42
DO 7 J=2,13
IF(NU(I,J).EQ.-2)GO TO 7
IF(NU(I,J).EQ.2)GO TO 53
IF(NU(I,J).EQ.7)GO TO 54
FREE NODE
59 IP=I+1
IM=I-1
IXP=IXM=1
GO TO 55
LAND BOUNDARY NODE
54 ISC=ISCA(I,J)
GO TO(56,57,58,59)ISC
56 IP=I+1
IM=I
IXP=1
IXM=-1
GO TO 55
57 IP=I
IM=I-1
IXP=-1
IXM=1
GO TO 55
58 IP=IM=I
IXP=IXM=-1
GO TO 55
BOUNDARY CONDITIONS
55 IF(J.EQ.16)GO TO 60
DARDANELLEN NODES
FORWARD DIFFERENCES
H22(I,J)=R1*(AS*H2(I,J)+H2(I,J)+H2(I+1,J))-R2*(H2(I,J)-
*DB(I,J))*(U2(I+1,J)-U2(I,J))-R2*U2(I,J)*(H2(I+1,J)-H2(I,J))
*-DB(I+1,J)+DB(I,J))
U12(I,J)=R1*(AS*U1(I,J)+U1(I+1,J)+U1(I,J))-R3*(H1(I+1,J)-H1
V12(I,J)=R1*(AS*V1(I,J)+V1(I+1,J)+V1(I,J))
GO TO 7
BOSPHORUS NODES
60 IF(I.EQ.35)GO TO 71
IF(I.EQ.37)GO TO 72
IP=J+1
IM=I-1
IXP=IXM=1
GO TO 73
72 IP=I

```

```

73 H12(I,J)=P1*(H1(IP,J)+H1(IM,J)+AS*H1(I,J))-R2*(H1(I,J)-
*H2(I,J))*(IXP*U1(IP,J)-IXM*U1(IM,J))-R2*U1(I,J)
***(H1(IP,J)-H1(IM,J)-H2(IP,J)+H2(IM,J))
U22(I,J)=P1*(IXP*U2(IP,J)+IXM*U2(IM,J)+AS*U2(I,J))-
*R2*U2(I,J)*(IXP*U2(IP,J)-IXM*U2(IM,J))-R4*(H1(IP,J)-
*H1(IM,J))-R5*(H2(IP,J)-H2(IM,J))
V22(I,J)=P1*(V2(IP,J)+V2(IM,J)+AS*V2(I,J))-R2*U2(I,J)*
*(V2(IP,J)-V2(IM,J))
GO TO 7
SUBROUTINE ROUTING
55 CALL FTS(I,J)
7 CONTINUE
SECOND TIME STEP
DO 9 I=1,42
DO 9 J=2,13
IF(NU(I,J).EQ.-2)GO TO 9
IF(NU(I,J).EQ.2)GO TO 62
IF(NU(I,J).EQ.0)GO TO 63
FREE NODE
69 JP=J+1
JM=J-1
JYP=JYM=1
GO TO 65
LAND BOUNDARY NODE
65 JSC=JSCA(I,J)
GO TO(66,67,68,69)JSC
66 JP=J+1
JM=J
JYP=1
JYM=-1
GO TO 65
67 JP=J
JM=J-1
JYP=-1
JYM=1
GO TO 65
68 JP=JM=J
JYP=JYM=-1
GO TO 65
BOUNDARY CONDITIONS
62 IF(J.EQ.1)GO TO 74
BOSPHORUS ENTRANCE
IF(J.EQ.36)GO TO 16
GO TO 17
BACKWARD DIFFERENCES
10 H1(I,J)=(1./(AS+1.))*(H12(I,J)*AS+H12(I,J-1))-(DT/DI)*
*(H12(I,J)-H22(I,J))*(V12(I,J)-V12(I,J-1))-(DT/DI)*
*(H12(I,J)-H12(I,J-1)-DB(I,J)+DB(I,J-1))*V12(I,J)
U2(I,J)=(1./(AS+1.))*(U22(I,J)*AS+U22(I,J-1))+CA*DT*V22(I,J)
*-(DT/DI)*V22(I,J)*(U22(I,J)-U22(I,J-1))-(DT*G*U22(I,J))*
*SQR(U22(I,J)**2.+V22(I,J)**2.)/(C**2.)*(H22(I,J)-DB(I,J))
*(SQR(U22(I,J)**2.+V22(I,J)**2.)*(U12(I,J)-U22(I,J))*DT*F
*/(H22(I,J)-DB(I,J))
V2(I,J)=(1./(AS+1.))*(V22(I,J)*AS+V22(I,J-1))-CA*DT*U22(I,J)
*-(DT/DI)*V22(I,J)*(V22(I,J)-V22(I,J-1))-(DT/DI)*G*(UD/BD)
*(H12(I,J)-H12(I,J-1))-(DT/DI)*G*((BD-UD)/BD)*(H22(I,J)-
*H22(I,J-1))-(DT*G*V22(I,J))*
*SQR(U22(I,J)**2.+V22(I,J)**2.)/(C**2.)*(H22(I,J)-DB(I,J))
*(SQR(U22(I,J)**2.+V22(I,J)**2.)*(V12(I,J)-V22(I,J))*DT*F
*/(H22(I,J)-DB(I,J))

```

CENTRAL DIFFERENCES

```

17 JP=J
   JM=J-1
   JYP=-1
   JYM=1
   A2=SQRT((U22(I,J)*U22(I,J))+(V22(I,J)*V22(I,J)))/
   *(H22(I,J)-DB(I,J))
   H1(I,J)=R1*(H12(I,JP)+H12(I,JM)+AS*H12(I,J))
   *-R2*(H12(I,J)-H22(I,J))*(JYP*V12(I,JP)-JYM*V12(I,JM))
   *-R2*V12(I,J)*(H12(I,JP)-H12(I,JM)-H22(I,JP)+H22(I,JM))
   U2(I,J)=R1*(U22(I,JP)+U22(I,JM)+AS*U22(I,J))+R6*V22(I,J)
   *-R2*V22(I,J)*(U22(I,JP)-U22(I,JM))-R3*A2*U22(I,J)
   *-RI*A2*ABS(U12(I,J)-U22(I,J))
   V2(I,J)=R1*(JYP*V22(I,JP)+JYM*V22(I,JM)+AS*V22(I,J))
   *-R5*U22(I,J)-R2*V22(I,J)*(JYP*V22(I,JP)-JYM*V22(I,JM))
   *-R4*(H12(I,JP)-H12(I,JM))-R5*(H22(I,JP)-H22(I,JM))-R6*A2
   *V22(I,J)-RI*A2*ABS(V12(I,J)-V22(I,J))
   GO TO 9
DARDANELLEN ENTRANCE
74 IF(J.EQ.4)GO TO 77
   IF(J.EQ.5)GO TO 78
   JP=J
   JM=J-1
   JYP=-1
   JYM=1
   GO TO 18
78 JP=J+1
   JM=J-1
   JYP=JYM=1
   GO TO 18
77 JP=J+1
   JM=J
   JYP=1
   JYM=-1
16 A1=SQRT((U12(I,J)*U12(I,J))+(V12(I,J)*V12(I,J)))/
   *(H12(I,J)-H22(I,J))
   H2(I,J)=R1*(H22(I,JP)+H22(I,JM)+AS*H22(I,J))-R2*(H22(I,J)
   *-DB(I,J))*(JYP*V22(I,JP)-JYM*V22(I,JM))-R2*V22(I,J)
   *(H22(I,JP)-H22(I,JM)-DB(I,JP)+DB(I,JM))
   U1(I,J)=R1*(U12(I,JP)+U12(I,JM)+AS*U12(I,J))+R6*V12(I,J)
   *-R1X/(H12(I,J)-H22(I,J))-RI*A1*ABS(U12(I,J)-U22(I,J))
   V1(I,J)=R1*(JYP*V12(I,JP)+JYM*V12(I,JM)+AS*V12(I,J))-R6*U12(I,J)
   *-R3*(H12(I,JP)-H12(I,JM))
   *-R1Y/(H12(I,J)-H22(I,J))-RI*A1*ABS(V12(I,J)-V22(I,J))
   GO TO 9
SUBROUTINE ROUTING
65 CALL STS(I,J)
   9 CONTINUE
   2 CONTINUE
   CALL RESULT(ITA)
   1 CONTINUE
   RESULT DUMPING
   CALL RESDUMP(IEN)
   STOP
   _END

```

```

SUBROUTINE RESULT(ITA)
DIMENSION NI(43),IDU(43,19),IHF1(43,19),IDLL(43,19)
COMMON /S3/H1(43,19),U1(43,19),V1(43,19),H2(43,19)
*,U2(43,19),V2(43,19)
COMMON /S5/NU(43,19),DB(43,19)
COMMON /S8/QLD,QUD,QLB,QUB
INITIALIZATION
DO 543 I=1,43
NI(I)=1
543 CONTINUE
DO 100 I=1,43
DO 100 J=1,19
IDU(I,J)=IHF1(I,J)=IDLL(I,J)=0
100 CONTINUE
I1=I7=I8=I9=0
NOS=NH=NM=NS=N1=N2=N3=0
DO 101 I=1,43
DO 101 J=1,19
IF(NU(I,J).EQ.-2)GO TO 102
IDU(I,J)=INT(H1(I,J)-H2(I,J))
IHF1(I,J)=INT((H1(I,J)-1400.)*100.)
IDLL(I,J)=INT(H2(I,J)-DB(I,J))
GO TO 101
102 IDU(I,J)=IHF1(I,J)=IDLL(I,J)=1000000
101 CONTINUE
DO 544 I=1,43
DO 544 J=1,19
IF(NU(I,J).EQ.-2)GO TO 545
GO TO 544
545 U1(I,J)=V1(I,J)=U2(I,J)=V2(I,J)=10000000.
544 CONTINUE
OUTPUT FILE
CONVERSION TO HOURS
NOS=ITA
NH=INT(NOS/3600)
N1=NH*3600
N2=NOS-N1
NM=INT(N2/60)
N3=NH*60
NS=N2-N3
WRITE(12,110)NOS,NH,NM,NS
110 FORMAT(///,40X,13HRESULTS AFTER,/
*,41X,12HELAPSED TIME,1X,15,1X,7HSECONDS,/,40X,I2,1X,
*5HHOURS,2X,I2,1X,7HMINUTES,2X,I2,1X,7HSECONDS)
VELOCITIES
WRITE(12,112)
112 FORMAT(4)X,41HUPPER LAYER HORIZONTAL VELOCITIES (M/SEC),/,/
*,41(1H=),//)
DO 113 J=19,1,-1
WRITE(12,130)J,(U1(I,J),I=1,15)
113 CONTINUE
WRITE(12,131)(NI(II),II=1,15)
DO 114 J=19,1,-1
WRITE(12,132)J,(U1(I,J),I=16,29)
114 CONTINUE
WRITE(12,133)(NI(II),II=16,29)

```

```

WRITE(12,133)(NI(II),II=30,43)
WRITE(12,510)
510 FORMAT(5(/),40X,39HUPPER LAYER VERTICAL VELOCITIES (M/SEC),
*,39(1H-),//)
DO 116 J=19,1,-1
WRITE(12,130)J,(V1(I,J),I=1,15)
116 CONTINUE
WRITE(12,131)(NI(II),II=1,15)
DO 117 J=19,1,-1
WRITE(12,132)J,(V1(I,J),I=16,29)
117 CONTINUE
WRITE(12,133)(NI(II),II=16,29)
DO 118 J=19,1,-1
WRITE(12,132)J,(V1(I,J),I=30,43)
118 CONTINUE
WRITE(12,133)(NI(II),II=30,43)
WRITE(12,119)
119 FORMAT(//////,40X,41HLOWER LAYER HORIZONTAL VELOCITIES (M/SEC)
*,//,40X,41(1H-),//)
DO 120 J=19,1,-1
WRITE(12,130)J,(U2(I,J),I=1,15)
120 CONTINUE
WRITE(12,131)(NI(II),II=1,15)
DO 121 J=19,1,-1
WRITE(12,132)J,(U2(I,J),I=16,29)
121 CONTINUE
WRITE(12,133)(NI(II),II=16,29)
DO 122 J=19,1,-1
WRITE(12,132)J,(U2(I,J),I=30,43)
122 CONTINUE
WRITE(12,133)(NI(II),II=30,43)
WRITE(12,123)
123 FORMAT(5(/),40X,39HLOWER LAYER VERTICAL VELOCITIES (M/SEC)
*,//,40X,40(1H-),//)
DO 124 J=19,1,-1
WRITE(12,130)J,(V2(I,J),I=1,15)
124 CONTINUE
WRITE(12,131)(NI(II),II=1,15)
DO 125 J=19,1,-1
WRITE(12,132)J,(V2(I,J),I=16,29)
125 CONTINUE
WRITE(12,133)(NI(II),II=16,29)
DO 126 J=19,1,-1
WRITE(12,132)J,(V2(I,J),I=30,43)
126 CONTINUE
WRITE(12,133)(NI(II),II=30,43)
130 FORMAT(1)X,I2,1X,1H0,3X,15(F5.3,2X))
131 FORMAT(16X,15(I2,5X),//)
132 FORMAT(1)X,I2,1X,1H0,3X,14(F5.3,2X))
133 FORMAT(16X,14(I2,5X),//)

```

HEIGHTS

UPPER LAYER DEPTH

WRITE(12,135)

```
135 FORMAT(////,40X,21HELEVATIONS AND DEPTHS,/,40X,21(1H-),////,
*40X,24HDEPTH OF UPPER LAYER (M),/,40X,24(1H-),///)
```

WRITE(12,138)(NI(II),II=1,22)

```
136 FORMAT(/,17X,22(I2,2X),/,17X,22(2H--,2X))
```

DO 136 J=19,1,-1

WRITE(12,137)J,(IDU(I,J),I=1,22)

```
137 FORMAT(10X,I2,1X,1H0,3X,22(I2,2X))
```

138 CONTINUE

WRITE(12,141)(NI(II),II=23,43)

```
141 FORMAT(/,17X,21(I2,2X),/17X,21(2H--,2X))
```

DO 139 J=19,1,-1

WRITE(12,140)J,(IDU(I,J),I=23,43)

```
140 FORMAT(10X,I2,1X,1H0,3X,21(I2,2X))
```

139 CONTINUE

LOWER LAYER DEPTH

WRITE(12,142)

```
142 FORMAT(////,40X,24HDEPTH OF LOWER LAYER (M),/,40X,24(1H-),///
```

WRITE(12,145)(NI(II),II=1,22)

```
145 FORMAT(/,13X,22(I2,3X),/,13X,22(2H--,3X))
```

DO 143 J=19,1,-1

WRITE(12,144)J,(IDL(I,J),I=1,22)

```
144 FORMAT(5X,I2,1X,1H0,3X,22(I4,1X))
```

143 CONTINUE

WRITE(12,146)(NI(II),II=23,43)

```
146 FORMAT(/,13X,21(I2,3X),/,13X,21(2H--,3X))
```

DO 147 J=19,1,-1

WRITE(12,148)J,(IDL(I,J),I=23,43)

```
148 FORMAT(5X,I2,1X,1H0,3X,21(I4,1X))
```

147 CONTINUE

FLUCTUATIONS

WRITE(12,149)

```
149 FORMAT(////,40X,39HFLUCTUATIONS AROUND MEAN SEA LEVEL (CM),/
*40X,39(1H-),///)
```

WRITE(12,150)(NI(II),II=1,22)

```
150 FORMAT(/,17X,22(I2,2X),/,17X,22(2H--,2X))
```

DO 151 J=19,1,-1

WRITE(12,152)J,(IHF1(I,J),I=1,22)

```
152 FORMAT(10X,I2,1X,1H0,3X,22(I2,2X))
```

151 CONTINUE

WRITE(12,153)(NI(II),II=23,43)

```
153 FORMAT(/,17X,21(I2,2X),/17X,21(2H--,2X))
```

DO 154 J=19,1,-1

WRITE(12,155)J,(IHF1(I,J),I=23,43)

```
155 FORMAT(10X,I2,1X,1H0,3X,21(I2,2X))
```

154 CONTINUE

RETURN

END

```

SUBROUTINE FTS(I,J)
COMMON /S1/IP,IM,IXP,IXM
COMMON /S3/H1(43,19),U1(43,19),V1(43,19),H2(43,19),U2(43,
*,V2(43,19)
COMMON /S4/H12(43,19),U12(43,19),V12(43,19),H22(43,19)
*,U22(43,19),V22(43,19)
COMMON /S5/NU(43,19),DB(43,19)
COMMON /S6/SX(43,19),SY(43,19)
COMMON /S7/AS,R1,R2,R3,R4,R5,R6,R7,RI,RB,RWX,RWY,GR
H12(I,J)=R1*(H1(IP,J)+H1(IM,J)+AS*H1(I,J))-R2*(H1(I,J)
*-H2(I,J))*(IXP*U1(IP,J)-IXM*U1(IM,J))-R2*U1(I,J)*
*(H1(IP,J)-H1(IM,J)-H2(IP,J)+H2(IM,J))
U12(I,J)=R1*(IXP*U1(IP,J)+IXM*U1(IM,J)+AS*U1(I,J))-R2*
*U1(I,J)*(IXP*U1(IP,J)-IXM*U1(IM,J))-R3*(H1(IP,J)-H1(IM,J)
V12(I,J)=R1*(V1(IP,J)+V1(IM,J)+AS*V1(I,J))-R2*U1(I,J)
***(V1(IP,J)-V1(IM,J))
H22(I,J)=R1*(H2(IP,J)+H2(IM,J)+AS*H2(I,J))-R2*(H2(I,J)-
*DB(I,J))*(IXP*U2(IP,J)-IXM*U2(IM,J))-R2*U2(I,J)
***(H2(IP,J)-H2(IM,J)-DB(IP,J)+DB(IM,J))
U22(I,J)=R1*(IXP*U2(IP,J)+IXM*U2(IM,J)+AS*U2(I,J))-
*R2*U2(I,J)*(IXP*U2(IP,J)-IXM*U2(IM,J))-R4*(H1(IP,J)-
*H1(IM,J))-R5*(H2(IP,J)-H2(IM,J))+SX(I,J)
V22(I,J)=R1*(V2(IP,J)+V2(IM,J)+AS*V2(I,J))-R2*U2(I,J)*
*(V2(IP,J)-V2(IM,J))
H12(I,J)=H12(I,J)+R7*(H22(I,J)-H2(I,J))
RETURN
END

```

```

SUBROUTINE STS(I,J)
COMMON /S2/JP,JM,JYP,JYM
COMMON /S3/H1(43,19),U1(43,19),V1(43,19),H2(43,19),U2(43,19)
*,V2(43,19)
COMMON /S4/H12(43,19),U12(43,19),V12(43,19),H22(43,19)
*,U22(43,19),V22(43,19)
COMMON /S5/NU(43,19),DB(43,19)
COMMON /S6/SX(43,19),SY(43,19)
COMMON /S7/AS,R1,R2,R3,R4,R5,R6,R7,RI,RB,RWX,RWY,GR
A1=SQRT((U12(I,J)*U12(I,J))+(V12(I,J)*V12(I,J)))/
*(H12(I,J)-H22(I,J))
H1(I,J)=R1*(H12(I,JP)+H12(I,JM)+AS*H12(I,J))-R2*(H12(I,J)
**H22(I,J))*(JYP*V12(I,JP)-JYM*V12(I,JM))-R2*V12(I,J)
***(H12(I,JP)-H12(I,JM)-H22(I,JP)+H22(I,JM))
U1(I,J)=R1*(U12(I,JP)+U12(I,JM)+AS*U12(I,J))+R6*V12(I,J)-
*R2*V12(I,J)*(U12(I,JP)-U12(I,JM))+RWX/(H12(I,J)-H22(I,J))-
*RI*A1*ABS(U12(I,J)-U22(I,J))
V1(I,J)=R1*(JYP*V12(I,JP)+JYM*V12(I,JM)+AS*V12(I,J))-R6*U12
**R2*V12(I,J)*(JYP*V12(I,JP)-JYM*V12(I,JM))-R3*(H12(I,JP)-
*H12(I,JM))+RWY/(H12(I,J)-H22(I,J))-RI*A1*ABS(V12(I,J)-V22(I
A2=SQRT((U22(I,J)*U22(I,J))+(V22(I,J)*V22(I,J)))/
*(H22(I,J)-DB(I,J))
H2(I,J)=R1*(H22(I,JP)+H22(I,JM)+AS*H22(I,J))
**R3*(H22(I,J)-DB(I,J))*(JYP*V22(I,JP)-JYM*V22(I,JM))
**R2*V22(I,J)*(H22(I,JP)-H22(I,JM)-DB(I,JP)+DB(I,JM))
U2(I,J)=R1*(U22(I,JP)+U22(I,JM)+AS*U22(I,J))+R6*V22(I,J)
**R2*V22(I,J)*(U22(I,JP)-U22(I,JM))-R3*U22(I,J)*A2
**RI*A2*ABS(U12(I,J)-U22(I,J))
V2(I,J)=R1*(JYP*V22(I,JP)+JYM*V22(I,JM)+AS*V22(I,J))
**R6*U22(I,J)-R2*V22(I,J)*(JYP*V22(I,JP)-JYM*V22(I,JM))
**R4*(H12(I,JP)-H12(I,JM))-R5*(H22(I,JP)-H22(I,JM))-R6*A2
**V22(I,J)-RI*A2*ABS(V12(I,J)-V22(I,J))+SY(I,J)
J=SQRT(FLOAT(I)**2.+FLOAT(J-4)**2.)
B1=SQRT(1492.)
B2=(B1-B)/B1
H1(I,J)=H1(I,J)+R7*(H2(I,J)-H22(I,J))-GR*B2/1782.
RETURN
END

```

```

FUNCTION NTD(I1,J1)
  IF(I1.EQ.-2) GO TO 131
  IF(J1.EQ.-2) GO TO 182
  NTD=4
  GO TO 190
132 NTD=1
  GO TO 190
181 IF(J1.EQ.-2) GO TO 133
  NTD=2
  GO TO 190
183 NTD=3
190 RETURN
  END

SUBROUTINE RESDUMP(IEN)
  COMMON /S3/H1(43,19),U1(43,19),V1(43,19),H2(43,19),U2(43,1
  *,V2(43,19)
  COMMON /S4/H12(43,19),U12(43,19),V12(43,19),H22(43,19)
  *,U22(43,19),V22(43,19)
  COMMON /S5/NU(43,19),DB(43,19)
  WRITE(13,700)IEN
700 FORMAT(/,20X,17HEXECUTION NUMBER=,1X,13,/)
  DO 701 I=1,43
  WRITE(13,702)(U1(I,J),J=1,19)
701 CONTINUE
  DO 703 I=1,43
  WRITE(13,702)(V1(I,J),J=1,19)
703 CONTINUE
  DO 704 I=1,43
  WRITE(13,702)(U2(I,J),J=1,19)
704 CONTINUE
  DO 705 I=1,43
  WRITE(13,702)(V2(I,J),J=1,19)
705 CONTINUE
702 FORMAT(1X,19F6.3)
  DO 706 J=1,19
  WRITE(13,707)(NU(I,J),I=1,43)
706 CONTINUE
707 FORMAT(1X,43I2)
  RETURN
  END

```

APPENDIX III
NUMERICAL RESULTS

VELOCITY FIELD IN THE ABSENCE OF WIND

Sea Level Difference 10 cm

Interfacial Elevation Difference 12 m

LOWER LAYER LONGITUDINAL VELOCITIES (M/SEC)

19	0	*****	*****	*****	*****	*****	*****	*****	*****	*****	*****	*****	*****	*****	*****	
18	0	*****	*****	*****	*****	*****	*****	*****	*****	*****	*****	*****	*****	*****	*****	
17	0	*****	*****	*****	*****	*****	*****	*****	*****	*****	*****	*****	*****	*****	*****	
16	0	*****	*****	*****	*****	*****	*****	*****	*****	*****	*****	*****	*****	*****	*****	
15	0	*****	*****	*****	*****	*****	*****	*****	*****	*****	*****	*****	*****	*****	*****	
14	0	*****	*****	*****	*****	*****	*****	*****	*****	*****	*****	*****	*****	*****	*****	
13	0	*****	*****	*****	*****	*****	*****	*****	*****	*****	*****	*****	*****	*****	*****	
12	0	*****	*****	*****	*****	*****	*****	*****	*****	*****	*****	*****	*****	*****	*****	
11	0	*****	*****	*****	*****	*****	*****	*****	*****	*****	*****	*****	*****	*****	*****	
10	0	*****	*****	*****	*****	*****	*****	*****	*****	*****	*****	*****	*****	*****	*****	
9	0	*****	*****	*****	*****	*****	*****	*****	*****	*****	*****	*****	*****	*****	*****	
8	0	*****	*****	*****	*****	*****	*****	*****	*****	*****	*****	*****	*****	*****	*****	
7	0	*****	*****	*****	*****	*****	*****	*****	*****	*****	*****	*****	*****	*****	*****	
6	0	.025	.017	.010	.007	.006	.005	.004	.003	.002	.001	*****	*****	*****	*****	
5	0	.025	.017	.010	.008	.006	.005	.004	.003	.001	.001	*****	*****	*****	*****	
4	0	.025	.016	.007	*****	*****	*****	*****	*****	.000	.000	.000	.000	.000	.000	
3	0	*****	*****	*****	*****	*****	*****	*****	*****	.000	.000	.000	.000	.000	.000	
2	0	*****	*****	*****	*****	*****	*****	*****	*****	*****	.000	.000	.000	.000	.000	
1	0	*****	*****	*****	*****	*****	*****	*****	*****	*****	*****	*****	*****	*****	*****	
		1	2	3	4	5	6	7	8	9	10	11	12	13	14	15
19	0	*****	*****	*****	*****	*****	*****	*****	*****	*****	*****	*****	*****	*****	*****	*****
18	0	*****	*****	*****	*****	*****	*****	*****	*****	*****	*****	*****	*****	*****	*****	*****
17	0	*****	*****	*****	*****	*****	*****	*****	*****	*****	*****	*****	*****	*****	*****	*****
16	0	.006	.006	.006	.006	.005	.006	.006	.007	.008	.009	.009	.010	.010	.011	.008
15	0	.006	.006	.007	.007	.007	.008	.008	.009	.010	.011	.012	.013	.014	.015	.017
14	0	.006	.006	.007	.007	.008	.009	.010	.011	.012	.013	.014	.015	.017	.019	.022
13	0	.006	.006	.007	.007	.008	.009	.011	.012	.013	.015	.017	.019	.021	.023	*****
12	0	.006	.006	.007	.008	.008	.010	.011	.012	.014	.016	.017	.019	.021	.023	*****
11	0	.005	.006	.007	.007	.008	.010	.011	.012	.014	.016	.017	.019	.021	.022	*****
10	0	.004	.005	.006	.006	.007	.008	.009	.011	.012	.014	.015	.016	.017	.019	.020
9	0	.002	.004	.006	.007	.008	.009	.010	.011	.013	.014	.015	.015	.016	.017	.017
8	0	.003	.004	.005	.006	.007	.008	.009	.010	.011	.012	.012	.012	.012	.012	.014
7	0	.003	.004	.004	.005	.006	.007	.008	.009	.010	.010	.010	.009	.005	*****	*****
6	0	*****	*****	.002	.004	.005	.005	.007	.008	.009	.009	.006	.007	.003	*****	*****
5	0	*****	*****	*****	*****	*****	.003	.005	.007	.008	.008	.008	.006	.004	.003	*****
4	0	*****	*****	*****	*****	.001	.002	.005	.006	.007	.008	.007	.006	.005	.003	*****
3	0	.000	.000	*****	.002	.001	.001	*****	*****	*****	*****	*****	*****	*****	.001	*****
2	0	.000	*****	*****	*****	*****	*****	*****	*****	*****	*****	*****	*****	*****	*****	*****
1	0	*****	*****	*****	*****	*****	*****	*****	*****	*****	*****	*****	*****	*****	*****	*****
		16	17	18	19	20	21	22	23	24	25	26	27	28	29	*****
19	0	*****	*****	*****	*****	*****	*****	*****	*****	*****	*****	*****	*****	*****	*****	*****
18	0	*****	*****	*****	*****	*****	*****	*****	*****	*****	*****	*****	*****	*****	*****	*****
17	0	*****	*****	*****	*****	*****	*****	*****	*****	*****	*****	*****	*****	*****	*****	*****
16	0	*****	*****	*****	*****	*****	.006	.005	.002	*****	*****	*****	*****	*****	*****	*****
15	0	.024	.028	.030	.030	.027	.017	.010	.003	-.002	-.001	*****	*****	*****	*****	*****
14	0	.025	.028	.029	.029	.026	.020	.012	.005	*****	.000	.000	*****	*****	*****	*****
13	0	.026	.027	.026	.027	.024	.019	.013	.007	.004	.002	.001	.000	*****	*****	*****
12	0	.025	.026	.026	.024	.022	.018	.013	.008	.005	.003	.001	.001	.000	*****	*****
11	0	.023	.024	.023	.022	.020	.016	.012	.008	.005	.003	.002	.001	.000	*****	*****
10	0	.020	.021	.020	.019	.017	.014	.011	.008	.005	.003	.002	.001	.000	*****	*****
9	0	.017	.017	.017	.017	.014	.011	.010	.007	.003	*****	*****	*****	*****	*****	*****
8	0	.012	.012	.012	.014	.012	.006	*****	*****	*****	*****	*****	*****	*****	*****	*****
7	0	.004	.006	.004	*****	*****	*****	*****	*****	*****	*****	*****	*****	*****	*****	*****
6	0	.002	.003	.002	*****	*****	*****	*****	*****	*****	*****	*****	*****	*****	*****	*****
5	0	.002	.002	.001	.001	-.001	.000	*****	.000	.000	*****	*****	*****	*****	*****	*****
4	0	.002	.001	.000	-.001	-.001	-.001	-.001	.000	.000	*****	*****	*****	*****	*****	*****
3	0	.001	.001	.000	*****	*****	.000	.000	.000	*****	*****	*****	*****	*****	*****	*****
2	0	*****	*****	*****	*****	*****	*****	*****	*****	*****	*****	*****	*****	*****	*****	*****
1	0	*****	*****	*****	*****	*****	*****	*****	*****	*****	*****	*****	*****	*****	*****	*****
		30	31	32	33	34	35	36	37	38	39	40	41	42	43	*****

VELOCITY FIELD IN THE ABSENCE OF WIND

Sea Level Difference 16 cm

Interfacial Elevation Difference 12 m

LOWER LAYER LONGITUDINAL VELOCITIES (M/SEC)

	1	2	3	4	5	6	7	8	9	10	11	12	13	14	15
19 0	*****	*****	*****	*****	*****	*****	*****	*****	*****	*****	*****	*****	*****	*****	*****
18 0	*****	*****	*****	*****	*****	*****	*****	*****	*****	*****	*****	*****	*****	*****	*****
17 0	*****	*****	*****	*****	*****	*****	*****	*****	*****	*****	*****	*****	*****	*****	*****
16 0	*****	*****	*****	*****	*****	*****	*****	*****	*****	*****	*****	*****	*****	*****	*****
15 0	*****	*****	*****	*****	*****	*****	*****	*****	*****	*****	*****	*****	*****	*****	*****
14 b	*****	*****	*****	*****	*****	*****	*****	*****	*****	*****	*****	*****	*****	*****	*****
13 0	*****	*****	*****	*****	*****	*****	*****	*****	*****	*****	*****	*****	*****	*****	*****
12 0	*****	*****	*****	*****	*****	*****	*****	*****	*****	*****	*****	*****	*****	*****	*****
11 0	*****	*****	*****	*****	*****	*****	*****	*****	*****	*****	*****	*****	*****	*****	*****
10 b	*****	*****	*****	*****	*****	*****	*****	*****	*****	*****	*****	*****	*****	*****	*****
9 b	*****	*****	*****	*****	*****	*****	*****	*****	*****	*****	*****	*****	*****	*****	*****
8 0	*****	*****	*****	*****	*****	*****	*****	*****	*****	*****	*****	*****	*****	*****	*****
7 0	*****	*****	*****	*****	*****	*****	*****	*****	*****	*****	*****	*****	*****	*****	*****
6 0	.035	.024	.013	.010	.008	.006	.005	.004	.003	.002	.001	*****	*****	*****	*****
5 0	.035	.024	.014	.011	.009	.007	.005	.004	.002	.001	*****	*****	*****	*****	*****
4 b	.035	.023	.010	*****	*****	*****	*****	*****	*****	*****	*****	*****	*****	*****	*****
3 b	*****	*****	*****	*****	*****	*****	*****	*****	*****	*****	*****	*****	*****	*****	*****
2 0	*****	*****	*****	*****	*****	*****	*****	*****	*****	*****	*****	*****	*****	*****	*****
1 0	*****	*****	*****	*****	*****	*****	*****	*****	*****	*****	*****	*****	*****	*****	*****
19 b	*****	*****	*****	*****	*****	*****	*****	*****	*****	*****	*****	*****	*****	*****	*****
18 0	*****	*****	*****	*****	*****	*****	*****	*****	*****	*****	*****	*****	*****	*****	*****
17 0	*****	*****	*****	*****	*****	*****	*****	*****	*****	*****	*****	*****	*****	*****	*****
16 0	.006	.006	.007	.006	.005	.006	.007	.008	.009	.010	.011	.012	.013	.014	.015
15 0	.006	.006	.007	.007	.007	.008	.009	.010	.011	.012	.013	.014	.015	.016	.017
14 0	.006	.007	.007	.007	.008	.009	.010	.011	.012	.013	.014	.015	.016	.017	.018
13 0	.006	.007	.007	.008	.008	.009	.011	.012	.013	.014	.015	.017	.019	.021	.023
12 0	.006	.006	.007	.008	.009	.010	.011	.013	.014	.016	.017	.019	.021	.023	.023
11 0	.006	.006	.007	.008	.009	.010	.011	.013	.014	.016	.017	.019	.021	.022	.022
10 0	.005	.005	.006	.007	.008	.009	.011	.012	.014	.015	.016	.018	.019	.020	.020
9 0	.003	.005	.006	.007	.008	.009	.010	.011	.013	.014	.015	.015	.016	.017	.017
8 0	.003	.004	.005	.006	.007	.008	.009	.010	.011	.012	.012	.012	.012	.012	.014
7 0	.003	.004	.004	.005	.006	.007	.008	.009	.010	.010	.010	.009	.005	*****	*****
6 0	*****	*****	.002	.004	.005	.005	.007	.008	.009	.009	.009	.007	.003	*****	*****
5 b	*****	*****	*****	*****	*****	.003	.005	.007	.008	.008	.008	.008	.006	.004	.003
4 b	*****	*****	*****	*****	.001	.002	.005	.006	.007	.007	.008	.007	.005	.003	.003
3 0	.000	.000	*****	.000	.001	.001	*****	*****	*****	*****	*****	*****	*****	*****	.001
2 0	.000	*****	*****	*****	*****	*****	*****	*****	*****	*****	*****	*****	*****	*****	*****
1 0	*****	*****	*****	*****	*****	*****	*****	*****	*****	*****	*****	*****	*****	*****	*****
	16	17	18	19	20	21	22	23	24	25	26	27	28	29	
19 0	*****	*****	*****	*****	*****	*****	*****	*****	*****	*****	*****	*****	*****	*****	*****
18 0	*****	*****	*****	*****	*****	*****	*****	*****	*****	*****	*****	*****	*****	*****	*****
17 0	*****	*****	*****	*****	*****	*****	*****	*****	*****	*****	*****	*****	*****	*****	*****
16 0	*****	*****	*****	*****	*****	*****	*****	*****	*****	*****	*****	*****	*****	*****	*****
15 0	.024	.028	.030	.030	.027	.017	.010	.003	-.002	-.001	*****	*****	*****	*****	*****
14 0	.025	.028	.029	.029	.026	.020	.012	.005	*****	.000	.000	*****	*****	*****	*****
13 b	.026	.027	.028	.027	.024	.019	.013	.007	.004	.002	.001	.000	*****	*****	*****
12 b	.025	.026	.026	.024	.022	.018	.013	.008	.005	.003	.001	.001	.000	*****	*****
11 0	.023	.024	.023	.022	.020	.016	.012	.006	.005	.003	.002	.001	.000	*****	*****
10 0	.021	.021	.021	.020	.017	.014	.011	.008	.005	.003	.002	.001	.000	*****	*****
9 0	.017	.017	.017	.017	.015	.011	.010	.007	.003	*****	*****	*****	*****	*****	*****
8 0	.012	.012	.012	.014	.012	.006	*****	*****	*****	*****	*****	*****	*****	*****	*****
7 0	.004	.006	.004	*****	*****	*****	*****	*****	*****	*****	*****	*****	*****	*****	*****
6 0	.002	.003	.002	*****	*****	*****	*****	*****	*****	*****	*****	*****	*****	*****	*****
5 0	.002	.002	.001	.000	-.001	.000	*****	.000	.000	*****	*****	*****	*****	*****	*****
4 0	.002	.001	.000	-.001	-.001	-.001	.000	.000	.000	*****	*****	*****	*****	*****	*****
3 0	.001	.001	.000	*****	*****	*****	.000	.000	.000	*****	*****	*****	*****	*****	*****
2 0	*****	*****	*****	*****	*****	*****	*****	*****	*****	*****	*****	*****	*****	*****	*****
1 0	*****	*****	*****	*****	*****	*****	*****	*****	*****	*****	*****	*****	*****	*****	*****
	30	31	32	33	34	35	36	37	38	39	40	41	42	43	

VELOCITY FIELD WITH WIND BLOWING FROM SOUTH-SOUTHWEST
WITH A SPEED OF 20 M/S

Sea Level Difference 8 cm

Interfacial Elevation Difference 10 m

VELOCITY FILED WITH WIND BLOWING FROM SOUTH-SOUTHWEST
WITH A SPEED OF 20 M/S

Sea Level Difference 24 cm

Interfacial Elevation Difference 12 m

VELOCITY FIELD WITH WIND BLOWING FROM NORTH-NORTHEAST
WITH A SPEED OF 17 M/S

Sea Level Difference 16 cm

Interfacial Elevation Difference 12 m

VELOCITY FIELD UNDER WIND BLOWING FROM NORTHEAST
WITH A SPEED OF 13 M/S

Sea Level excess 15 cm

Interfacial Elevation Difference 12 m

